Assessment of Potential Void Zones along the Adama–Awash Expressway using Integrated Geophysical and Geotechnical Approaches.

Sadik Husen Ukee

A Thesis submitted to the department of civil engineering

College of civil engineering and architecture

Presented in Partial Fulfilment of the Requirement of Masters of Science in Civil Engineering (Specialization in Geotechnical Engineering)

office of graduate studies

Adama science and technology university

may,2025

Adama, Ethiopia

Assessment of Potential Void Zones along the Adama–Awash Expressway using Integrated Geophysical and Geotechnical Approaches.

Sadik Husen Ukee

Advisor

Siraj Mulugeta (Ph.D.)

A Thesis submitted to the department of civil engineering

College of civil engineering and architecture

Presented in Partial Fulfilment of the Requirement of Masters of Science in Civil Engineering (Specialization in Geotechnical Engineering)

office of graduate studies

Adama science and technology university

may,2025

Adama, Ethiopia

Declaration

I declare that this thesis entitled "Assessment of Potential Void Zones along the Adama–Awash Expressway using Integrated Geophysical and Geotechnical Approaches." is my own work and has not been submitted to any university for similar purpose. The references used in this proposal are duly recognized by proper citations.

_____	_____	_____
Name of student	Signature	Date

Recommendation of Advisors

I, the major advisor/supervisor of this research, hereby certify that I have closely advised/supervised the student while developing this thesis and read the draft thesis entitled **"Assessment of Potential Void Zones along the Adama–Awash Expressway using Integrated Geophysical and Geotechnical Approaches."** prepared under my guidance by Sadik Husen. Therefore, I recommend the submission of the thesis to the department for further review and evaluation.

_____	_____	_____
Major Advisor/Supervisor	Signature	Date
_____	_____	_____
Co-advisor/Co-supervisor	Signature	Date

Approval Sheet

I/we hereby certify that the recommendation and suggestion given by the thesis review committee are appropriately incorporated into the final thesis entitled **"Assessment of Potential Void Zones along the Adama–Awash Expressway using Integrated Geophysical and Geotechnical Approaches."** By Sadik Husen.

Major Advisor/Supervisor	Signature	Date
Co-advisor/Co-supervisor	Signature	Date

Approval of Board of Reviewers

We, the undersigned, members of the Board of Reviewers of the thesis open defence by

Sadik Husen have read and evaluated the thesis entitled “Assessment of Potential Void Zones along the Adama–Awash Expressway using Integrated Geophysical and Geotechnical Approaches.” and assessed the understanding of the candidate about the proposed research. This is, therefore, to certify that the thesis is accepted and we recommend the implementation of the thesis. ----------.

_____	_____	_____
Chairperson	Signature	Date
_____	_____	_____
Reviewer 1	Signature	Date
_____	_____	_____
Reviewer 2	Signature	Date

Final approval and acceptance of the thesis is contingent upon submission of its final copy to the Office of Postgraduate Studies (OPGS) through the Department Graduate Council (DGC) and School Graduate Committee (SGC).

_____	_____	_____
Department Head	Signature	Date
_____	_____	_____
College Dean	Signature	Date
_____	_____	_____
Office of Postgraduate Studies, Dean	Signature	Date

ACKNOWLEDGEMENTS

I am sincerely grateful to all who contributed to the successful completion of this thesis. I extend my deepest appreciation to my advisor, Dr. Siraj Mulugeta, for his invaluable guidance, unwavering support, and insightful feedback throughout this research. I am also thankful to Dr. Argaw Asha for his thoughtful suggestions and consistent encouragement.

My heartfelt thanks go to the faculty of the Civil Engineering Department, whose instruction laid the groundwork for this study. I especially thank Mr. Shume for his assistance during the laboratory work. I also appreciate the support provided by Core Consulting Engineers Laboratory, particularly Mr. Meareg, and by Mr. Akthar from the ICT Laboratory for access to their facilities.

To my family, your love and encouragement have been my foundation I am forever grateful. I also wish to acknowledge my friends and colleagues for their motivation, collaboration, and meaningful discussions that enriched this journey.

Special thanks to the volunteers and institutions that offered data, resources, and support. Lastly, I recognize the academic contributions of geotechnical researchers whose work inspired and guided this study.

This thesis would not have been possible without the collective efforts of everyone mentioned. Thank you for your invaluable contributions.

TABLE OF CONTENTS

List of Table

List of figures

ACRONYMS

AASHTO	American Association of State Highway and Transportation Officials
ASTM	American Society for Testing and Materials
BH	Borehole
CBR	California Bearing Ratio
CL	Clay of Low Plasticity (USCS classification)
CH	Clay of High Plasticity (USCS classification)
ERT	Electrical Resistivity Tomography
GIS	Geographic Information System
GPR	Ground Penetrating Radar (if referenced)
GPS	Global Positioning System
LL	Liquid Limit
ML	Silt of Low Plasticity (USCS classification)
NP	Non-Plastic
PI	Plasticity Index
PL	Plastic Limit
pH	Potential of Hydrogen
RQD	Rock Quality Designation
SPT	Standard Penetration Test
SRT	Seismic Refraction Tomography
TDS	Total Dissolved Solids
UCS	Unconfined Compressive Strength
USCS	Unified Soil Classification System
VES	Vertical Electrical Sounding (if used alongside ERT)
Vp	Primary Wave Velocity
Vs	Shear Wave Velocity

Abstract

Potential void zones pose a serious geotechnical threat, particularly in regions underlain by unconsolidated, moisture-sensitive, or soluble materials that can lead to surface subsidence or collapse. This study evaluates the factors contributing to potential void formation along a section of the Adama–Awash Expressway in Ethiopia, spanning chainages 25+060 km to 25+180 km, through a multidisciplinary approach. A combination of geophysical methods—Electrical Resistivity Tomography (ERT) and Seismic Refraction Tomography (SRT) was employed alongside geotechnical investigations, including Dynamic Cone Penetrometer (DCP) testing, Atterberg limits, California Bearing Ratio (CBR), Proctor compaction, and permeability assessments. These techniques were supported by borehole logs and laboratory analyses, offering a comprehensive view of subsurface conditions. ERT results identified several low-resistivity anomalies (<29 Ω·m), most notably along survey Lines 3 and 5, indicative of saturated zones, dissolution features, or potential subsurface voids. Complementary SRT data revealed near-surface layers with seismic velocities below 400 m/s, highlighting the presence of loose, mechanically weak soils. Geotechnical characterization classified the soils primarily as CL (low to medium plasticity) under the Unified Soil Classification System, with Liquid Limits ranging from 38% to 50% and Plasticity Indices between 17% and 27%, suggesting poor bearing strength. At Borehole 105, the 1-meter layer exhibited moderate compaction (MDD = 1.5 g/cm³; OMC = 12.4%), cohesion of 30 kPa, and shear strength of 50 kPa, while the 3-meter depth contained finer, more moisture-retentive material (OMC = 18.7%) with higher cohesion (40 kPa) and shear strength (60 kPa), but increased risk due to potential volume changes. Similar patterns were observed at Borehole 106. In contrast, Borehole 107 revealed lower compaction levels (MDD = 1.3–1.4 g/cm³), reduced shear strength (45–48 kPa), and cohesion (25–28 kPa), indicating lower mechanical stability yet reduced susceptibility to moisture-induced deformation. However, hydrogeological tests from Borehole 107 indicated low permeability (hydraulic conductivity = 8.8 × 10⁻⁶ cm/s) and slightly alkaline conditions (pH = 8.5), factors that may promote carbonate dissolution and void development in confined aquifer conditions. based on integrated analysis, Boreholes 105 and 107 were identified as higher-risk areas for potential void formation. Mitigation recommendations include deploying deep foundations, pressure grouting in critical zones, enhancing surface drainage systems, and instituting ongoing geophysical monitoring. The outcomes of this research offer valuable insights for void risk management and long-term stability planning along the Adama–Awash Expressway.

Keywords

Dynamic cone penetrometer (DCP), Electrical Resistivity Tomography (ERT), Karst Terrain, Seismic Refraction Tomography (SRT) and Potential Void Zone.

CHAPTER 1

INTRODUCTION

1.1. Background of the study

Potential Void Zones, considered a naturally occurring hydrogeological event, pose significant risks to public safety and can cause major structural damage. Potential Void Zones have a significant financial impact. For example, in the United States, potential Void Zones are expected to cause annual budgetary losses of more than $300 million. The Florida Office of Insurance Regulation observed an increase in insurance claims linked with potential Void Zones in Florida, ranging from 2,360 in 2006 to 6,694 in 2010, with the total costs spent during this span being around $1.4 billion(Survey, 2018).

To mitigate these negative effects, it is critical to have a full grasp of the site's physiographic characteristics, geological composition, topographical features, climatic conditions, and soil distribution. Addressing building defects needs a thorough examination of the local geology, fracture orientations, and groundwater flow patterns. This analysis includes determining the types, depths, and compositions of subsurface soils and lithological formations, as well as a thorough examination of groundwater conditions, such as the location of the water table, its fluctuations, and the potential influx of surface water into excavated areas. For example, slope failures along road cuts are typically related with pre-existing planes, highlighting the importance of determining their direction. As a result, it is critical to investigate the direction and features of joints and weak zones. Furthermore, the level of weathering along these joints should be carefully assessed(Laekemariam et al., 2016).

A potential Void Zone is a naturally occurring cavity in the earth caused by a variety of reasons such as water and soil erosion. These elements are primarily responsible for the formation of potential Void Zones, particularly in places with limestone rock, as they can cause surface collapse. When a potential Void Zone forms, the surrounding ground destabilizes, which can cause foundation concerns. Potential Void Zones are essentially pits produced underground. They often arise when water collects and causes the ground to give way, frequently where a surface stream disappears underneath, resulting in the hole. This occurs when there is insufficient support, posing substantial challenges for both people and structures in the area.(Al-Shaqsi, n.d.-a,2019)

Potential Void Zones are a hazardous geohazard that can cause significant damage to infrastructure, disrupt daily life, and threaten public safety. They frequently arise when the stability of subsurface layers is jeopardized, either by the dissolving of soluble rocks such as limestone or the instability of loose sediments, particularly when groundwater flow affects the supporting materials below. This is especially concerning in situations where fragile surface materials come into contact with cracked bedrock.

Potential Void Zones present a number of challenges for site and civil engineers around the world. One major issue is that potential Void Zones are unavoidable natural disasters that pose a risk to property and human safety, making them challenging to control. But with time, human-caused carelessness can be corrected. Additionally, there is a dearth of research into how potential Void Zones emerge unexpectedly and possible ways to stop them from happening.

Particularly in places like Ethiopia's Oromia region, where geological and hydrological factors combine to create conditions that are favourable for their formation, potential Void Zones are a significant geohazard that pose serious risks to infrastructure. These geological depressions are created when the structural integrity of the subsurface is compromised, usually by the instability of unconsolidated sediments or the dissolution of soluble rocks. Groundwater movement, weak overburden materials, and fractured bedrock often interact to enable potential Void Zone development.

The Adama-Awash Express Road, a vital transportation corridor in Ethiopia, has often developed potential Void Zones, particularly near the 25-kilometer mark. The regional geology is distinguished by the presence of easily erodible sediments (sand, silt, and clay) underlying fractured basalt. This stratigraphy has been studied for its impact on the road's mechanical stability, as groundwater traverses these material layers, increasing pore pressures and accelerating erosive processes that can lead to subsurface voids and subsequent collapse.

The inability to accurately predict or control potential Void Zone formation endangers not only road users and infrastructure, but also the economic activities that rely on this critical route. As a result, a full understanding of subsurface geological conditions, material interactions, and mechanical qualities is critical to developing appropriate engineering solutions. This study intends to fill a knowledge gap by using sophisticated geophysical and geotechnical

methodologies to determine the underlying causes and mechanisms of potential Void Zone formation along the Adama-Awash expressway.

Potential Void Zones are a serious geohazard that can jeopardize public safety and infrastructure, especially in places with delicate geological characteristics like those with loose sediments or soluble rocks. Their growth is influenced by a number of factors, such as the stability of underlying materials and groundwater circulation. For effective mitigation methods, it is essential to comprehend the local geology and hydrological circumstances in areas like Ethiopia's Oromia region, where potential Void Zones have been found along the Adama-Awash Express Road. In-depth research employing contemporary geophysical and geotechnical methods can assist in identifying the fundamental causes of potential Void Zone formation, resulting in improved engineering solutions that strengthen infrastructure resilience and safeguard commercial operations that depend on these vital transportation routes.

Potential Void Zones are a major geohazard that can endanger infrastructure and public safety, particularly in areas with vulnerable geological properties, such as those containing soluble rocks or loose sediments. A variety of factors influence their growth, including groundwater circulation and subsurface material stability. In regions such as Ethiopia's Oromia region, where the Adama-Awash Express Road has encountered potential Void Zones, understanding the local geology and hydrological conditions is critical for developing efficient mitigation solutions. Detailed investigations using modern geophysical and geotechnical techniques can help reveal the core reasons of potential Void Zone development, leading to better engineering solutions that improve infrastructure resilience and protect economic activities that rely on these critical transportation corridors.

1.2 Statement of the Problem

Potential Void Zone formation is a severe geotechnical hazard on Ethiopia's Adama-Awash Expressway, a vital traffic route. Potential Void Zones, particularly those between 25+060 km and 25+180 km in length, pose a major threat to road infrastructure, public safety, and long-term structural stability. These potential Void Zones are caused mostly by the breakdown of soluble bedrock, which collapses surface soils and creates subsurface voids. However, the underlying mechanisms that contribute to potential Void Zone formation in this location have

not been adequately researched or characterized, resulting in a limited understanding of the geotechnical, geological, and chemical conditions involved.

The lack of understanding about specific subsurface circumstances such as geological formations, soil qualities, groundwater behaviour, and dissolution processes impedes the development of efficient mitigation solutions. The combination of geophysical anomalies, thin soil layers, and groundwater movement is still unclear, making it difficult to quantify the risk and apply preventative steps to prevent potential Void Zones. Furthermore, there is a scarcity of complete, integrated methodologies that combine geophysical, geotechnical, and chemical data to identify high-risk zones and provide appropriate engineering solutions for potential Void Zone mitigation.

Given the fundamental importance of the Adama-Awash Expressway to Ethiopia's transportation network, addressing the absence of comprehensive data on potential Void Zone risk and mitigation is critical. This study aims to bridge this knowledge gap by examining the subsurface conditions and causes of potential Void Zone formation, identifying high-risk sites, and suggesting targeted engineering solutions to reduce potential Void Zone occurrences while ensuring the expressway's long-term safety and stability.

1.3 Research Questions

These research questions address key aspects of the study, such as subsurface conditions, geological formations, geotechnical behaviour, chemical influences, and practical engineering implications for potential Void Zone risk assessment and mitigation along the Adama-Awash Expressway (Chainage 25+060 km to 25+180 km):

- What influence do geological formations and lithological variations along the studied section of the highway have on void zone formation?
- What are the key physical and chemical properties of soils in the study area, such as plasticity, permeability, pH, and compaction, based on results from laboratory and field testing?
- How do moisture variations affect the mechanical behaviour of soils and sediments in the region, impacting their load-bearing capacity and risk of collapse?
- What types of subsurface anomalies, including voids, dissolution zones, and weak soil layers, can be detected using geophysical techniques in the study area?

- How can the integration of geotechnical, geophysical, and geological data improve the accuracy of potential Void Zone risk zoning and help identify high-risk locations along the highway?
- What are the most effective engineering mitigation measures for reducing potential Void Zone risks in the high-risk areas identified along the study section of the highway?

1.4 Research Objectives

1.4.1 General Objective

To study the mechanisms of potential void zone formation along the Adama-Awash Expressway (chainages 25+060 km to 25+180 km) using integrated geotechnical, geological and geophysical approaches, with the goal of identifying high-risk zones and proposing effective mitigation strategies to improve infrastructure safety and resilience.

1.4.2 Specific Objectives

- To evaluate the geological formations and lithological variations along the study portion of the highway and determine their impact on potential void zone development.
- To assess soil physical and chemical qualities, such as plasticity, permeability, pH, and compaction, utilizing laboratory and in-situ testing methods.
- To investigate the mechanical behaviours of soils and sediments under various moisture conditions in order to estimate their load-bearing capability and risk of collapse.
- To discover subsurface anomalies such as voids, dissolution zones, and weak soil layers using geophysical techniques.
- To integrate geotechnical, geophysical, and geological data for precise potential Void Zone risk zoning and identifying high-risk locations.
- To offer appropriate engineering mitigating measures.

1.5 Scope of the Study

This study aims to evaluate the mechanisms behind potential Void Zone formation and assess the associated risks within a defined segment of Ethiopia's Adama–Awash Expressway, specifically between chainages 25+060 km and 25+180 km. The research is confined to this section due to observed geological and geotechnical indicators of ground instability, which are suspected to be related to karstic activity and the presence of underlying voids.

The research integrates geological, geotechnical, geophysical, and chemical investigations to characterize subsurface conditions and identify areas prone to potential Void Zone development. Geological analysis includes stratigraphic interpretation and lithological profiling to understand the role of soluble rocks and structural discontinuities in promoting karstification. Geotechnical investigations comprise laboratory and field tests such as Atterberg limits, California Bearing Ratio (CBR), Proctor compaction, permeability, and Dynamic Cone Penetrometer (DCP) testing to assess soil strength, plasticity, and This MSc research focuses on assessing potential Void Zone formation mechanisms and danger along a specific portion of Ethiopia's Adama-Awash Expressway, between chainages 25+060 km and 25+180 km. The investigation is limited to this corridor, which has shown geological and geotechnical signals of instability that may be linked to karst processes and subsurface cavities.

The research integrates geological, geotechnical, geophysical, and chemical investigations to characterize subsurface conditions and identify areas prone to potential Void Zone development. Geological analysis includes stratigraphic interpretation and lithological profiling to understand the role of soluble rocks and structural discontinuities in promoting karstification. Geotechnical investigations comprise laboratory and field tests such as Atterberg limits, California Bearing Ratio (CBR), Proctor compaction, permeability, and Dynamic Cone Penetrometer (DCP) testing to assess soil strength.

1.6 Significance of the Study

This study is of great significance due to its practical relevance in addressing potential Void Zone hazards and its scholarly contributions to geotechnical engineering, geophysics, and geohazard management. By integrating geophysical surveys such as Electrical Resistivity Tomography (ERT) and Seismic Refraction Tomography (SRT) with geotechnical assessments involving California Bearing Ratio (CBR), Atterberg limits, compaction, permeability, this research provides a comprehensive understanding of subsurface conditions along the Adama–Awash Expressway.

The identification of vulnerable zones, including voids and soft layers, allows for the creation of accurate hazard maps, which are essential for ensuring safer infrastructure development. Specifically, the findings will enhance the safety and resilience of the Adama-Awash Expressway, a critical transportation route in Ethiopia, by identifying high-risk areas such as Boreholes 105 and 107. This will enable the implementation of targeted mitigation measures,

including deep foundations, pressure grouting, and improved drainage systems, thereby preventing potential Void Zone damage and safeguarding public safety.

Furthermore, this study promotes sustainable engineering practices by recommending proactive measures such as continuous geophysical monitoring and the establishment of early warning systems. These solutions are expected to significantly enhance the long-term structural stability of the expressway, ensuring that it can withstand environmental stressors and geological changes without compromising safety. In addition to its engineering contributions, the study will offer valuable insights for policymakers and urban planners by revealing the interactions between geological formations, groundwater, and soil properties. This knowledge can guide the development of safer infrastructure designs in regions with similar geological conditions, ultimately contributing to better land-use management policies by discouraging construction in potential Void Zone-prone areas.

Academically, the study advances potential Void Zone research by adopting a multidisciplinary approach that combines geophysics, geotechnics, and hydrochemistry, providing a clearer understanding of karstification processes, carbonate material dissolution, and their roles in subsidence and subsurface instability. These findings have broader implications for other regions facing karst-related hazards. Finally, the study will propose engineering solutions and preventive measures for managing potential Void Zone risks in karst areas. Recommendations for ground stabilization, grouting, and surface drainage systems will be applicable to other transportation networks in Ethiopia and similar regions, improving long-term road maintenance and reducing the likelihood of potential Void Zone formation in vulnerable areas.

1.7 Limitations of the Study

Although this research applied a wide range of methods, it encountered some important limitations. The limited time available for fieldwork reduced both the number of sites that could be tested and the overall coverage of the study area. There were also constraints in accessing advanced geophysical equipment and fully equipped laboratories, which may have influenced the depth and precision of certain tests. Since the study was concentrated on a short section of the Adama–Awash Expressway, the results may not reflect conditions in other areas. Additionally, because few previous studies have been conducted on potential Void Zones in Ethiopia, there was a lack of local data and literature for comparison. These challenges

highlight the need for more detailed and broader research on potential Void Zone risks across the country.

1.8 Validity of the Study

The credibility of this research is strengthened by its integrated, multidisciplinary approach, which combines geophysical, geotechnical, geological, and chemical data to assess potential Void Zone vulnerability along the Adama–Awash Expressway section between 25+060 km and 25+180 km.

Non-invasive geophysical tools like Electrical Resistivity Tomography (ERT) and Seismic Refraction Tomography (SRT) were used to identify subsurface irregularities—such as areas with low resistivity or low seismic velocity that often signal the presence of voids, water-saturated zones, or structurally weak materials linked to potential Void Zone formation. Geotechnical evaluations, including tests like the Atterberg limits, Dynamic Cone Penetrometer (DCP), California Bearing Ratio (CBR), and Proctor compaction, offered critical data on soil properties such as strength, consistency, and compaction. These tests helped pinpoint zones with low structural stability and poor load-bearing characteristics. Laboratory findings complemented the field observations, revealing soils with moderate to high plasticity and low CBR values—conditions typically associated with materials prone to collapse.

Furthermore, hydrogeological data gathered from borehole logs, particularly Borehole 107, revealed low permeability and alkaline groundwater conditions (pH 8.5), both of which promote carbonate dissolution and karst formation. These findings support the geophysical and geotechnical interpretations, improving internal consistency and triangulation of data across independent approaches.

The study's geographical focus on a well-defined road stretch, as well as the consistency of results across different test lines (e.g., ERT Lines 3 and 5, Boreholes 105 and 107), provide additional support for the construct and external validity. Furthermore, the recommended mitigation techniques are based on actual site-specific characteristics, which strengthens the conclusions' practical validity and application.

Overall, the convergence of many lines of data lends significant credence to the study's findings and validates the conclusions obtained on potential Void Zone vulnerability and potential mitigation along the Adama-Awash Expressway.

CHAPTER TWO

2. LITRETURE REVIEW

2.1 Introduction

Potential Void Zones are a major worry in geohazards, frequently developing unexpectedly and causing severe structural and economic consequences. They are particularly problematic in regions with soluble bedrock, strong groundwater flow, and unconsolidated surface materials. This literature study looks at the elements that contribute to potential Void Zone formation, geophysical and geotechnical diagnosis tools, and the subsurface conditions that exist along Ethiopia's Adama-Awash Express Road. Understanding these processes is critical for creating effective mitigation methods that improve infrastructure safety and resilience.(Ahmad et al., 2022)

A potential Void Zone is a depression in the ground that lacks external surface drainage and is created by a process in which rocks disintegrate. Underground water steadily dissolves the limestone bedrock beneath the ground's surface, leaving a network of underground holes. Above the limestone layer are layers of sand, clay, and soil. According to Taheri (2016), these layers are often sturdy enough to support the infrastructure and utilities that are erected upon them. If the holes are too close to the surface, or if they develop in size and move closer to the surface, the surface layers may collapse unexpectedly. Even heavy rain can cause the top layer to become overly heavy. When subsurface water is tapped excessively, the holes dry out and can no longer sustain the weight of the layer above them. A pore is then developed; this is what geologists refer to as karst terrain (Al-Shaqsi, n.d.-a, 2019).

In carbonate-rich locations, karst voids provide substantial engineering issues. These holes can cause a variety of concerns, such as road and highway subsidence, structural collapses of building foundations, and dam leaking. The creation of huge holes in karst environments can result in rapid and catastrophic pavement failures, whereas the slow movement of tiny particles from the sub-base may lead to gradual ground subsidence and possible collapse over time. (Al-Shaqsi, n.d.-b)These conditions have significant financial ramifications for engineering designs, particularly in infrastructure projects. Subsurface cavities provide a significant risk in areas with carbonate rocks, with potential Void Zones causing key issues such as foundation collapses, road subsidence, and damage to utilities that are generally located beneath road subgrades. Furthermore, these subsurface holes might pose serious public safety hazards in civil engineering projects. Underestimating foundation dimensions frequently causes

catastrophic subsidence of structures and roadways due to potential Void Zone occurrences(Farhan et al., 2024).

A potential Void Zone is a depression in the ground that lacks external drainage and is generated when rocks dissolve. Groundwater gradually erodes the limestone bedrock beneath the surface, forming a network of underground caverns. Above this limestone layer, there are usually sand, clay, and soil layers that are strong enough to sustain the structures and utilities that are placed on it. However, if these cavities reach too close to the surface or expand, the layers above may collapse unexpectedly. Heavy rainfall can also contribute to this by putting additional weight on the surface. Furthermore, over-extraction of groundwater can dry out the holes, reducing their ability to sustain the weight above, resulting in the formation of what geologists refer to as karst topography. Potential Void Zones can form owing to both natural processes and human activity. Natural potential Void Zones result from erosion induced by underground water(Al-Shaqsi, n.d.-a, 2019).

Potential Void Zones present significant threats to the stability and safety of infrastructure, requiring careful investigation and effective mitigation strategies. This research addresses a recurring potential Void Zone issue along a driveway in Nashville, Tennessee, where periodic pavement subsidence and collapse have occurred over several years despite numerous repairs. The study involved extensive site assessments, including field drilling and investigations into soil, rock, and groundwater conditions. The subsurface examination revealed a complex geological structure primarily composed of the Ordovician Hermitage Formation, with karst-related geology leading to soil erosion and subsidence. The site consists of a mix of soil and rock types, with fill materials covering underlying natural clay and limestone bedrock. Various mitigation methods were explored, such as the standard inverted rock filter potential Void Zone repair, land bridge construction, and compaction grouting. Ultimately, compaction grouting was chosen as the most effective solution(Alimohammadi, 2024).

Several mitigating strategies were considered, including standard inverted rock filter potential Void Zone repair, land bridge construction, and compaction grouting. Compaction grouting was chosen as the preferable procedure because it is effective in stabilizing the area and preventing future potential Void Zones while also being feasible and cost-effective. The proposed compaction grouting repair plan is thorough, including methodology, materials, and construction specifications. Based on evaluations and specialist consultations, recommendations are made to implement the compaction grouting program. This study gives

useful insights into potential Void Zone mitigation measures that may be applied to similar geological circumstances around the world, emphasizing the significance of ongoing monitoring and maintenance to address potential future potential Void Zones. Furthermore, the findings seek to inform the establishment of improved design standards and building procedures for potential Void Zone restorations in karst settings(Alimohammadi, 2024).

2.2 Soluble rocks

Water moving through fractures and voids in soluble rock formations can gradually dissolve materials such as limestone, dolomite, gypsum, anhydrite, and salt. This process of chemical and physical dissolution removes material from fractures and bedding planes, significantly increasing the permeability of these rocks over relatively brief geological timescales—ranging from several decades to around 100,000 years. As these underground voids expand, they pose a serious threat of mechanical failure and ground surface deformation when larger cavities begin to collapse. In this study, karst features and subterranean cavities are documented within rock layers found in the southern parts of the Harz Mountains and the Kyffhäuser Hills in Germany. In this region, bands of limestone, dolomite, anhydrite, and gypsum extend across a kilometre-wide zone along the base of the Harz Mountains. These rock units, originally laid down during the Zechstein stage of the Permian period, were subsequently buried and later exposed through tectonic uplift. The exposed rocks exhibit widespread karst formations, although sizable underground cave systems disconnected from the surface have also been identified, primarily through accidental encounters during mining activities(Kaufmann & Romanov, 2019).

High secondary permeability, which results from water passing through the rock and dissolving the soluble fracture walls, is a characteristic of soluble rocks including gypsum, limestone, and anhydrite. This highly selective dissolving process expands cracks into voids and eventually cavities, which carry the majority of flow across an aquifer via preferential flow routes. We use a computational model that describes the growth of secondary porosity in soluble rocks to investigate the evolution of isolated fractures in various rock types. Identifying shallow vs deep flow channels and their evolution for different types of rock, the impact of precipitation on the dissolved material in the fracture, and the complexity of fracture growth in fractures composed of many soluble materials are our three main areas of interest. Our results show that although the time scale is very different, the development of gypsum and limestone cracks is similar. Because of a difference in the kinetical rate law that explains the removal of soluble rock, anhydrite evolves more quickly than both limestone and anhydrite. Changes in the hydro

chemical conditions can cause the dissolved rock to precipitate, which can quickly obstruct fractures and alter the soluble rock's preferred channel pattern(Kaufmann et al., 2016).

Soluble rocks dissolve, resulting in the formation of caverns and voids, which may eventually create a potential Void Zone. The collapse mechanism may be natural or man-made. One of the harms caused by soluble rocks is ground collapse, which can range from moderate saucer-shaped depressions that build over time to a catastrophic collapse, which is a potential Void Zone that occurs unexpectedly. Soluble rock dissolution can cause ground subsidence, building and road collapse, and damage to utilities including water, gas, and drainage. It occurs when water flows through soluble rocks, creating cavern networks and subterranean chambers. It occurs when water flows through soluble rocks, creating cavern networks and subterranean chambers(Al-Shaqsi, n.d.,2023).

The underlying rocks and sediments may collapse locally as a result of these voids, which weaken the ground above. Additionally, it may result in bad ground conditions and engineering issues. Dolomite, limestone, chalk, gypsum, and salt are the five primary soluble rock types that are found around the world. Each has a unique solubility, rate of dissolving, and geological location(Kaufmann & Gabrovsek, 2017).

Water, which may include carbon dioxide, sulphides, or other organic acids, dissolves soluble rocks including limestone, dolostone, gypsum, and anhydrite. This activity takes place both on the surface of the rock and within underlying fractures and faults, particularly throughout the rock's teleogenetic history. In contrast to insoluble rocks, where permeability remains relatively constant due to continuous subsurface flow routes, soluble fractured aquifers exhibit significant permeability increase with time. This results in very efficient drainage channels, where surface water flow can be completely eliminated as the expanded fractures accommodate massive amounts of water, even during major recharge periods. These favourable subsurface flow pathways frequently result in the formation of huge holes, sometimes meter-wide or greater, which offer access to caverns capable of carrying entire underground rivers (Kaufmann & Gabrovsek, 2017).

Water seepage under hydraulic structures often leads to the dissolution of evaporite rocks, posing significant global challenges. This process is crucial in the degradation of rock and contributes to karst features such as caves and potential Void Zones, which facilitate water leakage and increase the risk of dam collapse. Prominent sulphate rocks like gypsum ($CaSO4{\cdot}2H2O$) and anhydrite ($CaSO4$) are common in the Earth's crust and contribute to these

issues. Many dams worldwide face challenges related to the dissolution of these sulphate rocks(Aziz et al., 2024).

2.3 Factors Contributing to Potential Void Zone Formation

Potential Void Zones usually have a higher probability of occurrence and a greater genetic diversity in evaporite terrains than in carbonate karst areas. This is because evaporites have a higher solubility, and commonly a lower mechanical strength. Subsidence damage resulting from evaporite dissolution generates substantial losses throughout the world, but the causes are only well-understood in a few areas(Gutiérrez et al., 2008).

Potential Void Zones are caused by a complex interplay of natural and anthropogenic factors. The dissolution of soluble bedrock (karst processes), groundwater fluctuations, soil erosion, and human activities such as over-extraction of groundwater or poorly planned construction significantly influence their development. Potential Void Zone formation caused by leaking pipes in karst soluble rocks is a significant concern, leading to infrastructure damage and safety risks(Pipe et al., 2024).

The rapid formation of potential Void Zones in recent years has been strongly linked to significant changes in hydrogeological conditions, particularly the rapid decline in the Dead Sea (DS) water level over the past decades (Arkin, 1993; Arkin and Gilat, 2000; Wachs et al., 2000). This phenomenon has been closely associated with the accelerated drop in the DS level, which has drastically altered the subsurface dynamics near the shoreline. Over the last 30 years, the DS level has decreased by approximately 20 meters, at an average rate of about 80 centimetres per year. Such a dramatic reduction has triggered a series of profound geological and hydrological transformations(Yechieli et al., 2003).

As the sea level dropped, the shoreline retreated toward the center of the basin, reducing the size of the sea significantly. This retreat has caused existing springs near the shoreline to shift in location, while new springs have emerged along the receding shoreline. Concurrently, subsurface changes have occurred, including a notable decline in the regional groundwater level. This drop has also shifted the position of the fresh-saline water interface, which has moved progressively closer to the basin's centre (Yechieli et al., 1995).

These alterations in the groundwater system have exacerbated the susceptibility of the near-shore regions to potential Void Zone formation. The rapid shifts in hydrogeological conditions,

coupled with the destabilization of the subsurface due to changes in water saturation and salt dissolution, have created an environment where potential Void Zones form more frequently and unpredictably(Yechieli et al., 2003).

The drop in the Dead Sea (DS) water level and the resulting shift in the fresh-saline water interface have exposed subsurface salt layers to groundwater that is undersaturated with respect to halite. This process initiates significant geological transformations. Fresh groundwater, moving through conduits such as faults or joints, dissolves the salt, leading to the formation of caverns within the salt layer. Over time, the ceilings of these caverns collapse, followed by the gradual collapse of overlying unconsolidated sediments into the voids. In some cases, relatively consolidated layers within the sedimentary sequence may temporarily support the structure before eventually giving way. This sequence of events culminates in the development of potential Void Zones on the surface(Yechieli et al., 2003).

Additionally, the decline in DS water level may reduce hydrostatic pressure in the subsurface, particularly in pre-existing cavities. This reduction in pressure can further destabilize the subsurface structure, contributing to the formation of potential Void Zones. These combined processes highlight the complex interplay of hydrological and geological factors driving potential Void Zone development in the region(Yechieli et al., 2003).

Subsurface exploration revealed a complex geological profile dominated by the Ordovician Hermitage Formation, with karst-prone geology contributing to soil erosion and subsidence (Alimohammadi, 2024).

Potential Void Zones are a geological hazard that result from the collapse of a surface layer into a void beneath. These depressions can have devastating effects on infrastructure, property, and human life. A variety of natural and anthropogenic factors contribute to their formation, which can be broadly categorized into geological, hydrological, and human-induced factors(Campus et al., 2024).

2.3.1 Geological Factors

Water flowing through soluble rocks such as limestone, dolomite, gypsum, anhydrite, and salt can gradually dissolve these materials, expanding voids and fissures. This process, driven by both physical and chemical dissolution, significantly increases the permeability of the rocks. Over relatively brief geological periods—ranging from decades to 100,000 years—these voids

can grow large enough to threaten the structural stability of the rocks. When these enlarged cavities become unstable, they may collapse, leading to surface deformation and potential hazards(Kaufmann & Romanov, 2019).

The primary geological condition that facilitates potential Void Zone formation is the presence of soluble bedrock, such as limestone, gypsum, or dolomite. These materials are prone to dissolution by slightly acidic groundwater over time, leading to the formation of subterranean cavities. Karst landscapes, characterized by features like caves, potential Void Zones , and underground drainage, are particularly susceptible (Ford & Williams, 2007). The type and thickness of the overlying sediments also influence potential Void Zone formation. Loose, unconsolidated sediments are more likely to collapse into voids compared to compacted or cohesive soils.

Groundwater dynamics also play a significant role in potential Void Zone development in mining regions. Water infiltrating abandoned voids can erode the cavity walls and dissolve soluble minerals, enlarging the voids and increasing the likelihood of collapse. Seasonal changes in the water table, particularly during periods of rapid drainage or heavy rainfall, can destabilize the overburden, making it more susceptible to subsidence(Witkowski et al., 2023).

Mitigating potential Void Zone risks in shallow mining areas requires a combination of detailed geological surveys and stabilization efforts. Technologies like ground-penetrating radar (GPR) are instrumental in detecting voids and weak zones beneath the surface. Stabilization measures, such as backfilling voids with grout or other materials, can reinforce the subsurface and reduce collapse risks. Furthermore, integrating historical mining data into land-use planning is essential to avoid development on high-risk sites. By addressing these factors, the likelihood of potential Void Zone formation can be minimized, protecting infrastructure and communities in affected areas(Gutiérrez et al., 2008).

2.3.2 Hydrological Factors

Groundwater is defined as water which is located underground in between sediment particles and the zones of porous sediments are called aquifers. Subsequently, most of Long Island’s freshwater supply comes from pumping these underground aquifers. The groundwater level (GWL) fluctuations occur naturally due to various factors including seasonal changes, precipitation levels, and also human activity (Tamiru et al. 2018).

Underground erosion happens when groundwater breaks down sediment particles, forming fractures that lead to further erosion. When significant underground erosion occurs, these fractures expand until the groundwater reaches a non-porous sediment layer. Potential Void Zones develop when subsurface sediment layers experience chemical weathering or dissolution due to groundwater movement from surface water or precipitation. This process typically involves the natural dissolution of rocks like limestone by circulating underground water. Over time, the surface above the eroded area loses stability and collapses inward, forming a potential Void Zone(Hope & Marsellos, 2024a).

Potential Void Zone formations present substantial risks to infrastructure and public safety, with Long Island, NY witnessing a recent increase in such events. The potential link between frequent fluctuations in groundwater levels (GWL) and accelerated subterranean erosion, which may contribute to potential Void Zone development, was explored. Analysing GWL data from USGS monitoring stations pinpointed areas on Long Island displaying various GWL fluctuations. Although the findings do not show a strong individual correlation between high-frequency GWL fluctuations and potential Void Zone occurrences, regions with predominantly high-frequency GWL oscillations tend to experience a greater number of potential Void Zones (Hope & Marsellos, 2024b).

Changes in groundwater dynamics play a critical role in potential Void Zone development. Fluctuations in the water table, often caused by prolonged droughts or heavy rainfall, can destabilize subsurface voids. Rapid water infiltration following heavy rainfall increases soil erosion and accelerates cavity collapse (Gutiérrez et al., 2014). Additionally, the withdrawal of groundwater for agricultural or industrial purposes reduces hydraulic pressure, leading to the collapse of supporting structures in karst systems(Hope & Marsellos, 2024b).

Chalk streams often have several sink points spread over significant distances, with the locations shifting depending on water flow. In low flow conditions, water infiltrates further upstream through sediments into the chalk beneath. Over time, sink points evolve as sediment blocks existing ones, and new openings emerge. Some streams vanish into surface depressions or blind valleys, while others overflow to different sinks or catchments during high flows. Human interventions, such as modifications for drainage or rerouting, have altered many of these natural systems(Maurice et al., 2023).

The electrical resistivity technique is a widely used geophysical method for detecting groundwater potential. This approach is effective, non-destructive, and cost-efficient, making

it a reliable way to identify potential groundwater sources. It involves taking surface measurements to gather subsurface resistivity data, which provides a clearer understanding of the subsurface characteristics. This information is crucial for accurately locating aquifers with high groundwater yield(Sulaiman et al., 2022).

2.3.3Human-Induced Factors

Human activities often act as triggers for potential Void Zone formation in these areas. Construction, road building, or alterations to land use can add stress to the surface above old mining voids. Vibrations from machinery or vehicles can precipitate collapse, especially in zones where subsurface structures are already compromised. Additionally, insufficient records of historical mining operations increase the risk of unexpected potential Void Zone occurrences, as potential danger zones may go unidentified(Witkowski et al., 2023).

Potential Void Zones frequently develop in areas of shallow mining due to the inherent instability caused by the voids left behind after resource extraction. These voids, often unsupported, create conditions conducive to surface collapse over time. The process begins with the collapse of the rock strata forming the roof of mining excavations. These rock layers, typically lacking the plasticity to deform without breaking, are subjected to stress from the weight of overlying materials. Over time, fractures form, and the roof eventually collapses into the voids, creating a chain reaction that affects the overburden(Witkowski et al., 2023).

As the rock layers collapse, the overlying unconsolidated sediments, such as Quaternary deposits, begin to settle into the space created by the collapse. These sediments, being loose and lacking cohesion, easily shift downward, leading to depressions at the surface and forming potential Void Zones. This process is often exacerbated by the passage of time, as abandoned mining areas experience progressive weakening. Weathering of exposed surfaces within the voids and infiltration of groundwater further degrade the stability of the excavation walls and roof, causing delayed potential Void Zone formation even long after mining operations have ceased(Witkowski et al., 2023).

The "fill sinks" method has been effectively utilized in various studies; however, the features identified through this approach often tend to be overestimated and lack accuracy in defining potential Void Zone boundaries. As a result, depressions derived from topographic data typically require further refinement, which is commonly achieved through post-processing and human visual inspection of RGB imagery(Rafaeli et al., 2024).

Anthropogenic activities significantly contribute to potential Void Zone formation. Urbanization and infrastructure development alter natural drainage patterns and impose additional loads on the subsurface. Construction activities, such as drilling or mining, can directly destabilize karst features, leading to sudden collapses. Furthermore, improper waste disposal and leaky sewer systems introduce additional water into the subsurface, exacerbating dissolution processes the formation of the potential Void Zone at Oana Crater was closely studied, revealing that changes in subsurface heat distribution, particularly shifting from the northwest to the northeast, significantly influenced nearby fumarole activity. This thermal redistribution triggered the release of molten sulfur and intensified fumarole emissions(Oishi, n.d., 2021).

Historical analysis of the site indicated similar hydrothermal events in 1966, suggesting a recurring pattern of subsurface thermal energy movement. These events highlighted the role of hydrothermal fluids and volcanic gases in weakening the surface geology, which contributed to the 2021 potential Void Zone formation. Unlike earlier potential Void Zones associated with mud eruptions, the 2021 event occurred independently, implying a potential alteration in thermal energy pathways within the shallow subsurface.

The persistent geothermal and fumarolic activities at Oana Crater continue to shape its volcanic environment. Among these, the W-6 fumarole stands out, emitting white plumes that rise as high as 100 meters above the crater. Additionally, fumarolic activity is widely dispersed throughout the crater and the nearby Tsubakurosawa fissure, underscoring the dynamic nature of the geothermal landscape (Oishi, n.d., 2021).

2.3.4 Climate Change and Potential Void Zones

Potential Void Zones typically form when water erodes detrital or evaporite rock beneath the Earth's surface, creating a cavity that eventually collapses. Increased underground water mobility may lead to accelerated potential Void Zone development, especially upon more frequent warming temperatures due to climate change(Hubbs & Marsellos, 2024).

over the past few decades, numerous scientists have extensively studied climate change by analysing temperature extremes, weather variations, ice core data, and more. Despite the broad consensus in the scientific community regarding the reality of climate change, its link to specific geohazards remains underexplored. Frequently examined connections include those between climate change and hurricanes, volcanic activity, floods, and heat waves. According to the map provided by the Centre for Climate and Energy Solutions (2024) and Earthjustice

(2024), the years 2020-2023 have recorded the highest incidences of extreme weather events, such as tropical storms, droughts, and severe storms. This trend strongly suggests an influence of climate change on these occurrences.(Hubbs & Marsellos, 2024)

Emerging research highlights the role of climate change in influencing potential Void Zone occurrences. Rising global temperatures and altered precipitation patterns are expected to intensify the hydrological processes that trigger potential Void Zones. Regions experiencing extreme weather events, such as heavy storms or prolonged droughts, are particularly vulnerable (Waltham et al., 2005).

The potential Void Zone at Oana Crater was meticulously observed to provide detailed insights into its formation. The investigation revealed that changes in heat distribution beneath the crater, particularly from the northwest to the northeast, significantly affected the activity of nearby fumaroles. This redistribution of thermal energy led to the emergence of molten sulfur and heightened fumarole activity.(Oishi, n.d., 2021)

2.4 Geophysical Methods for Potential Void Zone Investigation

Geophysical techniques provide non-invasive means to investigate subsurface conditions and identify potential potential Void Zone-prone zones. Geophysical surveys have been utilized in civil engineering investigations since the late 1920s, starting with seismic and resistivity surveys for dam site studies. Today, these techniques are commonly employed in geological investigations to gather site parameter information. They are effective in identifying areas of concern that are not visible at the surface. Additionally, geophysical methods aid in distinguishing boundaries between residual soils, weathered rock, and fresh rock. These techniques can also pinpoint unusual foundation features such as dykes, cavities, fault zones, and buried river channels.(Eze et al., 2023)

Potential Void Zones often form due to geological and hydrological processes, such as the dissolution of soluble rocks beneath the surface, alterations in groundwater flow, or human activities like over-extraction of water. To study these phenomena, geophysical investigations are employed as non-invasive tools that allow engineers and geologists to analyse the subsurface. These techniques help detect anomalies and provide valuable information without the need for extensive excavation.(Alimohammadi, 2024)

The primary goals of geophysical investigations include identifying the root causes of potential Void Zone formation, such as voids, fractures, or destabilized rock layers resulting from natural

processes or human activity. Additionally, these investigations aim to determine the depth and extent of the affected area, which is essential for assessing the associated risks. Methods like ground-penetrating radar (GPR), electrical resistivity tomography (ERT), and seismic refraction are commonly used for this purpose. Based on the findings, experts can recommend appropriate mitigation measures, such as filling voids with grout, stabilizing soils, redirecting water flow, or reinforcing structures to minimize further damage and enhance safety.(Alimohammadi, 2024)

Potential Void Zones are a global phenomenon which can have devastating consequences. There are many different causes, but all are based on the overburden's soil pressures. The pressures increase to a breaking point where then the overburden material, the material above an underground cavity, falls into the cavity, leaving in many cases a conical shape and circular ground opening.(Lamb & Shiau, n.d.)

2.4.1 Electrical Resistivity Tomography (ERT)

Electrical Resistivity Tomography (ERT) has emerged as one of the most widely used and accessible geophysical techniques in geotechnical and environmental research. Its popularity stems from its efficiency in subsurface investigations and its ability to adapt to challenging terrains, including mountainous regions. By employing various electrode configurations, ERT not only accelerates measurement processes but also provides high-resolution data on subsurface characteristics. This non-invasive method is particularly effective in analysing key geophysical parameters, such as structural stability, moisture content, and the composition of subsurface fluids, making it a highly sensitive and versatile tool for diverse applications.(Alam et al., 2024)

Electrical Resistivity Tomography (ERT) is an advanced subsurface imaging method that collects numerous data points to generate a two-dimensional, either grayscale or color-coded, representation of underground conditions. In recent years, this method has significantly evolved beyond traditional resistivity sounding techniques. It now offers the ability to detect changes in both horizontal and vertical soil structures across a considerable area, providing detailed insights into subsurface variations(Alam et al., 2024)

An extensively utilized non-invasive geophysical technique for examining subsurface properties is electrical resistivity tomography (ERT). By reconstructing the electrical resistivity (ER) data distribution beneath the acquisition line, this method offers comprehensive insights.

To describe both horizontal and vertical fluctuations in ER, ERT integrates a number of electrical techniques. (Jabrane et al., 2023)

In karst areas, cracks and joints that weaken the earth frequently cause operational and safety issues related to potential Void Zone subsidence. Advanced indirect subsurface exploration techniques must be added to traditional methods like geological mapping and geotechnical drilling in order to adequately define these structures. In this study, the two-dimensional and three-dimensional geometry of sediment-filled potential Void Zones created by the interaction of fractures and joints in karst terrains is analysed using near-surface geophysical techniques, specifically Electrical Resistivity Tomography (ERT) and Seismic Refraction Tomography (SRT).(Jabrane et al., 2023)

The electrical resistivity method essentially involves injecting a high-voltage Direct Current (DC) into the ground through two current electrodes, C1 and C2, placed at a specific distance apart. The deeper the current penetrates, the greater the distance between the electrodes. This generates electrical currents in the ground, which in turn create electrical voltage. This voltage is measured using potential electrodes, P1 and P2, which are positioned closer together than the current electrodes. As the distance between C1 and C2 is adjusted, the potential difference measured by the potential electrodes will vary based on the type of rock or soil at the survey location.(Listanti et al., 2018)

The Electrical Resistivity Tomography (ERT) technique measures the potential difference generated when a known electrical current is injected into the ground. Variations in the electrical resistance of subsurface materials arise due to differences in material properties, such as fracture density, composition, and saturation levels. This process involves the use of four metal electrodes: two for injecting the current and two for detecting the resulting potential difference(Hussain et al., 2020).

The ERT observations were carried out using the modern state of the art Advanced Geophysical Instruments (AGI), Superstring R1/IP electrical resistivity unit, USA. Supersting is a portable IP/RES unit which is widely applied for Resistivity and Induced polarization surveys.

The 2D Electrical Tomography (ERT) survey was conducted using Wenner array. The field observations were made every 5m interval to get detail information and meet the target depth

15- 20m. Electrodes were laid out in a straight line using a constant spacing (a=5m) between adjacent electrodes. After completing the sequence measurement with the minimum spacing "a" (5m in our case) then the next sequence of measurement was carried out with "2a" which is 20m. The same process is repeated with "3a", "4a", 5a up to 7a. The data with increased spacing enables deeper investigations. Moreover, to get the best results, the measurements in the field survey were carried out in a systematic manner, so that, high quality data are obtained(Underwood, 2009).

The 2D-electrical imaging resistivity data were processed using a Geo-electrical Imaging 2D & 3D, Geotomo software. The program makes use of the least- squares method based on a quasi- Newton optimization technique (Loke and Baker 1996a). The two-dimensional modelling approach employed in this software represents the subsurface as a grid of rectangular elements. It then estimates the resistivity of each block in a way that the resulting apparent resistivity pseudo section closely matches the observed field data. The optimization algorithm works by minimizing discrepancies between the simulated and actual apparent resistivity

values through iterative adjustments to the resistivity values assigned to each block. The effectiveness of this process is quantified using the root-mean-square (RMS) error, which indicates how well the model replicates the measured data(Sulaiman et al., 2022).

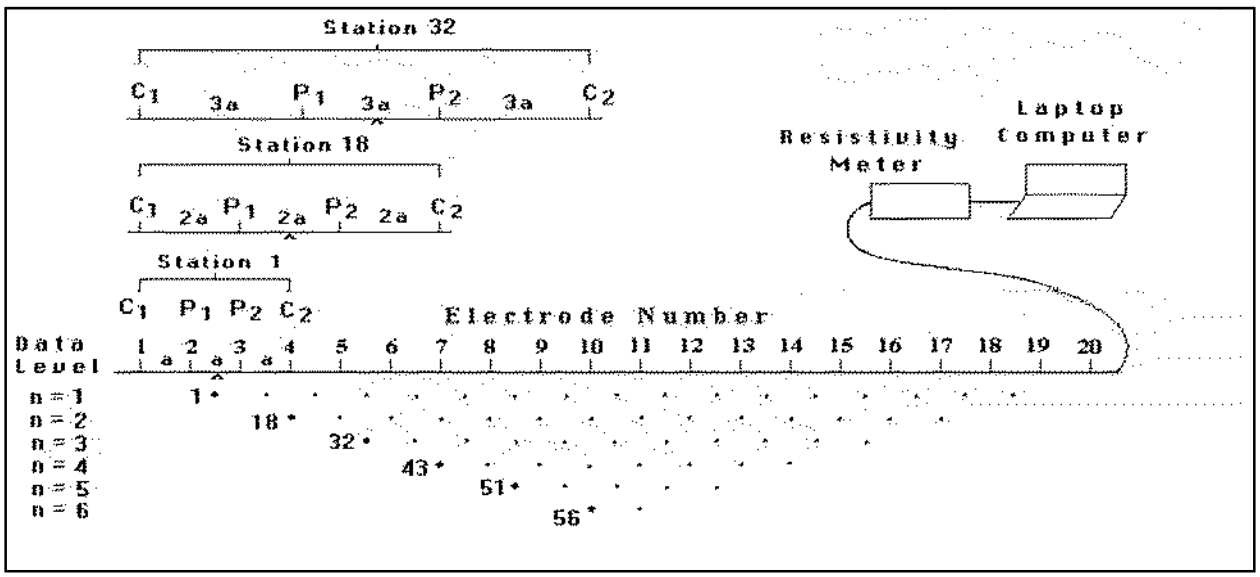

Figure 2-1: Sequence of Measurements to Build up a Pseudo-Section

2.4.2Ground Penetrating Radar (GPR)

GPR examines shallow subsurface features using high-frequency electromagnetic radiation. It is effective in detecting shallow voids and fractures but may be limited by the presence of highly conductive soils(Alam et al., 2024).

Depending on the antenna and local soil properties, Ground Penetrating Radar (GPR) provides the best resolution of all the geophysical methods. This technique sends electromagnetic waves into the earth at various frequencies to produce a subsurface picture. Energy waves emitted by the antenna interact with subsurface materials. The waves are either absorbed or reflected, depending on the characteristics of these materials, such as voids, cracks, moisture content, or clay composition.(Hussain et al., 2020)

The reflected energy is captured by a receiver, which helps construct detailed images of the subsurface. The radar pulse amplitude plays a crucial role in this process, as it carries information about the ground's properties. After converting the travel time of the waves into depth, these amplitudes are used to map subsurface discontinuities. Higher contrasts at material interfaces generate stronger amplitudes, while weaker contrasts result in lower amplitudes. Radar stratigraphy is employed to interpret these reflections, analysing patterns caused by variations in soil and lithological properties. Factors such as grain composition, size, shape, orientation, packing, sorting, and porosity influence the radar reflections, providing detailed insights into subsurface structures and material properties.(Jabrane et al., 2023)

2.4.3Seismic Refraction Tomography (SRT)

SRT uses seismic wave propagation to determine the stiffness of subsurface materials. Potential Void Zone-prone locations frequently have low seismic velocities, which correspond to lose or water-saturated materials. (Jabrane et al., 2023).

Finding the seams and fractures that weaken the earth is the first step in addressing operational and safety issues associated with potential Void Zone subsidence in karst regions. Indirect subsurface exploration methods must be used in addition to geotechnical boreholes and geological mapping in order to describe such structures. This work aims to determine the 2D and 3D geometry of sediment-infilled potential Void Zones formed by the combination of fractures and joints in karst settings using near-surface geophysical techniques including seismic refraction tomography (SRT) and electrical resistivity tomography (ERT). (Jabrane et al., 2023)

Seismic Refraction Tomography (SRT) is a geophysical method for determining the mechanical characteristics of subsurface materials by monitoring seismic wave propagation. The technique entails creating ground vibrations and then monitoring the speed and behaviour of the ensuing waves. It focuses on compression waves, or P-waves, which refract at layer boundaries in the subsurface. The velocity of these P-waves (VP) is calculated by tracking their initial arrivals following direct wave events. Geophones measure travel times, which are then utilized to infer underlying structures. (Jabrane et al., 2023)

The data gathering system used in this method is often modern equipment such as the SUMMIT II Compact, a 24-channel system housed in a sturdy metal enclosure. Plug & Trace technology is used in this system, which makes setup easier and guarantees effective functioning even under challenging conditions. A pseudo-2D processing technique may generate artefacts in places with significant lateral velocity changes. Rayfract is a software that reconstructs the travel routes of the refracted waves to build 2D models of VP.(Jabrane et al., 2023)

The system comprises a manual process for determining the arrival times of P-waves, known as first breaks, for each geophone and shot. Forward modelling approaches, such as finite difference methods, are used to simulate travel times and wave patterns, allowing for iterative modifications to align observed and forecast data. To improve modelling accuracy, the Wave Path Eikonal Travel Time Inversion (WET) method is used, which employs "fat rays" or Fresnel volumes rather than standard "thin rays." This technique compensates for wave dispersion and energy transmission, delivering more realistic subsurface velocity distributions and lowering resolution loss over longer distances.(Jabrane et al., 2023)

The SmartSeis system from Geometrix in the United States was used for the seismic refraction survey. This 24-channel seismograph, outfitted with cutting-edge hardware and software, was linked to a plotter for accurate data display. Geophones with a natural frequency of 10Hz, equipped with dampening resistors and standard sensitivity and receptivity, were used to receive wave signals. A 7kg sledgehammer was used as the energy source.(Underwood, 2009)

A high-resolution seismic data gathering approach with seven shots per spread was used, resulting in high-quality data up to a depth of 40 meters. There were four sorts of shots: direct, three centrals, reverse, and both direct and reverse offset shots. Shot points were set at 25-meter intervals. Furthermore, two consecutive spreads were overlapped using four geophones and an in-line profiling survey technique. The spacing and geometry details are illustrated in Figure 2-2, and the project parameters are summarized in Table 2-1.

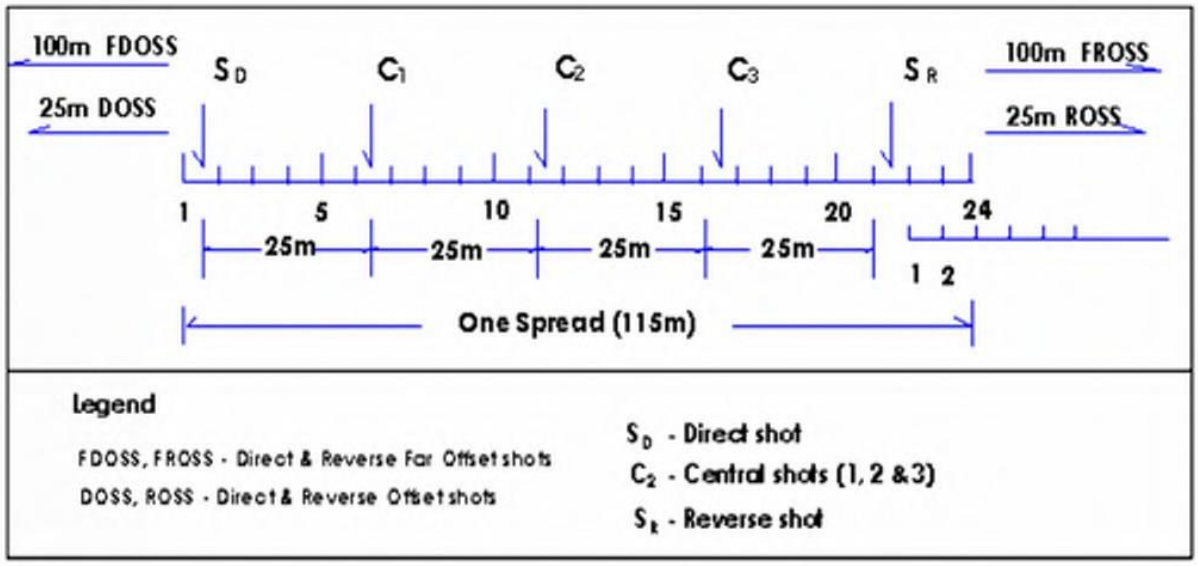

Figure 2-2: Geometry of Refraction Seismic Shooting (5m Geophone Spacing)

Description	Type/magnitude
Energy source	Sledge Hammer
Geophone distance	5m
Length of spread	115m
Shot position	-22.5, 2.5, 27,5, 52.5, 77.5, 102.5, 127.5…
Recording Time	128ms – 512ms
Sampling	0.125
Filtering	Open
Amplification	Auto trace (mostly)

Table 2-1: Parameters of refraction seismic used during fieldwork

2.5 Geotechnical Techniques

2.5.1 Soil Testing

soil testing for potential Void Zone identification often requires the integration of multiple geophysical and geotechnical methods, each providing unique insights into subsurface conditions. By combining tests like DCP, ERT, and SRT, engineers can obtain a thorough understanding of the ground's behaviour, which is essential for preventing potential Void Zone-related damage. These tests, while individually useful, offer enhanced results when used together, ensuring more reliable identification of potential Void Zone risks in diverse environments.

Geotechnical engineering, a specialized branch of geology and civil engineering, focuses on the engineering properties and behaviour of earth materials. The main goals of soil investigations in this field are to examine the geological condition of the soil and to provide construction recommendations and design criteria. This process typically involves drilling and sampling at the study site. The collected soil samples are then analysed for various geotechnical parameters.(Temitope & Blessing, 2024)

A critical aspect of geotechnical analysis is the Atterberg tests, conducted in standard engineering geology laboratories. These tests determine the plastic limit, liquid limit, plasticity index, and grain size distribution of soil samples. The plastic and liquid limits, collectively known as consistency limits, are observed to assess the plasticity of the soil using a plasticity chart. The Atterberg limits serve as fundamental measures of the characteristics of fine-grained soil.(Temitope & Blessing, 2024)

Depending on its water content, soil can exist in four states: solid, semi-solid, plastic, and liquid. Each state corresponds to different soil behaviours and engineering properties. The boundaries between these states are defined by changes in soil behaviour. The Atterberg limits help distinguish between silt and clay soils(Temitope & Blessing, 2024).

2.5.2 Dynamic Cone Penetration Test (DCP)

A range of methods are used in soil testing to evaluate the behaviour and structural integrity of subsurface materials in order to identify potential Void Zones. The Dynamic Cone Penetration Test (DCP) is one of these techniques that is particularly useful for assessing the soil's strength and compaction(Civil Concept, 2023).

The DCP works by driving a conical tip into the ground through the force of a hammer, with penetration depth recorded after a set number of blows. The rate of penetration can provide an indication of soil strength, as loose or fractured soils tend to show higher penetration rates, which may be a sign of areas vulnerable to potential Void Zone formation. The test is also relatively quick, inexpensive, and can be performed in areas where access may be limited. This makes it especially useful for detecting weak zones in karst terrains where potential Void Zones are more likely to occur(Civil Concept, 2023).

The DCP test is frequently used alongside other geotechnical and geophysical testing methods to provide a more comprehensive understanding of subsurface conditions. Seismic refraction tomography (SRT) and electrical resistivity tomography (ERT), for example, can be combined

with DCP to identify voids, fractures, and variations in material properties beneath the surface. While DCP gives direct insight into the soil's compaction and resistance, ERT can help map the extent of moisture and mineral content in the soil, and SRT can reveal variations in material stiffness, both of which are critical in identifying areas of potential instability(Civil Concept, 2023).

2.6 Mitigation and Risk Management

Detecting subsurface cavities will help engineers identify their location and take appropriate precautions when dealing with them. These subterranean cavities promote surface sinking and collapse, resulting in the formation of potential Void Zones. Thus, determining the location of these cavities is the first step in resolving the issue. In general, cavity locations are unavailable since they are not recorded in databases or geographical maps. Various technologies, such as electromagnetic and seismic methods, were efficient in locating these voids(Al-Shaqsi, n.d.2019).

Knowledge about potential Void Zones helps to alleviate many of the problems associated with their occurrence. Understanding the nature of karst, dissolution and potential Void Zones, subsidence, and the hazards and risks associated with these natural phenomena causes people to contemplate the gravity of the situation. This knowledge influences their conduct in dealing with issues, causing them to be more mindful of the impacts, causes, and consequences. Their conduct will include reducing behaviours that may produce potential Void Zones, following proper processes before construction work begins, and understanding the best methods and actions required to manage them. These practical efforts reduce the occurrence of potential Void Zones , the expense of damage restoration, and environmental degradation(Al-Shaqsi, n.d.2019).

Mitigating potential Void Zone risks necessitates a complex strategy that includes geotechnical study, engineering solutions, and policy frameworks. Combining these aspects can lower the risk of potential Void Zones arising while also minimizing their impact on infrastructure and public safety. The following are important measures for effective potential Void Zone mitigation:

2.6.1Ground Stabilization

Ground stabilization procedures are critical for improving subsurface integrity in areas prone to potential Void Zone formation. Soil grouting, which includes injecting a cementitious or chemical grout into the ground to fill voids and consolidate loose soils, is a common way of preventing potential Void Zones. Compaction methods, which involve compacting soil to increase its density and load-bearing capacity, are also critical for reducing ground instability. These treatments harden the earth, making it more resistant to subsurface vibrations that could result in potential Void Zones (Alimohammadi & Memon, 2024).

2.6.2Drainage Improvements

Effective drainage systems are critical for reducing potential Void Zone risks, particularly in areas where water infiltration speeds up erosion or undermines ground stability. Proper drainage management diverts excess water away from sensitive soil and rock formations, reducing the risk of erosion, which can weaken the ground structure. Installing well-designed stormwater drainage systems can significantly reduce water accumulation in high-risk areas, ensuring that surface runoff does not exacerbate potential Void Zone formation. By controlling water flow and preventing excess moisture from penetrating the soil, the potential for potential Void Zones to develop is greatly reduced. Treatment design features enhance the effectiveness of a control. During the construction process, construction staff should stabilize the upland soils of an infiltration basin to ensure that it does not become clogged with sediment(Wisconsin Department of Natural Resources, 2004).

Infiltration basins are large-scale facilities that have long been utilized by municipalities and site developers for both quantity and quality management. They are possible in several parts of the nation, especially in areas with sandy soils. When addressing an excessively large drainage area, infiltration basins often have significant failure rates. Generally speaking, they work best in places with relatively little drainage. Although fewer than five acres is preferable, under the correct circumstances, less than ten acres may be acceptable(Wisconsin Department of Natural Resources, 2004).

The most crucial element in determining the location of infiltration basins is the soil. For the basin to be able to absorb rainwater rapidly enough, the soils should be very permeable.

Groundwater pollution may result from soils that permeate too quickly because they may not offer enough treatment. It is recommended that the infiltration rate be between 0.5 and 3 inches per hour. Furthermore, the soils should have less than 40 percent silt/clay and no more than 20 percent clay(Wisconsin Department of Natural Resources, 2004).

2.6.3Monitoring Systems

Installing monitoring systems is an important proactive measure in potential Void Zone risk management. Groundwater levels and subsurface movements can be monitored using a variety of sensors, such as piezometers to measure water pressure and geophysical sensors to detect ground shifts. These monitoring systems provide early warnings of potential potential Void Zone activity by detecting changes in subsurface conditions, such as fluctuating groundwater levels or unusual shifts in soil or rock. Real-time data from these systems can be used to trigger alerts, enabling timely interventions to prevent potential Void Zone formation and protect both people and infrastructure(Hyun Nam et al., 2018).

It is a multidisciplinary undertaking to conduct a thorough evaluation of potential Void Zone risk and susceptibility at the regional or site-specific level. In addition to geotechnical and hydrogeological factors that affect the location and timing of potential Void Zones, a thorough risk assessment incorporates property developers, urban planners, and several other fields that are not often included in geoscience operations. But from a geotechnical and hydrogeological perspective, risk in terms of collapse vulnerability is still a crucial component of a site's potential Void Zone assessment(Hyun Nam et al., 2018).

2.6.4Land Use Regulations

Land-use planning aims to decrease the number of disputes and negative environmental repercussions on society and nature. In the first place, land-use planning entails gathering and analysing essential data to enable the development of plans. The ensuing policies are influenced by economic, sociological, and political factors, as well as perceptions of the situation. As previously said, land use planning is a political process, with decisions typically made at various levels of government, depending on the project, after recommendations from professional officers. The planner gives recommendations on planning proposals, but when a specialty area is involved, the recommendations are only as good as the advice provided by a professional in geological context.(Bell, n.d.,2023)

Implementing land use rules based on detailed potential Void Zone risk assessments is an important technique for long-term potential Void Zone control. Geological and hydrological zoning restrictions can limit development in potential Void Zone-prone areas. Authorities can lessen the risk of potential Void Zones for persons and property by banning construction in high-risk zones. Risk maps developed by geological surveys and risk assessments can help guide urban planning and development decisions, ensuring that new infrastructure is placed in safer areas. This preventive technique lessens the likelihood of potential Void Zones interrupting urban areas and minimizes the expenses of damage and restoration(Bell, n.d.,2023).

2.6.5Policyand Public Awareness

Beyond engineering and regulatory measures, effective potential Void Zone risk reduction requires raising public awareness and implementing regulations. Public education campaigns can educate communities and businesses in potential Void Zone-prone locations about the warning indications of potential Void Zone activity, emergency preparedness, and safety practices. Furthermore, policies that encourage regular inspections of infrastructure, particularly roads and buildings in hazardous regions, can aid in the identification of early warning signals and the prevention of catastrophic potential Void Zone incidents. Collaboration among government agencies, engineers, and the general public ensures that potential Void Zone risk management techniques are well understood and supported (Bell, n.d.,2023).

2.7 Research Gap

Despite extensive research on potential Void Zone formation and its impacts, critical gaps remain, particularly concerning the Adama-Awash Express Road in Ethiopia. While global studies have provided valuable insights into potential Void Zone mechanisms and hazard assessment localized investigations focusing on the unique geological, hydrological, and climatic conditions of the Adama-Awash region are lacking. The geological and hydrological context of Ethiopia—characterized by volcanic rocks, basaltic plateaus, and varying groundwater dynamics—presents specific challenges that need to be explored in more detail. Local studies are essential to better understand the interaction between these factors and potential Void Zone development in the Ethiopian context, as most global research does not address the region's specific conditions(Zaminkar & Fotohi, 2020).

Furthermore, while studies on potential Void Zone formation emphasize the role of soil properties such as composition, structure, permeability, and moisture content(Hope & Marsellos, 2024b), the relationship between these factors and potential Void Zone susceptibility in the Ethiopian context remains underexplored. For example, variations in soil moisture content and its interaction with seasonal rainfall patterns are critical but often overlooked in many studies(Abdulbariu Ibrahim et al., 2024). Detailed research on soil characteristics—particularly in relation to groundwater fluctuation and seasonal moisture—could significantly improve potential Void Zone hazard assessments in the region.

Additionally, most research on potential Void Zones tends to focus on static geological conditions, often overlooking the dynamic factors, such as fluctuating groundwater levels and seasonal changes, that influence subsurface stability(Soltanpour et al., 2023). While there is significant understanding of how geology contributes to potential Void Zone formation, groundwater dynamics and seasonal moisture variations have not been adequately considered in the context of dynamic potential Void Zone hazard assessments. This gap calls for comprehensive research that evaluates both static geological and dynamic hydrological factors in influencing ground stability, particularly along major infrastructure routes such as the Adama-Awash Express Road.

The effectiveness of potential Void Zone mitigation strategies specific to the Adama-Awash corridor also remains underexplored. Much of the current research focuses on generic mitigation methods such as grouting, ground stabilization, and drainage improvements(Ha, 2024), with little attention paid to the unique geological and hydrological conditions of Ethiopian roads. Localized mitigation strategies, including advanced geotechnical techniques and geophysical methods, need further exploration for their application to Ethiopia's specific subsurface conditions. In subsurface characterisation for potential Void Zone identification, methods including Ground Penetrating Radar (GPR), Seismic Refraction Tomography (SRT), and Electrical Resistivity Tomography (ERT) have shown promise. (Ibrahim et al., 2024), but these methods have been underutilized in the context of Ethiopian infrastructure and potential Void Zone risk mitigation.

Finally, there remains a pressing need to bridge the gap between scientific research and actionable policy recommendations. While much of the existing research on potential Void Zone management offers theoretical insights(Aziz et al., 2024), effective land-use planning and policy development based on localized, data-driven studies remain underdeveloped. There is a

need for updated policy frameworks that incorporate findings from recent potential Void Zone studies and integrate them into practical guidelines for infrastructure development and zoning in potential Void Zone-prone areas. By incorporating the latest scientific data on potential Void Zone risk factors, such as those identified in recent studies on groundwater modelling and dynamic subsurface monitoring(Ahmad et al., 2022), it will be possible to create more resilient infrastructure and more informed land-use regulations.

Addressing these gaps will not only advance the understanding of potential Void Zone formation along the Adama-Awash Express Road but will also contribute to the development of more effective prediction models and mitigation strategies tailored to Ethiopia's specific needs. A multidisciplinary approach, combining geological, hydrological, geotechnical, and policy-based research, is essential for reducing potential Void Zone-related risks and enhancing the resilience of infrastructure in the region.

CHAPTER 3

MATERIALS AND METHODS

3.1 Introduction

This chapter provides a thorough explanation of the technique used in the inquiry. It includes the materials, methods, and processes used to ensure that the research objectives are satisfied successfully. The methodology is organized systematically to address the study's general and specialized objectives, with a clear description of the processes carried out throughout each phase of the research.

The research begins with a thorough desk review, which serves as the investigation's foundation. This step entails collecting and analysing existing data, maps, and past studies pertinent to the study area. The desk study was followed by rigorous field investigations aiming at gathering first-hand evidence and validating the conclusions of the original evaluation. These investigations were intended to capture the study region's unique characteristics, with a special emphasis on its geological, geotechnical, and geophysical elements.

Defining the study region and maintaining appropriate sample procedures were crucial. The establishment of sample size and preparation processes were critical steps in obtaining trustworthy and representative datasets. Samples were carefully collected to illustrate the variety of subsurface conditions across the study area, with an emphasis on weak and collapsible formations that lead to potential Void Zone formation.

To reinforce the analytical framework, a variety of geotechnical and sophisticated geophysical testing methodologies were used. These tests were conducted according to internationally accepted standards established by the American Society of Testing and Materials (ASTM) and the American Association of State Highway and Transportation Officials (AASHTO). Advanced testing techniques enabled detailed characterisation of subsurface formations, allowing for a more comprehensive assessment of the elements driving potential Void Zone formation and seismic risks in the area.

The study's laboratory phase took advantage of the capabilities of several cutting-edge institutions. Testing took place in the Core Consulting Engineers Laboratory, ICT Engineering PVT Central Laboratory in Addis Ababa, Ethiopian Engineering Corporation Laboratory, and KPIL Laboratory. Each facility contributed to distinct areas of the study, ensuring that diverse and specialized knowledge was used in the analysis.

By combining geotechnical and geophysical methodologies, the study provides a comprehensive assessment of potential Void Zone formation mechanisms and subsurface stability. These integrated methodologies provide a comprehensive understanding of the interaction between geological features and seismic activity, which is crucial for guiding engineering design and mitigation strategies in the area.

This methodological chapter establishes the foundation for addressing the various issues posed by the research area's geological and seismic setting. It is designed to assure the dependability and precision of the results while remaining consistent with the research's overall goals. This methodological chapter establishes the foundation for addressing the various issues posed by Geological and seismic characteristics of the research area. It is intended to ensure the dependability and precision of the results while remaining true to the research's overarching objectives. This methodological chapter lays the groundwork for tackling the many difficulties raised by the research area's geological and seismic environment. It is intended to ensure the dependability and precision of the results while remaining true to the research's overarching objectives. This methodological chapter lays the groundwork for tackling the many difficulties raised by the research area's geological and seismic environment. It is intended to ensure the dependability and precision of the results while keeping compatible with the research's overall goals.

3.2. Study Area

The research area is located in the Middle Eastern section of Ethiopia, within the Oromia Region. The principal route spans roughly 60 km and starts at Adama, as indicated by coordinates (E534109 & N944258, E543875 & N956366, and E564352 & N978403) or at the Addis-Adama expressway terminal. The path continues via Welenchiti and ends near Melkajilo Village at 60Km.The region is located in the Ethiopian Rift Valley, a section of the Great East African Rift system that runs from northeast to south of the country. This environment is characterized by various volcanic rock formations, with broad plains overlaid by thick deposits

of residual and silty clay soils generated from rock weathering followed by erosion and deposition processes.

The study area, which focuses on central Ethiopia's complex geological and seismic context, is part of the Nazareth geological map area (NC37-15), as defined by the Geological Survey of Ethiopia. It is made up of several lithological units, including the Nazareth Series, basaltic and ash flows, as well as adjacent formations such as the Bofa Basalt and Dina Formation. The variable stability and erodibility of these units are important factors in potential Void Zone formation.

Moreover, according to the revised Ethiopian Seismic Zoning Map (CES 160-2015), the project area is classified as Zone 4. With Peak Ground Acceleration (PGA) values ranging from 0.1 to 0.115, the combination of seismic activity and the prevalence of weak, collapsible formations introduces a significant risk, necessitating careful engineering and planning.

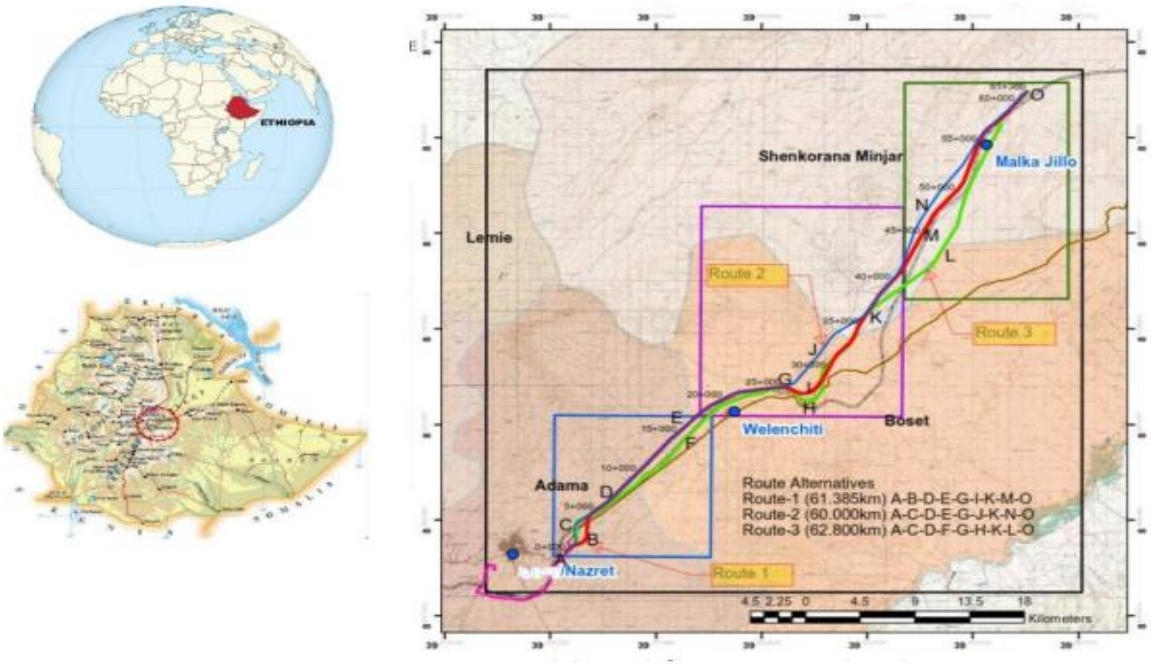

Figure 3-1: Geological Map of the study Area

3.3 Regional Geological Setting

The geological parameters of the project corridor, as indicated in the Geological Map of Nazaret (NC37-15) by the Geological Survey of Ethiopia, reveal a diversified and complicated landscape. This map, scaled at 1:250,000, provides a detailed overview of the region's

geological features, which are critical for understanding the challenges and opportunities associated with the project. The project's alignment is wholly within the scope of this survey, ensuring that the geological data is very relevant and area-specific. The desk research, supplemented by site reconnaissance inspections, enabled a thorough understanding of the geological formations, allowing conclusions to be tailored to local conditions.

Among the principal geological formations influencing the route alignment are volcanic rocks, sedimentary layers, and metamorphic complexes. Volcanic rocks, frequently basaltic in form, are common in the region and are noted for their durability and strength, making them useful for construction needs. However, their presence also suggests a history of volcanic activity, which may bring concerns such as seismic instability. Sandstone, shale, and limestone are common materials found in sedimentary strata. These rocks are more prone to erosion and weathering, necessitating careful planning and execution of the project to assure long-term stability.

Metamorphic complexes, such as schist and gneiss, add to the complexity of the geological landscape. These rocks, created under high pressure and temperature conditions, are generally stable but difficult to excavate and construct due to their hardness and variable nature. The extensive investigations conducted during the site reconnaissance survey provided vital insights into these formations, allowing possible dangers to be identified and mitigation solutions developed. The initiative seeks to strike a balance between development and sustainability by using geological data, engineering, and environmental issues.

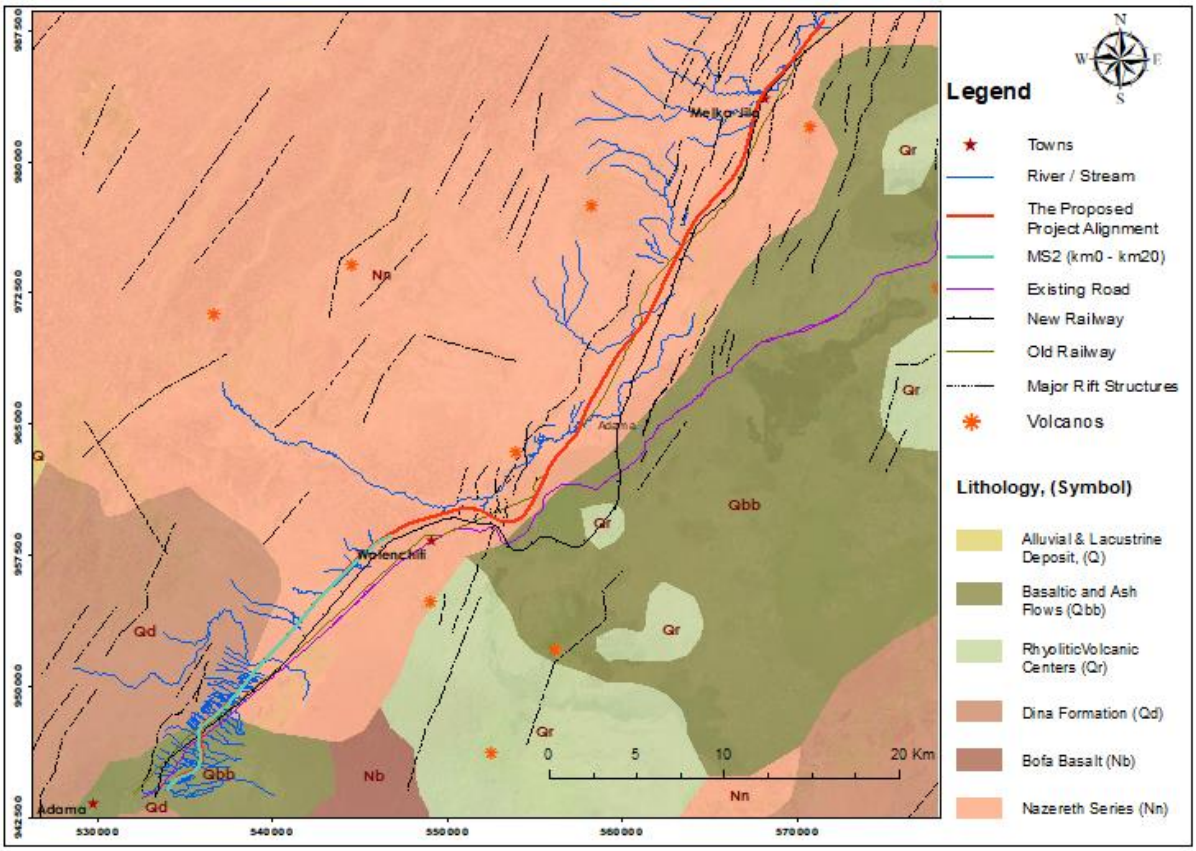

Figure 3-2 lithological Map of the Project Area

(Source: Geological Survey of Ethiopia, Geology of Nazareth Area scale 1:250,000)

3.3.1 Nazareth Series (Nn)

- **Description**: The Nazareth Series represents the oldest and most widespread lithological unit encountered along the corridor. This formation is primarily made up of ignimbrites, unwelded tuffs, and ash flows interspersed with pumice, rhyolitic flows, and trachyte layers.
- **Challenges**: The formation contains alternating layers of low-density ash/pumice, which exhibit low stability, and fractured ignimbrites that are relatively more competent. Additionally, the soils developed from this formation display high erodibility and moderate collapsibility, which pose significant concerns for structural integrity and surface stability.

3.3.2 Basaltic and Ash Flows (Qbb)

- **Description**: Extending through the first 5 km of the proposed alignment, this unit comprises pumice, spattered cones, and pyroclastic materials.
- **Challenges**: The ash and pumice layers in this formation are associated with surface and subsurface erosion, as well as ground fissuring in areas with tectonic weaknesses. These processes contribute to instability and necessitate careful geotechnical design considerations.

3.3.3 Adjacent Geological Formations

Although the Nazareth Series and Basaltic and Ash Flows dominate the route alignment, additional formations occur near the proposed corridor. These include:

- **Bofa Basalt**: Found in the southern section of the region, this formation consists of alkaline basalt that is relatively stable and competent. However, it does not intersect with the project alignment.

- **Dina Formation**: This unit primarily comprises ignimbrites, tuffs, coarse pumice, and water-lain pyroclastic rocks with occasional sediment intercalations. Located southwest of the alignment and underlying the basaltic and ash flow formations, it is prone to collapse and internal erosion when subjected to saturation and tectonic weaknesses.
- **Rhyolitic Volcanic Centres**: Representing volcanic activity in the region, this unit includes obsidian pitchstone, pumice, ignimbrite, tuff, and trachyte flows. These peralkaline materials are associated with volcanic vents and buried volcanic edifices, adding to the geological complexity near the project area.

  The project area is located in Central Ethiopia, which has been extensively studied for seismic risks due to its position within the East African Rift System. According to the **revised Compulsory Ethiopian Standard (CES) 160–2015**, Ethiopia is divided into five seismic zones (0–5), each with varying levels of seismic activity. Based on this classification, the project site lies in **Zone 4**, characterized by a Peak Ground Acceleration (PGA) range of **0.1 to 0.115**.

- **Seismic Implications**: This classification places the project in a moderately high-risk seismic region. The combination of active tectonics, weak subsurface formations, and potential ground fissures underscores the need for detailed seismic risk assessments and resilient engineering designs.
- **Data Sources**: Seismic maps and historical earthquake data were reviewed to gain a comprehensive understanding of regional seismicity and its implications on the structural stability of the project corridor.

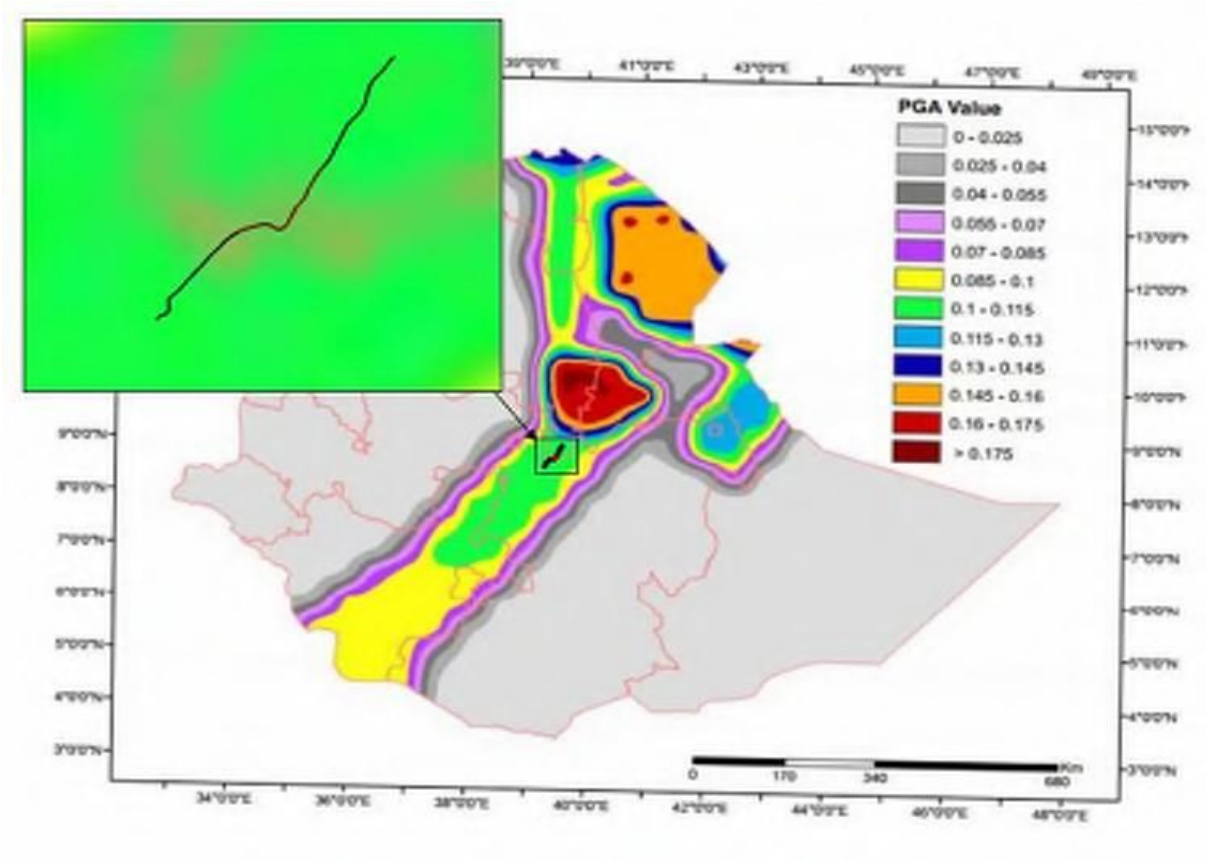

Figure 3-3: Seismic Hazard Map of Project Area

3.3.4 Rainfall

Rainfall data from the Meteorological Agency of Ethiopia at stations in Nazareth over a 35-year period (1981-2016) shows that the average maximum rainfall between July through September is between 100 and 220 millimetres. The months of November through January have the least amount of rainfall, which ranges from 5 to 10 mm. In the project region, the rainy

season begins in June and lasts until the end of September. Rainfall in the project region averages 828 mm per year.

Based on available meteorological data, the average monthly rainfall in the project area is summarized in Table 3-1 and Figure 3-4

Month	Jan.	Feb	Mar	Apr	May	June	Jul.	Aug.	sept	Oct	Nov	Dec
Rainfall, mm	10	20	50	60	60	63	220	200	100	30	10	5

Table 3-1 Average Monthly Rainfall

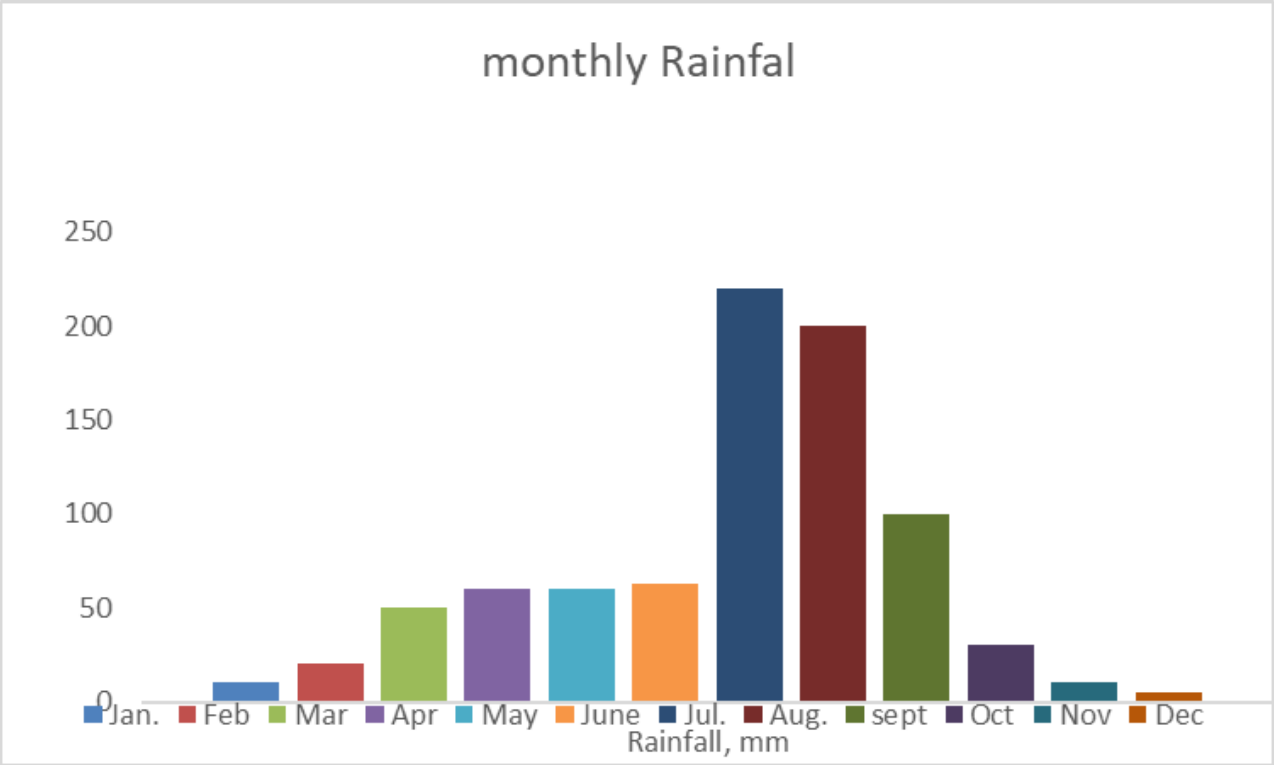

Figure 3-4 Monthly Rainfall (mm); (source NMA Website)

3.3.5 Temperature

For 35 years, from 1981 to 2016, temperature data was collected from stations operated by the Ethiopian Meteorological Agency in Nazareth. The maximum recorded temperature between April and June is 31°C, which is also the highest mean monthly temperature in May. The lowest temperature ever recorded is 10.8°C in December. The project area's average annual temperature is 21.1°C. The average monthly maximum and lowest temperature data are shown in Table 3-2 below.

Month	Jan.	Feb.	Mar.	Apr.	May	June	Jul.	Aug.	Sept.	Oct.	Nov.	Dec.
T. Max, ^{0}C.	27.8	29	30.3	30	31	30.3	27.2	26.8	27.9	27.8	27.2	26.9
T. Min., ^{0}C	11.8	13	14.2	14.9	15.2	15.9	15.2	15	14.5	12.2	11.4	10.8
T. Avg., ^{0}C	19.7	21	22.2	22.4	23.2	23.1	21.1	20.9	21.1	20	19.3	18.9

Table 3-2: Average Max and Min Temperature of the Research Area

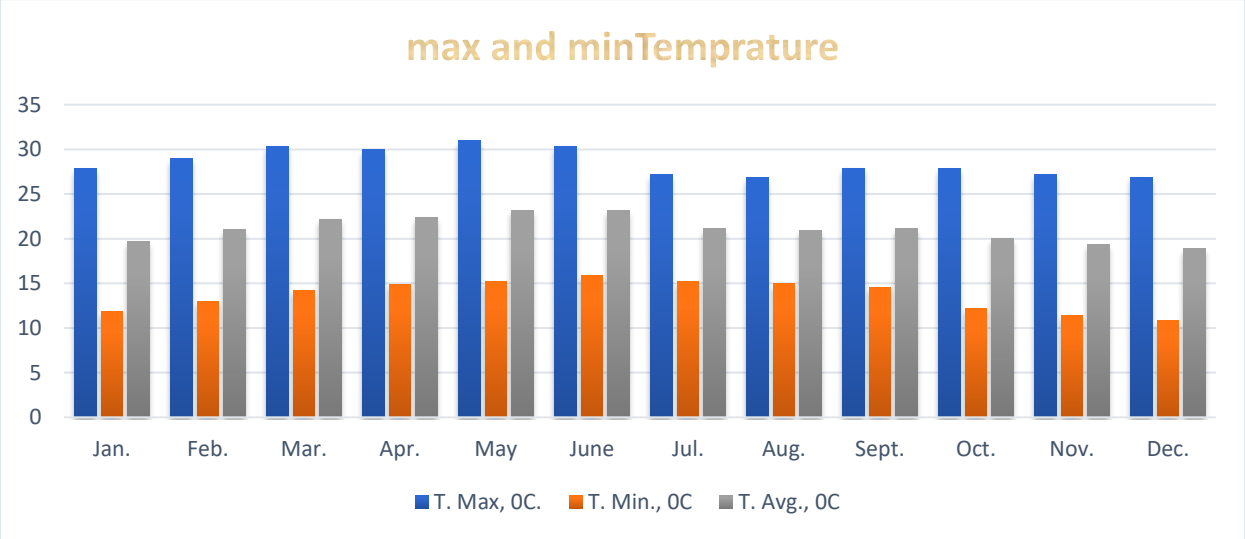

Figure 3-5: Temperatures at the monthly maximum and lowest (0C) (Source: NMA Website)

3.4 Methodological Approach

This research analyses potential Void Zone danger along the Adama-Awash Expressway using a mixed-methods methodology that blends quantitative and qualitative techniques. By integrating numerical data with interpretive interpretation, the study guarantees a comprehensive understanding of subsurface conditions and likely potential Void Zone causes.

Quantitative Methods: Geophysical and geotechnical data must be gathered and analysed as part of the quantitative approach. Subsurface resistivity variations are mapped using Electrical Resistivity Tomography (ERT) scans, which provide details about the geological structure and

likely holes or anomalies that point to potential Void Zone activity. Additionally, soil samples taken from boreholes (105, 106, and 107) are subjected to laboratory tests including Atterberg limits, permeability, CBR, and Proctor compaction in order to evaluate the physical characteristics of the soil along the route. To ascertain the correlation between physical attributes, potential Void Zone occurrence, and potential risk, these data are statistically analysed.

Qualitative Methods: The assessment of geological and geotechnical data in relation to past potential Void Zone incidents in the region is the qualitative component of this study. The geological elements that contribute to potential Void Zone formation may be contextualized by looking at the literature, reports, and records that are currently accessible on potential Void Zone events along the Adama-Awash Expressway. In order to assess the mechanisms behind potential Void Zone development and provide context for the quantitative findings, the study also incorporates expert opinion and observational data from field surveys.

Data Integration and Interpretation: A thorough risk assessment model is produced by combining the data from the two methods. While the qualitative data provide crucial contextual information about local geological conditions and past potential Void Zone patterns, the quantitative data from the ERT and soil testing serve as a baseline for identifying high-risk zones. The creation of mitigating methods for the prevention of potential Void Zones along the roadway is informed by the combined findings. A thorough risk assessment model is produced by combining the data from the two methods. While the qualitative data provide crucial background information regarding local geological conditions and past potential Void Zone patterns, the quantitative data from the ERT and soil testing serve as a baseline for identifying high-risk zones. The combined findings inform the development of mitigating solutions for potential Void Zone prevention along the highway.

3.4.1 study design

Potential Void Zone susceptibility along the Adama–Awash Expressway, especially between chainages 25+060 km and 25+180 km, is investigated using a multidisciplinary, field-based research methodology that combines geophysical, geotechnical, geological, and chemical methodologies. Its goal as an applied research project is to locate and evaluate geotechnical risks related to karst processes in a specific Ethiopian setting. Both direct and indirect inquiry strategies are used in this study.

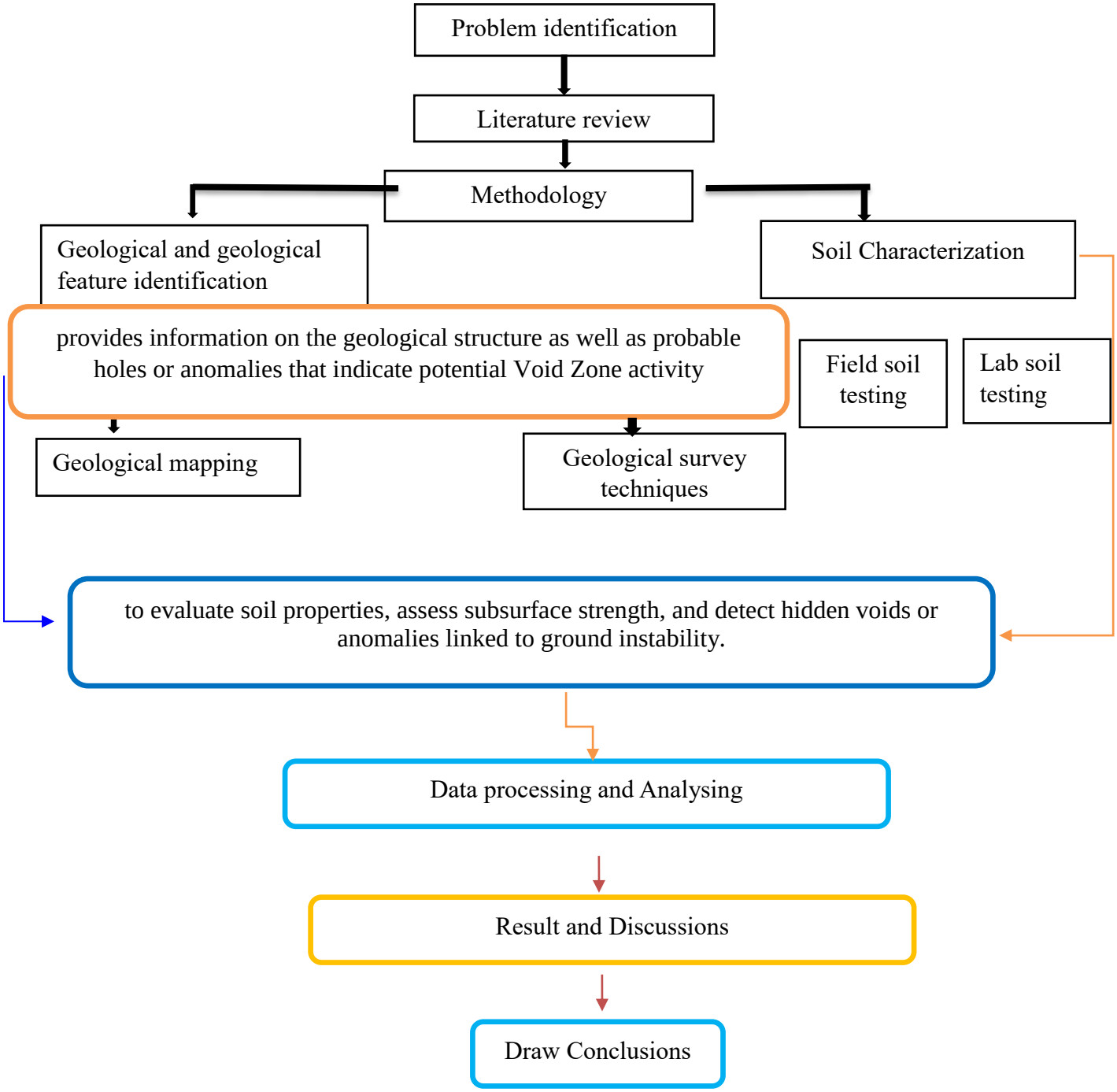

Figure 3-6 Flow chart illustrating the research methodology

3.5 Field Investigation Plan

The electrical resistivity survey is an important geophysical approach for determining the distribution of subsurface resistance using measurements acquired from the ground surface. These data allow for the determination of real resistivity in subsurface materials, which is impacted by a variety of geological parameters such as mineral composition, fluid content, porosity, and water saturation. For decades, the approach has been used extensively in hydrogeological, mining, geotechnical, and environmental engineering research.

Electrical resistivity surveys have recently become more popular in environmental research and site characterization in Environmental Engineering. Their ability to distinguish between fresh and saline groundwater is very useful, as resistivity tests are highly sensitive to conductive subsurface minerals. For this study, Electrical Resistivity Tomography (ERT) and core drilling methods will be used to collect precise subsurface geological data required for the project's basic design stages along the Adama-Awash Express Road.

The approach is based on Ohm's Law, which governs the flow of electricity into the ground. The equation defining Ohm's Law in vector form for current flow in a continuous medium includes the following components:

- **K**: A geometric factor dependent on the arrangement of the four electrodes.
- **R**: Resistance, determined from the measurements.

Geophysical tools like the SAS1000 Tera-meter measure resistance ($R = \Delta V/I$). However, the resistivity value obtained from this measurement is not the genuine resistivity of the subsurface, but rather its "apparent" resistivity. This apparent resistivity depicts a homogeneous subsurface that produces the same resistance value for the given electrode setup.

The inversion problem occurs when deriving the true resistivity distribution from apparent resistivity data, as the relationship between these values is complex. Advanced data processing and interpretation techniques will be used in later stages of this work to tackle the inversion problem and obtain accurate geological information. The inversion problem occurs when deriving the true resistivity distribution from apparent resistivity data, as the relationship between these values is complex. Advanced data processing and interpretation techniques will

be used in later stages of this work to tackle the inversion problem and obtain accurate geological information.

This research aims to improve understanding of subsurface conditions by focusing on potential Void Zone-prone locations and the geophysical signals associated with instability. The analysis will inform technical solutions and mitigation methods for infrastructure development along the expressway.

To estimate the severity, extent, and depth of the potential Void Zone area, the following geophysical studies will be performed:

3.5.1 Geophysical Methods

3.5.2 Seismic Refraction Tomography (SRT)

Geometrics' Smart Seis 24-channel seismograph was used during the seismic refraction survey (USA). This microprocessor-based system contains advanced hardware and software, which are interfaced with a plotter for effective data visualization (see Fig. 3.5). Geophones with a natural frequency of 10 Hz were utilized for signal reception, with dampening resistors added to increase sensitivity and receptivity to standard criteria. A 7-kilogram sledgehammer was used as the energy source for seismic signal creation.

High-Resolution Seismic Data Acquisition

A 7 shots per spread technique was used to enable high-quality data gathering at depths of up to 40 meters. This approach employed several shot types: direct shots, three central shots, reverse shots, direct offset shots, and reverse offset shots. Shot sites were placed at regular 25-meter intervals along the survey lines. Furthermore, two consecutive spreads were overlapped with four geophones to form an in-line profiling survey technique (see Fig. 3.4 for geometry).

Figure 3.4: Smart Seis of Geometrics of USA

Field Parameters

The field parameters used for the seismic refraction survey are presented in Table 3.1.

Description	Type/Magnitude
Energy Source	Sledgehammer
Geophone Distance	5 m
Length of Spread	115 m
Shot Position	-22.5, 2.5, 27.5, 52.5, 77.5, 102.5, 127.5…
Recording Time	128 ms – 512 ms
Sampling Interval	0.125
Filtering	Open
Amplification	Auto trace (mostly)

Table 3.1: Field Parameters for Seismic Refraction Survey

The use of this innovative technology ensured complete coverage and capture of high-resolution seismic data, which is critical for analysing subsurface layering and identifying weak zones connected with the potential Void Zone-prone area.

3.5.3 Electrical Resistivity Tomography (ERT)

Equipment and Setup

The Electrical Resistivity Tomography (ERT) survey was conducted using the **ABEM Tetrameter SAS 1000 resistivity meter**, a Swedish-made device designed for high-precision 2D resistivity imaging. The complete setup included:

- Two **LUND multi-electrode cables**, each with 21 take outs spaced at **5 meters** on the abutments and **20 meters** over the waterbody.
- **Electrode Selector ES10-64**, which facilitated automatic switching between electrodes.
- **21 stainless steel electrodes**, cable-to-electrode jumpers, and connectors.
- A **12V, 70Ah car battery** with an External Battery Adapter (EBA) to power the system.
- **RS232 cable** for data transfer to a laptop for further analysis.

The resistivity meter was programmed to take automatic readings utilizing bespoke protocols and address files, resulting in efficient and precise data collecting. The multi-electrode configuration enabled accurate measurement and analysis of subsurface resistivity. The 2D-electrical imaging resistivity data were analysed with Geo-electrical Imaging 2D & 3D, Geotomo software, August 2004. The program uses the least-squares method, which is based on a quasi-Newton optimization technique (Loke and Baker 1996a). This program's 2-D model separates the subsurface into many rectangular chunks. The resistivity of the rectangular blocks is then determined, resulting in an apparent resistivity pseudo section that is consistent with the actual data. The optimization method essentially attempts to reduce the discrepancy between the calculated and observed apparent resistivity values.

Field Procedure

The ERT survey was intended to supplement the results of the Seismic Refraction Tomography (SRT) survey by giving additional subsurface geological information. The steps are listed below:

Survey Line Preparation:

- The ERT was carried out along the same six survey lines as the SRT, with locations altered in the field based on ground conditions to optimize the effectiveness of potential Void Zone mapping.
- The Lund cables (100m in total length) were put out on the ground or water's surface. To ensure constant coverage, stainless steel electrodes were spaced at 10-meter intervals.

Overlapping Configuration:

- To guarantee seamless data acquisition, Takeout 21 of the first cable and Takeout 1 of the second cable were connected to the same electrode, resulting in an overlapping configuration.

Adaptation for Waterbody Survey:

- Because floating electrodes were unavailable, a static 2D resistivity survey mode was used for underwater profiling. The Lund multi-electrode cable was laid directly on the water's surface, allowing the exposed portion of the cable to conduct current to subsurface formations beneath the waterbed. A early test revealed that the technology gave results comparable to traditional mobile underwater surveys.

Data Collection:

- The WEN32SX electrode arrangement was used, with an inter-electrode spacing of 5m.
- Prior to data capture, a contact resistance test was performed to identify poorly connected electrodes or areas of high resistance. Problematic connections were repaired by reattaching electrodes or applying salt water to increase conductivity.
- To achieve precise and dependable data gathering, parameters such as stacking (2-4 measurements) and current injection (50-200 mA) were specified.
- One electrode position was used to overlap adjacent spreads, allowing for greater continuity and resolution in subsurface imaging.
- Collected data were automatically stored on the instrument and transferred to a laptop using an RS232 cable for further processing and interpretation.

Figure 3.6 Equipment used and field survey set up for ERT Survey

Objectives of the ERT Survey

- Mapping Resistivity Variations: Identifying voids and unstable zones beneath the potential Void Zone.
- Subsurface Characterization: Providing thorough information about the integrity and qualities of subsurface materials.
- Survey parameters
- Inter-Electrode Space: 5m (land) and 20m (waterbody).
- Total Length per Spread: 100m.
- Stacking: 2–4 readings.
- Current Injection Range: 50-200 mA.

The ERT survey supplemented the SRT data by providing new insights into resistivity changes, providing a more complete picture of the potential Void Zone-prone area's geology and geotechnical features. Together, these methodologies improved our understanding of subsurface anomalies and zones of instability, which is crucial for fulfilling the research goals.

This integrated process guarantees that subsurface characteristics are effectively mapped and analysed, providing significant insights for dealing with potential Void Zone concerns and establishing educated mitigation methods.

Integration of Methods

Both geophysical methods were implemented along six lines each, ensuring comprehensive coverage of the project area. The use of SRT and ERT together provided complementary datasets, enabling a thorough understanding of subsurface conditions. The coordinates and lengths of all survey lines are detailed in Table 3.2.

No.	Geophysical lines	Length of profile	Survey method	UTM Coordinates			
				Start		End	
				Easting (m)	Northing (m)	Easting (m)	Northing (m)
1	Line-L-1	230	ERT	551511	959956	551730	959889
2	Line-L-2	230	ERT	551513	959963	551732	959896
3	Line-L-3	230	ERT	551514	959968	551739	959899
4	Line-L-4	230	ERT	551515	959973	551741	959904
5	Line-L-5	230	ERT	551517	959979	551738	959912
6	Line-L-6	230	ERT	551523	960004	551747	959936
7	Line-L-1	240	SRT	551511	959956	551739	959886
8	Line-L-2	240	SRT	551513	959963	551742	959893
9	Line-L-3	240	SRT	551514	959968	551744	959897
7	Line-L-41	240	SRT	551515	959973	551745	959902
8	Line-L-5	240	SRT	551517	959979	551748	959908
9	Line-L-6	240	SRT	551523	960004	551757	959932

Table 3.2: UTM Coordinates (Datum Adindan, zone 37N) of Geophysical survey lines

To provide a full subsurface characterization, geophysical investigations were carried out along six survey lines utilizing both Seismic Refraction Tomography (SRT) and Electrical Resistivity Tomography (ERT). The combination of both methodologies produced complementary datasets, which improved the accuracy and reliability of subsurface interpretations. Each approach was used on six profiles to guarantee enough spatial coverage of the study area. The survey lines were designed consistently, with ERT profiles extending 230 meters and SRT profiles reaching 240 meters. The coordinates were referenced using the Universal Transverse

Mercator (UTM) coordinate system, which is based on the Adin dan datum and Zone 37N. This organized geophysical survey approach ensures a thorough analysis of subsurface conditions, allowing for the identification of significant geological features pertinent to the study.

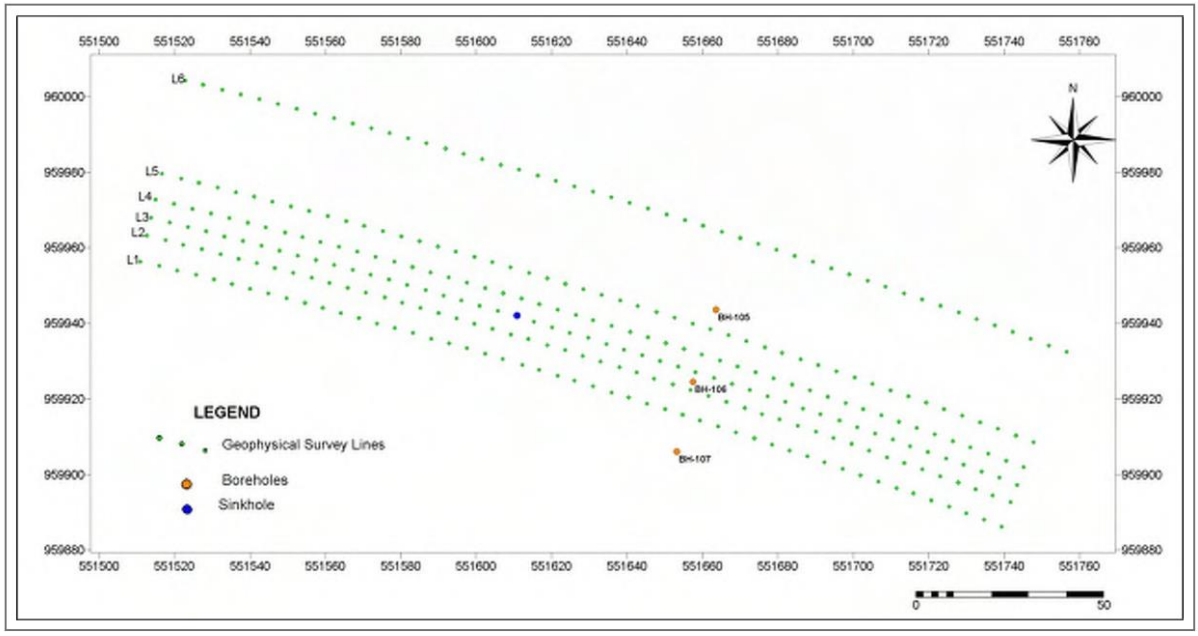

Figure 3-7: Geophysics Survey Lines

3.6: Sample Collection

To achieve a thorough understanding of the subsurface conditions in potential Void Zone-prone locations, a well-structured and systematic soil sampling strategy was developed. This methodology is critical for precisely identifying the geological, geotechnical, and hydrogeological elements that contribute to potential Void Zone development. The approach entails collecting soil samples at numerous depths to capture differences in material qualities across stratigraphic levels. By collecting samples at various depths, the study can identify crucial subsurface layers that may impact potential Void Zone formation, such as loose or weak zones, highly compressible soils, or moisture-sensitive materials prone to erosion or subsidence.

Geophysical survey data are used to influence the selection of sampling spots, which improves sample collection precision. Seismic Refraction Tomography (SRT) and Electrical Resistivity Tomography (ERT) offer detailed subsurface imaging, exposing abnormalities such as high porosity zones, moisture accumulations, and weak soil layers. This data-driven method guarantees that sampling is concentrated in regions of interest, increasing the usefulness of

obtained data for potential Void Zone investigation. Furthermore, samples will be collected from both unstable and stable areas to allow for comparison investigations, resulting in a better knowledge of the changes in material behaviour under different settings.

The appropriate sample techniques will be used based on the depth and soil type. Augers will be employed for shallow soil sampling, resulting in little disruption to the natural structure of loose sediments. Coring tools built exclusively for soil extraction will be used to collect samples from lower stratigraphic layers while conserving their in-situ properties. Proper handling and storage in airtight containers will be used to avoid changes in moisture content and chemical composition, which could compromise test findings. The gathered samples will be divided into two types: undisturbed and disturbed, based on the laboratory procedures they will undergo. Undisturbed samples are necessary for advanced geotechnical testing, including permeability, compaction, and strength analysis, as these qualities play an important role in soil stability and potential Void Zone susceptibility.

Following collecting, the samples will go through a battery of laboratory tests to determine their physical, mechanical, and chemical qualities. These tests will provide information about soil strength, permeability, porosity, and mineral composition, all of which are important elements determining potential Void Zone development. The combination of laboratory results and geophysical survey data will allow for a more comprehensive assessment of subsurface conditions, resulting in a better understanding of the mechanisms that drive potential Void Zone formation in the research area.

- Several typical images were obtained to visually illustrate the characteristics of potential Void Zone-prone locations. These photos provide vital insights into the surface manifestations of subsurface instability and serve as supporting evidence for geophysical survey results and soil sampling data. The photos illustrate significant geological and geotechnical features, such as surface deformation, fissures, soil erosion, and active ground settlement, which are critical for understanding the mechanisms that cause potential Void Zone development. The first set of photographs shows a well-developed potential Void Zone with a nearly round form and sheer vertical sides. The visual qualities observed are:

- **Steep and Exposed Walls:** The potential Void Zone exhibits nearly vertical walls, exposing stratified soil layers. This suggests a sudden collapse, possibly due to subsurface voids or weakened soil structure.
- **Cracked and Eroded Base:** The bottom of the potential Void Zone contains a cracked surface, indicating previous water accumulation and subsequent drying. The presence of sediment deposits suggests active erosional processes.
- **Loose and Displaced Soil Fragments:** Large chunks of soil and rock fragments are scattered within the potential Void Zone, showing signs of mechanical failure and progressive collapse.
- **Surface Instability Indicators:** The jagged edges and overhanging sections of the rim indicate ongoing erosion, increasing the risk of further expansion.

These characteristics provide important information about the nature of potential Void Zone collapse, emphasizing the significance of geophysical and geotechnical investigations for risk assessment. Another collection of pictures shows widespread ground fractures and surface deformations in a potential Void Zone-prone location. The main observations from these photos are:

- Irregular and Extended Surface Cracking: Deep and persistent fissures indicate unequal settlement and underlying weakness. These fractures are signs of impending potential Void Zone formation.
- Erosion and Soil Displacement: The fractures reveal loose and broken soil, implying ongoing erosion and loss of structural integrity. The variety in soil texture implies different amounts of compaction, which could contribute to instability.
- Field Markers and Personnel: The graphic depicts an active investigation, with survey markers put along the fissure to demonstrate an ongoing assessment of ground movement and hazard mapping.
- Potential Contributing Factors: Excavation or grading activities appear to have had an impact on the surrounding environment, possibly altering the natural drainage pattern and speeding soil erosion and instability.

The representative photographs serve as important documentation of potential Void Zone-related surface deformations, reinforcing the findings from geophysical and geotechnical studies. The visual characteristics observed provide crucial insights into the mechanisms of potential Void Zone formation, emphasizing the necessity of engineering mitigation strategies to address subsurface instability. The integration of photographic evidence with geotechnical data enhances the reliability of the study, contributing to a comprehensive assessment of potential Void Zone-prone zones. To further illustrate the field conditions and provide visual context to the study area, representative photographs of the potential Void Zone-prone locations are included below.

Figure 3-8: Representative pictures for potential Void Zone at km25

3.6.1 Sample Collection from Potential Void Zone-Prone Locations

Study Area and Sampling Points: This study focuses on the 25+060-25+180 km segment of the project, where intensive geophysical investigations and borehole drilling were carried out to determine the underlying causes of potential Void Zones and associated risks. Soil sampling was conducted at precise sites along this route, considering pre-identified weak zones and essential areas for study.

3.6.2 Sampling Procedures and Techniques

Sampling Procedures and Techniques

Given that soil samples were obtained at depths of 1 m, 2 m, and 3 m using a shield tube with a diameter of 100 mm operated by an excavator, the methodology is modified as follows.

Shallow Sampling Method (Excavation and Shield Tube): For depths of 1 m and 2 m, sampling was conducted using an excavator equipped with a shield tube (100 mm diameter). This approach ensured precise sampling with minimal disturbance to the soil's natural structure. The excavator facilitated controlled penetration of the shield tube into the soil layers.

Figure 3.9 excavation and shield tube

Sample Retrieval: After reaching the desired depth, the shield tube was extracted carefully, ensuring the sample remained intact inside the tube.

- **Labelling:** Collected samples were immediately labelled with site-specific information, including coordinates, depth, and date. This detailed documentation was crucial for traceability during analysis.
- **Storage:** Samples were transferred into air-tight plastic bags for preservation of their physical and moisture characteristics. Care was taken to prevent contamination during handling.

Deep Sampling Method (Coring with Shield Tube): At the greater depth of 3 m, the excavation and shield tube method were employed for core sampling. This procedure was effective in retrieving relatively undisturbed soil cores, particularly cohesive layers, for detailed analysis.

- **Critical Zone Sampling:** After geophysical tests (ERT and SRT), weak points identified along the section influenced the precise placement of the excavator for targeted coring.
- **Handling:** Once the shield tube containing the sample was extracted, it was immediately sealed using PVC caps to retain moisture content and structural integrity.
- **Preservation:** Samples were stored in sealed tubes or containers to protect them from environmental exposure and vibrations during transportation.

Sample Preservation and Transportation

Both shallow (1 m, 2 m) and deep (3 m) samples were preserved according to their characteristics:

- **Undisturbed Samples:** Sealed in PVC tubes to maintain in-situ properties like moisture and density.

Disturbed Samples: Air-dried and placed in clean, labelled plastic bags for tests like grain size and chemical composition. All samples were transported to the laboratory in moisture-proof containers, adhering to stringent sample logging protocols to ensure traceability.

Figure 3.10 sample preservation using wax

3.7 Laboratory Tests

This section describes a variety of laboratory experiments performed on soil samples collected at depths of 1 m, 2 m, and 3 m along the 25+060-25+180 km segment. The tests are designed to offer crucial information about the soil's physical, chemical, and mechanical properties, as well as its interactions with groundwater, structural stresses, and potential Void Zone formation processes.

3.7.1 Soil Physical Properties

Moisture Content: The natural moisture content of the soil was assessed using the AASHTO T-89-17 protocols. Moisture content (w) is the weight of water (Ww) in a soil mass divided by the weight of its solids (Ws), expressed as a percentage. The formula goes as follows:

$w = (Ww / Ws) \times 100$

Equipment Used:

- Drying oven
- Precision balance
- Moisture cans
- Gloves and tongs

Procedure:

- Soil samples were placed in moisture cans and measured to determine the wet weight.
- The samples were dried in an oven at a constant temperature of 105°C until their weight stabilized.
- After cooling, the dry weight was measured and the moisture content estimated using the formula.

Moisture content is an important aspect in understanding soil behaviour, such as its ability to shrink, swell, or transport water. High moisture content suggests higher permeability and probable instability, which are important elements in potential Void Zone formation.

Specific Gravity: Specific gravity, denoted as Gs, is the ratio of the weight of a specific volume of soil solids to the weight of an equivalent volume of distilled water. The test was conducted following ASTM D-854 (2002). The formula is given as:

Gs = Unit weight (or density) of soil solids / Unit weight (or density) of water

Equipment Used:

- Pycnometer
- Precision balance
- Distilled water

Procedure:

- Soil samples were passed through a No. 40 (425 µm) screen to guarantee homogeneity and remove bigger particles that could distort results.
- The pycnometer was filled with a predetermined volume of distilled water and its weight was recorded.
- A soil sample was added, and air bubbles were eliminated using gentle agitation.
- The final weight was recorded, and calculations were made with the formula.

Figure 3-11 specific gravity of soil

Significance: Specific gravity provides information about the soil's mineralogical composition and density. This knowledge is critical to understanding compaction behaviour and subsurface stability.

Grain Size Analysis: Grain size analysis is a fundamental test used to determine the particle size distribution in soil samples. This research sheds light on soil composition and classification, allowing us to predict how it will behave under various environmental and engineering scenarios. The test is especially useful for determining permeability, erosion potential, and load-bearing capacity, all of which are critical to understanding subsurface conditions in potential Void Zone-prone locations.

Methodology: Sieves were used to analyse coarse particles, and hydrometers to evaluate smaller particles. Grain size analysis employs two primary techniques: sieve analysis for coarser particles and hydrometer analysis for finer particles.

Sieve Analysis (For Sand and Gravel):

- **Equipment Used:**
  - A set of sieves with varying mesh sizes (e.g., 4.75 mm to 75 µm).
  - Sieve shaker.
  - Precision balance.

Procedure:

- The soil sample is oven-dried to remove any moisture content.
- A predetermined weight of the sample is placed in the topmost sieve of a stacked sieve set.
- The sieves are shaken mechanically or manually for a fixed time period.
- The weight of soil retained on each sieve is recorded, and the percentage of each size fraction is calculated.

Application: This test determines susceptibility to erosion and water infiltration. A higher sand proportion enhances permeability and groundwater flow, impacting subsurface stability.

Atterberg Limit Tests: The targeted area (25+060-25+180) was evaluated for potential Void Zone formation utilizing soil consistency analysis and Atterberg limit testing. These tests included measuring the liquid limit (LL), plastic limit (PL), and plastic index (PI), according to ASTM D-4318 (2010). Soil samples were obtained from potential Void Zone-prone regions and tested for particles smaller than the No. 40 sieve (425 μm). The tests were carried out on untreated soil samples to determine their flexibility and moisture behaviour. The plastic index, which is determined as the difference between the liquid and plastic limits, was used to identify the moisture content range in which the soil shows plastic behaviour. These factors are necessary for understanding the susceptibility of fine-grained soils to subsidence and potential Void Zone formation within the study.

The findings of the Atterberg limit tests offered insights into the physical qualities of the soil at Location 25+060–25+180, aiding in the detection of relationships between soil consistency and potential Void Zone occurrence. Detailed findings, including the liquid limit, plastic limit, and plastic index values, are reported in Appendix B.

Modified Proctor Test: The Modified Proctor test was used to measure the compaction properties of soil samples collected from potential Void Zone-prone locations at Locations 25+060-25+180. This test followed ASTM D-1557 (Standard Test Methods for Laboratory Compaction Characteristics of Soil Using Modified Effort), which uses more compact energy to better simulate field circumstances.

Soil samples were properly sieved to remove particles larger than 19 mm, ensuring that they met the test requirements. The earth was compacted in five stages using a cylindrical mould,

with each layer getting 56 blows from a 4.54 kg rammer dropped from a height of 457 mm. This approach provided the required energy for modified compaction.

The test results included determining the soil samples' maximum dry density (MDD) and optimum moisture content (OMC). These factors are critical for determining the soil's compaction potential and resistance to deformation or collapse, especially in potential Void Zone prone locations. The Modified Proctor test results provided useful insights into the soil's engineering behaviour and stability in field situations.

Detailed findings, including MDD and OMC values, are presented in Appendix B.

Figure 3-12 modified proctor test

California Bearing Ratio (CBR) Test: The California Bearing Ratio (CBR) test was used to assess the strength and load-bearing capacity of soil samples collected from potential Void Zone-prone locations at Location 25+060-25+180. This test followed ASTM D-1883 (Standard Test Method for CBR of Laboratory-Compacted Soils), with revisions to match the compaction intensity of the Modified Proctor method. Soil samples were sieved to remove particles larger than 19 mm and then compacted into five layers in a cylindrical mould. Each layer was compressed with 60, 30 and 10 blows of a 4.54 kg rammer dropped from a height of 457 mm. This multi-tiered technique ensured that the soil was compacted precisely under changing energy levels, simulating field conditions. The test involved penetrating the compacted soil sample with a standard piston at a constant rate of 1.27 mm/min. The loads required to achieve penetration depths of 2.5 mm and 5 mm were measured, and the CBR

values were calculated as the ratio of the measured load to the standard load, expressed as percentages.

The CBR test results gave critical information on the subgrade strength and load-bearing capacity of the soil at the research site. These findings help to better understand soil behaviour under applied stresses and its role in potential Void Zone development. Appendix B presents detailed results, including CBR values.

Figure3- 13California Bearing Ratio (CBR) Test

Direct Shear Test: The Direct Shear test was conducted to evaluate the shear strength parameters of soil samples collected from potential Void Zone-prone areas at Location 25+060–25+180. This test was performed following ASTM D-3080 (Standard Test Method for Direct Shear Test of Soils Under Consolidated Drained Conditions).

Soil samples were carefully prepared by sieving to remove particles larger than 2 mm and compacted using the Modified Proctor effort to achieve consistency with other tests. The specimens were placed in the direct shear box apparatus, which consists of a lower and upper half capable of independent horizontal movement.

The test was conducted under controlled normal stress conditions, with applied stress levels set to simulate field loads. A horizontal force was applied to the soil sample at a constant strain rate, causing shearing along a predetermined plane. The resulting shear force and displacement were recorded throughout the test.

The key parameters derived from this test included the shear strength, cohesion (c), and angle of internal friction (φ) of the soil. These parameters are critical for understanding the soil's resistance to shear stress and its potential contribution to potential Void Zone formation under applied loads. The results from the Direct Shear test provided valuable insights into the engineering behavior of soils in the study area.

Figure3- 14 picture of Direct Shear Test

Permeability Test: The Permeability Test was used to assess the hydraulic conductivity of soil samples taken from potential Void Zone-prone locations at Locations 25+060-25+180. This test is critical for understanding the circulation of water through the soil and its possible role in potential Void Zone development. The test used ASTM D-2434 (Standard Test Method for Permeability of Granular Soils [Constant Head]) for granular soils and ASTM D-5084 (Standard Test Methods for Measurement of Hydraulic Conductivity of Saturated Porous Materials) for fine-grained soils. Soil samples were sieved for particles larger than 2 mm in

fine-grained soils and 19 mm in granular soils. The permeability tests were carried out using two approaches, depending on the soil type.

The test results revealed information on the soil's hydraulic conductivity, which is important for determining the role of water infiltration and flow in the commencement or advancement of potential Void Zone formation. Appendix D contains detailed results, including permeability coefficients for the soils under study.

3.7.2 Soil Chemical Analysis

pH Test: The pH test was used to determine the acidity or alkalinity of soil samples taken from potential Void Zone-prone locations at Locations 25+060-25+180. The purpose of this test was to evaluate the chemical properties of the soil, which are important in understanding soil behaviour and susceptibility to potential Void Zone formation. Soil samples were properly sieved to remove particles larger than 2 mm. The test followed normal soil pH determination protocols, which used a 1:1 soil-to-water ratio. A representative soil sample was combined with distilled water, and the suspension was allowed to equilibrate before measuring the pH with a calibrated digital pH meter.

The pH test findings revealed vital information on the chemical environment of the soils in the study area. Soil pH can influence mineral dissolution and soil structure stability, both of which contribute to potential Void Zone development. The pH test results were utilized to connect chemical attributes with potential Void Zone susceptibility.

Detailed findings, including pH values for the studied soils, are summarized in Appendix C.

3.7.3 Field Tests

Field studies were conducted to assess the in-situ characteristics of soils in potential Void Zone-prone locations at 25+060-25+180. These tests comprised the Dynamic Cone Penetrometer (DCP) Test and the Field Density Test (FDT) employing a sand cone. These tests revealed essential information about the soil's strength, density, and load-bearing capability, which are crucial for understanding potential Void Zone development.

3.7.3.1Dynamic Cone Penetrometer (DCP) Test:

The Dynamic Cone Penetrometer (DCP) test was used to determine the in-situ strength and stiffness of the soil layers. The test followed ASTM D-6951 (Standard Test Method for Use of the Dynamic Cone Penetrometer in Shallow Pavement Applications).

The DCP apparatus was made out of a steel rod with a cone tip that was driven into the ground by dropping a weight from a standard height. The depth of penetration for each hammer strike was measured and recorded. The DCP index, which represents the rate of penetration, was used to measure the relative strength of the soil layers. This test provided significant information about the soil's carrying capacity and stability in potential Void Zone-prone areas.

Figure 3-15 Dynamic Cone Penetrometer (DCP) Test

3.7.3.2Field Density Test (FDT) by Sand Cone Method

To estimate the soil's in-situ density, a Field Density Test (FDT) was done using the sand cone method. This test adheres to ASTM D-1556 (Standard Test Method for Density and Unit Weight of Soil in Place by Sand Cone Method). The process entailed digging a small hole at the test location, carefully collecting the excavated soil for laboratory analysis, and then filling the hole with homogeneous, dry sand from a calibrated sand cone apparatus. The volume of the hole was determined using the mass of sand utilized. The bulk and dry densities of the soil were then calculated using the excavated soil's mass and moisture content.

These field studies supplied critical data on the soil's physical qualities, assisting in determining its role in potential Void Zone development. Appendix E presents the detailed results of both experiments, including DCP indices and field density values.

Figure 3-16 Field Density Test (FDT) by Sand Cone Method

Task	Method	Objective
Geophysical Surveys	SRT & ERT	Map subsurface anomalies and weak zones.
Soil Sampling	Auger & Core Drilling	Collect samples for physical, chemical, and mechanical analysis.
Dynamic Cone Penetration	DCP Test	Evaluate strength and consistency of subsurface layers.
Field Density Test	Sand Cone / Nuclear Gauge Method	Measure in-situ density and validate compaction results.
Laboratory Tests	Physical, Chemical, Mechanical	Analyze soil properties to assess stability and groundwater interaction.

Table 3.3 Geotechnical Investigation Methods and Their Objectives

Visual Additions:

- **Maps**: Show geophysical survey lines and sampling locations.
- **Photos**: Include images of field equipment (e.g., DCP test in progress) and laboratory setups

3.8 Identifying Geological Features

3.8.1 Geological Mapping

The first stage is to conduct a complete geological survey of the Adama-Awash Express Road. This mapping is to identify and record several geological formations in the area, with a focus on stratigraphy and bedrock types: Understanding the composition and distribution of underlying rock formations, particularly soluble rocks like limestone and gypsum that can dissolve and generate potential Void Zones.

Faults, fractures, and joints: Identifying fault zones, fractures, and joints to assess the area's susceptibility to potential Void Zones. These features usually act as routes for water penetration, hastening the disintegration of soluble rocks.

Soil Types: Mapping various soil types to determine how soil composition influences potential Void Zone formation. Some soils, particularly those high in clay content, may affect groundwater movement and contribute to potential Void Zones.

CHAPTER 4:

RESULTS AND DISCUSSION

This chapter examines the findings of the integrated studies done along the Adama-Awash Express Road corridor. The study uses a combination of geophysical, geotechnical, and chemical techniques to evaluate subsurface properties, soil behaviour, and geohazard vulnerabilities, with a focus on identifying potential Void Zone formation causes. The findings given in this chapter seek to get a better understanding of the complex interplay between geological processes and anthropogenic activities that are crucial to infrastructure resilience in this dynamic and seismically active region.

To accomplish this, a multidisciplinary strategy was used, with Electrical Resistivity Tomography (ERT) and Seismic Refraction Tomography (SRT) as the principal geophysical instruments for mapping subsurface abnormalities. These non-invasive approaches were supported by thorough borehole log data (BH 105, BH 106, and BH 107), which provided a better understanding of the stratigraphy and lithological properties of the research area. The connection of geophysical profiles with borehole data and generalized tables of compressional wave velocities (P-wave velocities) and resistivity values proved critical in understanding the composition and mechanical properties of subsurface layers.

Geotechnical and chemical studies extended this inquiry by offering critical insights on soils' physical, index, and mechanical properties, as well as their chemical makeup. Soil behaviour was studied under various conditions using tests such as grain size analysis, Atterberg limits, shear strength evaluation, and California Bearing Ratio (CBR) measurements. Complementary chemical tests, including pH and sodium content assessments, revealed the impact of groundwater interactions on soil stability, providing a more comprehensive understanding of potential failure causes.

This chapter analyses the key drivers of potential Void Zone formation as well as the critical risk zones throughout the corridor by combining geophysical data with geotechnical and chemical discoveries. The findings establish a solid platform for suggesting targeted mitigation methods to protect the region's vital infrastructure. This chapter contextualizes these findings within the larger geological and environmental framework of the Ethiopian Rift, drawing comparisons with previous studies and recommending topics for further research and practical applications. This section presents the results of the geophysical investigation. To help the

lithological description and interpretation of the current results, a generalized table of compressional wave velocities and resistivities is constructed in connection with the accessible borehole logs (BH 105, 106, 107) around the potential Void Zone.

No.	Rock and Soil Types	Range of P-wave velocity (m/sec)	Range of Resistivities (Ohm-m)
1	Unconsolidated sediments, very loose sand with clay, silty sandand silty sandy clay and decomposed materials	Below 1000	Below 29
	silty gravel and rock fragments as well as sand with clay and silty sand.	1000-1500	
2	Intensively decomposed to highly fractured and weathered basalt, silty gravel and rock fragments	1500 -1750	23-173
3	Highly fractured/weathered to moderately fractured/ weathered, scoraceous basalt, partially water saturated	1750-2500	25-141
4	Moderately to slightly fractured and weathered basalt	2500-3500	83-141
5	Slightly fractured/weathered to Fresh basalt	3500-4500	Above 141
7	Fresh to very fresh basalt	Above 4500	Above 141

Table 4-1: Range of P-wave velocities and Electrical Resistivity of rocks & Soils of the survey area

4.1 Electrical Resistivity Tomography (ERT) Results

This section gives the interpreted results of the Electrical Resistivity Tomography (ERT) study carried out along six profile lines (Lines 1–6) on the Adama-Awash Express Road. The primary goal of the study was to look at subsurface lithological variations and identify weak zones or geological structures that could lead to potential Void Zone formation. Color-coded resistivity data were used to understand the ERT profiles, which were then connected with accessible borehole logs to improve geological interpretation. Each survey line is discussed independently, and the interpretations are supported by the associated resistivity cross-sections (Figures 4-1 to 4-6).

4.1.1 Line L-1

The ERT section (Figure 4-1) shows a low resistivity zone (<28 Ω·m) northwest of station 115, shown by a dashed outline. This zone is regarded as a weak layer of silty clay on top of heavily worn and decomposed basalt. Borehole BH 107 supports the identification of a low-resistivity anomaly below 5 m between stations 140 and 150, indicating heavily worn and fragmented vesicular basalt formation. Higher resistivity values (>83 Ω·m) are observed from station 120 towards the southeast, indicating the presence of worn and fractured basalt. This unit outcrops from station 135 and reaches a depth of around 15.5m. defined boundary near station 120 marks the transition between low and high resistivity zones, which could represent a lithological contact or a structural discontinuity. Resistivity is low to intermediate northwest of the border, with a localized high-resistivity anomaly between stations 45 and 75 at 10.6 m depth.

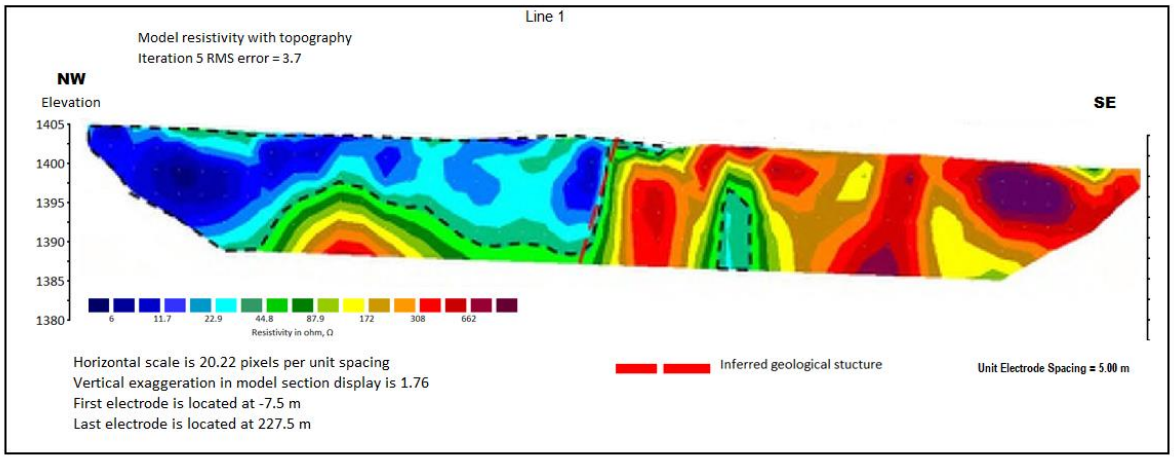

Figure 4-1: Electrical Resistivity Tomography (ERT) Section along Line 1

4.1.2 Line L-2

The ERT section in Figure 4-2 shows a low resistivity zone (<25 Ω·m) northwest of station 125, interpreted as a silty clay layer with variable thickness ranging from a few centimeters to around 15 m. An intermediate resistivity unit (25-118 Ω·m) occurs between stations 125 and 145, indicating moderately fragmented basalt. The area south-east of station 145 has high resistivity values (>118 Ω·m), indicating fragmented or large basalt. A known potential Void Zone near station 125 corresponds to zones with low to intermediate resistivity. However, due to basalt boulders and previous grouting treatments, precisely delineating subsurface characteristics in this location proved difficult. A structural element is implied near this location.

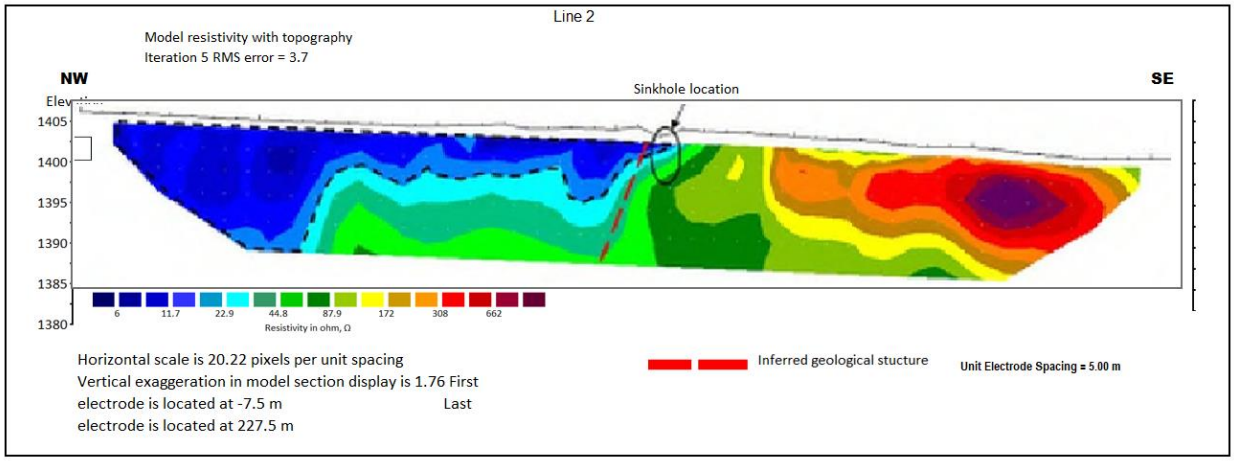

Figure 4-2: Electrical Resistivity Tomography (ERT) Section along Line 2

4.1.3 Line L-3

As illustrated in Figure 4-3, a low resistivity zone (<27 Ω·m), enclosed by a dashed line, is observed northwest of station 140. This zone likely consists of silty clay overlying weathered basalt, with a thickness ranging from 3.1 m to 11.9 m, showing minimum and maximum values at stations 140 and 25, respectively.The underlying layer exhibits intermediate resistivity (27–141 Ω·m), outcropping between stations 140 and 185. This is interpreted as weathered and moderately fractured basalt. A high resistivity layer (>141 Ω·m) appears southeast of station 185, interpreted as slightly fractured to massive basalt. A structural discontinuity is inferred near station 125, which coincides with a known potential Void Zone location. The locally reduced resistivity at this point is attributed to disturbed ground conditions and reduced bulk resistivity.

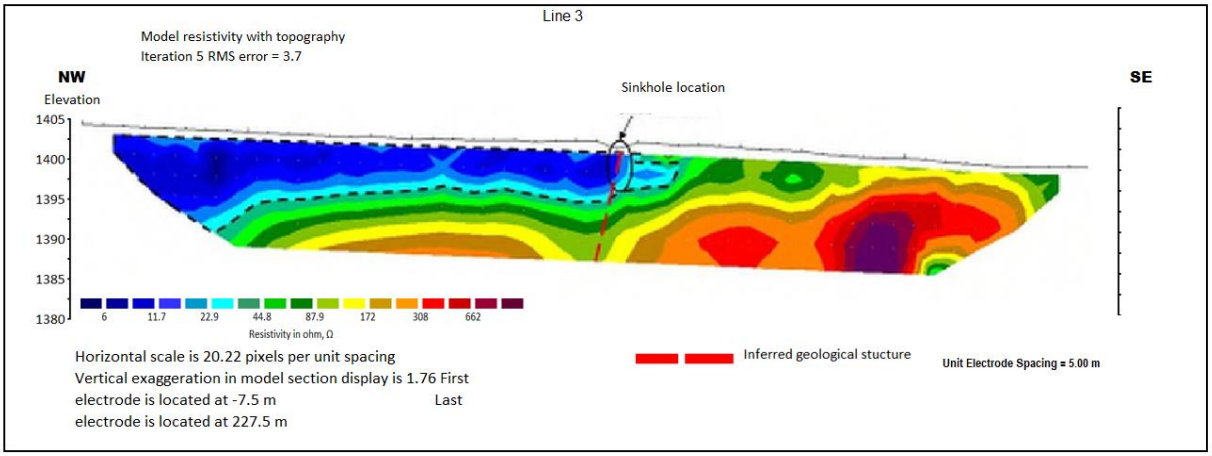

Figure 4-3: Electrical Resistivity Tomography (ERT) Section along Line 3

4.1.4 Line L-4

Figure 4-4 depicts a thin, low resistivity layer (<23 Ω·m) between stations 0 and 135, indicating silty clay. This layer can be as thick as 3.8 m. From station 135 south-eastward, a high resistivity zone (>172 Ω·m) implies fractured or massive basalt. The remaining profile has intermediate resistivity values (23-173 Ω·m), indicating silty gravel with fragmented rock underlying weathered and cracked basalt. In the neighborhood of station 125, a geological structure is inferred, which may influence the local resistivity distribution.

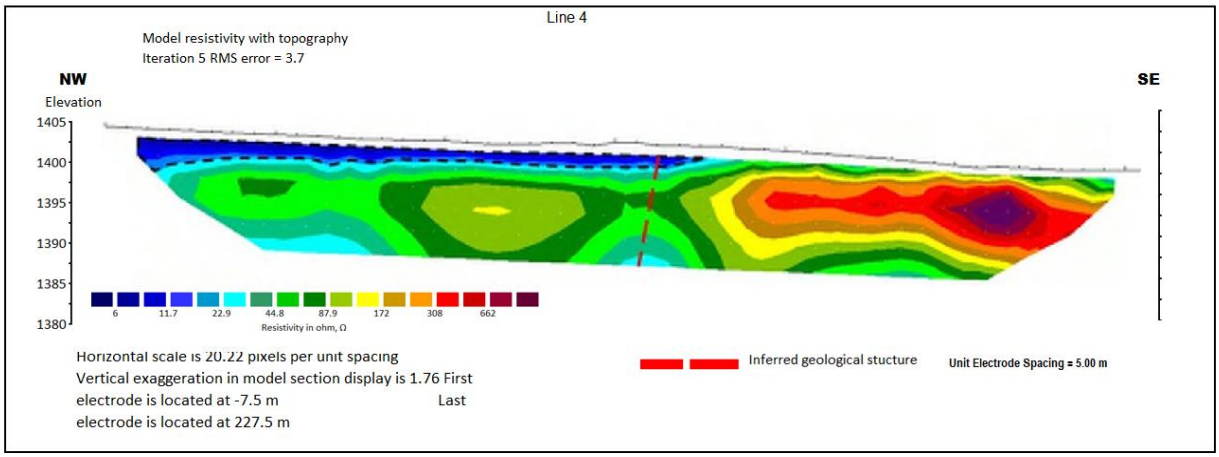

Figure 4-4: Electrical Resistivity Tomography (ERT) Section along Line 4

4.1.5 Line L-5

Figure 4-5 shows a low resistivity zone (<25 Ω·m), marked by a dashed line, northwest of station 140. This feature is characterized as silty clay underlain by worn basalt, with a thickness ranging from 2.5 to 11.3 meters.

The core region of the profile has an intermediate resistivity zone (25-62 Ω·m), which is likely caused by worn, fractured basalt soaked with groundwater. High resistivity readings (>98 Ω·m) around station 150 indicate the existence of strongly worn and fragmented scoraceous basalt, agreeing with borehole BH 105 results. A geological structure is inferred near station 130, where a thick, deep low-resistance zone is visible.

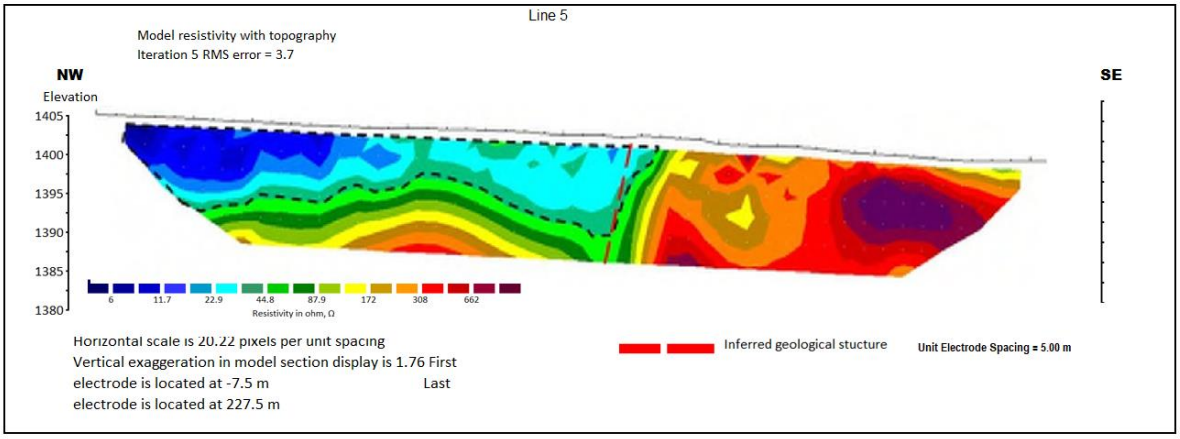

Figure 4-5: Electrical Resistivity Tomography (ERT) Section along Line 5

4.1.6 Line L-6

Figure 4-6 shows a shallow subsurface layer with low resistivity values (<29 Ω·m), indicating clay-rich soils or clayey sands with significant moisture content. These materials have high electrical conductivity due to the presence of tiny particles and water-filled pore spaces. The layer's thickness of up to 7.5 m indicates significant accumulation of surface sediments caused by weathering and deposition. Such a thin and conductive layer has significant consequences for geotechnical stability, as it may have low shear strength and contribute to greater risk of surface subsidence or collapse, particularly in places prone to karst formation. The moderately resistant zone (29-119 Ω·m) beneath the low-resistivity layer is thought to be weathered and fractured basalt. This zone most likely reflects the transitory contact between surface soils and more competent rock components.

The resistivity range implies partial saturation, increased porosity, and the occurrence of open fractures, all of which are frequent characteristics of basalt exposed to protracted chemical weathering. Such weathered basalt layers can display heterogeneous mechanical behavior, potentially acting as conduits for groundwater flow, which may hasten the breakdown of soluble rocks underneath them in karst terrains. This intermediate layer is critical for controlling fluid circulation and forming subsurface voids.

High resistivity values (>119 Ω·m) are recorded at deeper depths and center parts of the profile, particularly between stations 75-120 and 145-215. These zones are characteristic of minimally fragmented to large basalt, indicating more competent and undamaged bedrock with little groundwater saturation. The high resistivity indicates that these parts are less permeable and

more structurally stable. Notably, a subsurface structural anomaly is detected near station 130, which cuts through the profile's depth. This feature may be a fault zone, fracture network, or vertical dissolution conduit, and its presence has geotechnical implications. If soluble materials are encountered at depth, such subsurface structures can channel groundwater flow, accelerate weathering processes, and enhance the likelihood of potential Void Zone formation.

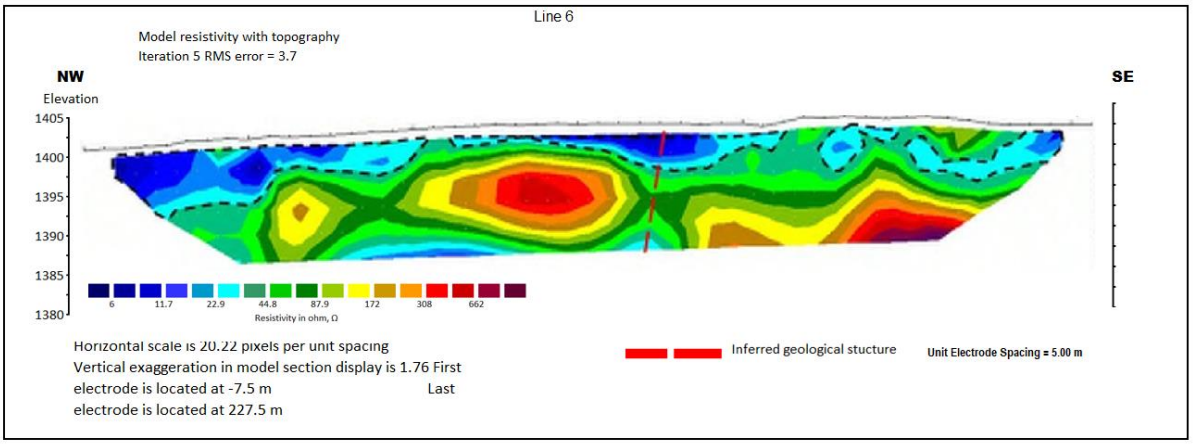

Figure 4-6: Electrical Resistivity Tomography (ERT) Section along Line 6

The Electrical Resistivity Tomography (ERT) survey conducted along Lines 1 through 6 of the Adama–Awash Expressway provided crucial insights into subsurface conditions linked to potential potential Void Zone development. The investigation revealed zones of low resistivity indicative of silty clays, weathered and fractured basalt, and several structural anomalies. These findings align with results from previous studies undertaken in similar volcanic and karstic environments.

Prior research has shown that near-surface low-resistivity anomalies (typically below 30 Ω·m) are often associated with materials rich in clay, saturated zones, or highly weathered rocks all of which are key factors in the development of potential Void Zones . For instance, (André et al., 2012), in their ERT-based study of karst collapse in China, observed that clay-filled voids and weathered zones displayed resistivity values ranging between 10–50 Ω·m. This range corresponds well with the low-resistivity features detected in the present study, notably along Lines 1, 2, 5, and 6.

In addition, the presence of intermediate resistivity values (25–141 Ω·m) interpreted as weathered and fractured basalt is comparable to observations by(Le Blond et al., 2015) , who highlighted that volcanic rocks altered by weathering processes commonly display intermediate resistivity because of water- and clay-filled fractures. In this investigation, such

zones were consistently found beneath the silty clay layers, particularly on Lines 3 and 5, highlighting zones of potential ground weakness.

The identification of high-resistivity areas (>100–150 Ω·m) across the profiles, attributed to massive or only slightly fractured basalt, also matches previous findings. According to Cardarelli et al. (2003), resistivity values exceeding 100 Ω·m typically indicate relatively unweathered and competent bedrock in volcanic settings. High-resistivity zones observed, especially in Lines 1, 2, and 6, suggest areas of comparatively stable geological conditions, although nearby structural features (e.g., at station 130 on Line 6) still pose potential geohazards by facilitating groundwater movement.

Structural discontinuities identified in the resistivity models inferred from sharp resistivity contrasts are consistent with interpretations by(Mancarella et al., 2012).Their work demonstrated that faults and fractures play a pivotal role in channelling groundwater, accelerating dissolution, and promoting void development in karst terrains. The discontinuities detected near stations 120 (Line 1), 125 (Line 3), and 130 (Lines 5 and 6) in this study mirror these dynamics, highlighting the necessity for detailed structural assessments in such environments.

Furthermore, the surface layers of low resistivity observed in this survey, reaching thicknesses up to 7.5 m (especially notable on Line 6), resemble findings reported by(André et al., 2012). These author emphasized that thick clay-rich surface deposits could mask deeper karstic voids, potentially leading to an overestimation of surface stability unless verified with borehole or additional geophysical data.

In summary, the resistivity distributions and geological interpretations derived from this study are largely consistent with established findings in similar geological contexts. Nonetheless, site-specific anomalies, such as grouted zones (noted along Line 2) and varying clay thicknesses (Lines 4 and 6), underline the necessity of combining ERT results with borehole investigations for a comprehensive understanding of subsurface conditions and potential Void Zone risk assessment.

4.2 Seismic Refraction Tomography (SRT) Results

Seismic Refraction Tomography (SRT) technology was utilized on six survey lines to assess subsurface conditions along the Adama-Awash Expressway. The primary goal was to identify

regions of weak and loose material, broken bedrock, and structural discontinuities that could cause ground subsidence or potential Void Zone development. The 2D P-wave velocity tomography models emphasize changes in lithology, degree of weathering, and subsurface heterogeneity, which are outlined for each line below.

4.2.1 SRT Survey Line 1

The survey extends from the starting position at 551,511 m E, 959,956 m N to the concluding point at 551,739 m E, 959,886 m N, using the Adindan Datum (Zone 37N), with an elevation range of 1404.8 m to 1398.7 m above sea level (a.s.l.). The two-dimensional P-wave velocity tomography for SRT Survey Line 1 (Figure 4-7) shows a near-surface zone with very low seismic velocities, often less than 1000 m/s. This upper layer, which has an average thickness of around 6 meters, is thought to be made of very weakly cemented and thoroughly degraded silty gravel, sandy clay, and rock fragments. These materials have poor compaction and significant porosity, indicating a low load-bearing capability and an increased susceptibility to erosion and settlement.

Underneath this surficial level is a more capable subsurface layer with P-wave velocities ranging from 1000 to 1750 m/s. This layer, which reaches a maximum depth of around 17 meters near station 95, is thought to be primarily composed of extremely worn and fractured basalt. The increase in seismic velocity with depth indicates a gradational improvement in material stiffness and cementation, while widespread fracturing and weathering indicate lower rock mass strength compared to un weathered bedrock.

These findings highlight the geotechnical significance of the investigated area, where a weak, unconsolidated surface layer and an uneven weathering rock horizon may present ground stability difficulties. The lateral difference in depth and continuity of the basaltic layer at the survey line's ends suggests zones of potential instability, which might be worsened by increasing water infiltration or load conditions.

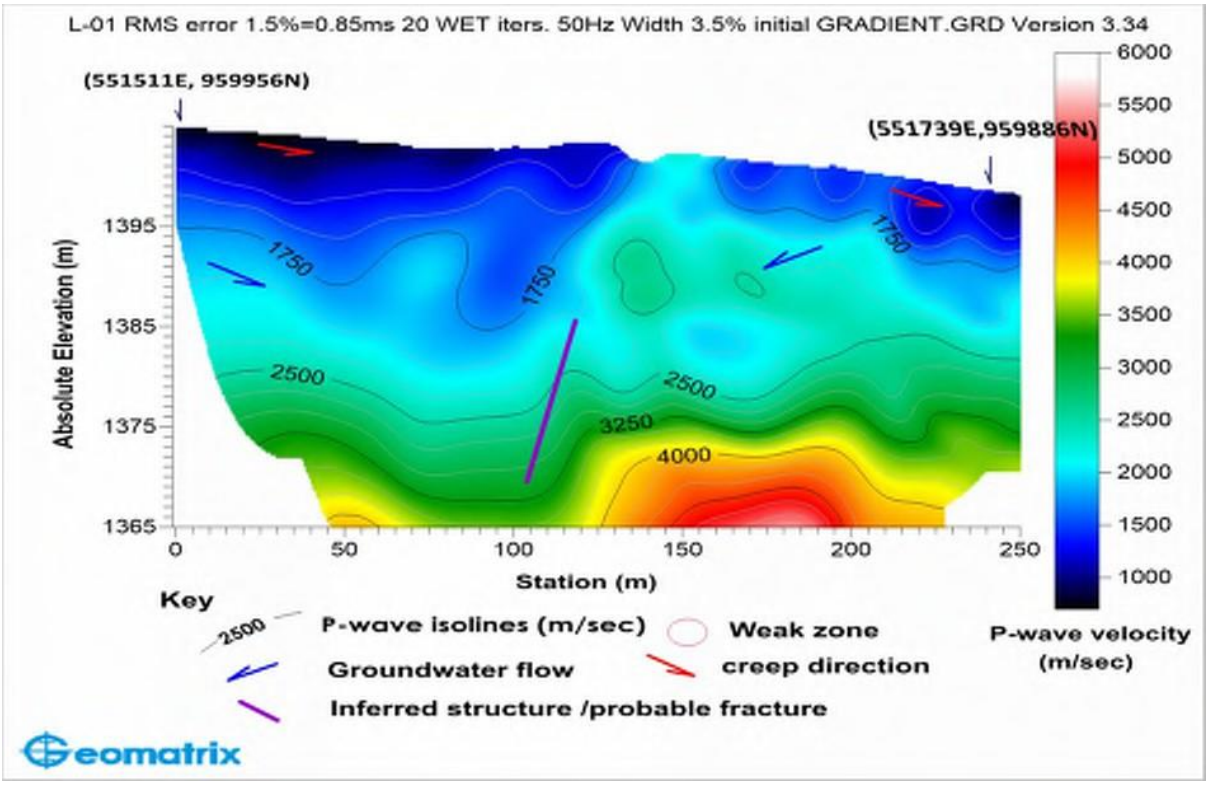

Figure 4-7: 2D P-wave Velocity Tomography along SRT Survey Line 1

4.2.2 SRT Survey Line 2

The survey extends from the starting point at 551,513 m E, 959,963 m N to the concluding position at 551,742 m E, 959,893 m N, using the Adindan Datum (Zone 37N), with an elevation range of 1405.0 m to 1398.7 m above sea level (a.s.l.). P-wave velocity tomography along SRT Survey Line 2 (Figure 4-8) shows a clear stratification of underlying material properties. The uppermost 12 meters have continuously modest seismic velocities, often less than 1250 m/s. These low-velocity zones are more visible and spread out toward both ends of the survey line, and they are interpreted as loosely compacted soils composed of sand, clay, and silty sand. These materials' variability and lateral continuity signal poor geotechnical properties, including inadequate shear strength and propensity for deformation under load.

A more compact and stiffer unit exists under this surficial layer, with P-wave velocities ranging from 1250 to 1750 m/s. This unit is thought to have severely weathered basalt interspersed with moderately well-cemented sandy clay and silty sand. The denser features of this layer imply increased load-bearing capacity, but they also signal prior events of structural weathering and mechanical disintegration of the parent rock mass. Notably, a geologically significant anomaly has been detected near station 130, where the subsurface layer appears to be offset and dips

toward station 80. This feature may correspond to a fault or fracture zone and is likely to operate as a preferred subsurface drainage conduit.

The presence of such a structure, as well as the resulting localized weakening of subsurface materials, raises concerns about fracture-controlled water infiltration and percolation. These processes can cause progressive subsurface erosion and increase the risk of potential Void Zone formation, especially in areas with low overburden cohesiveness.

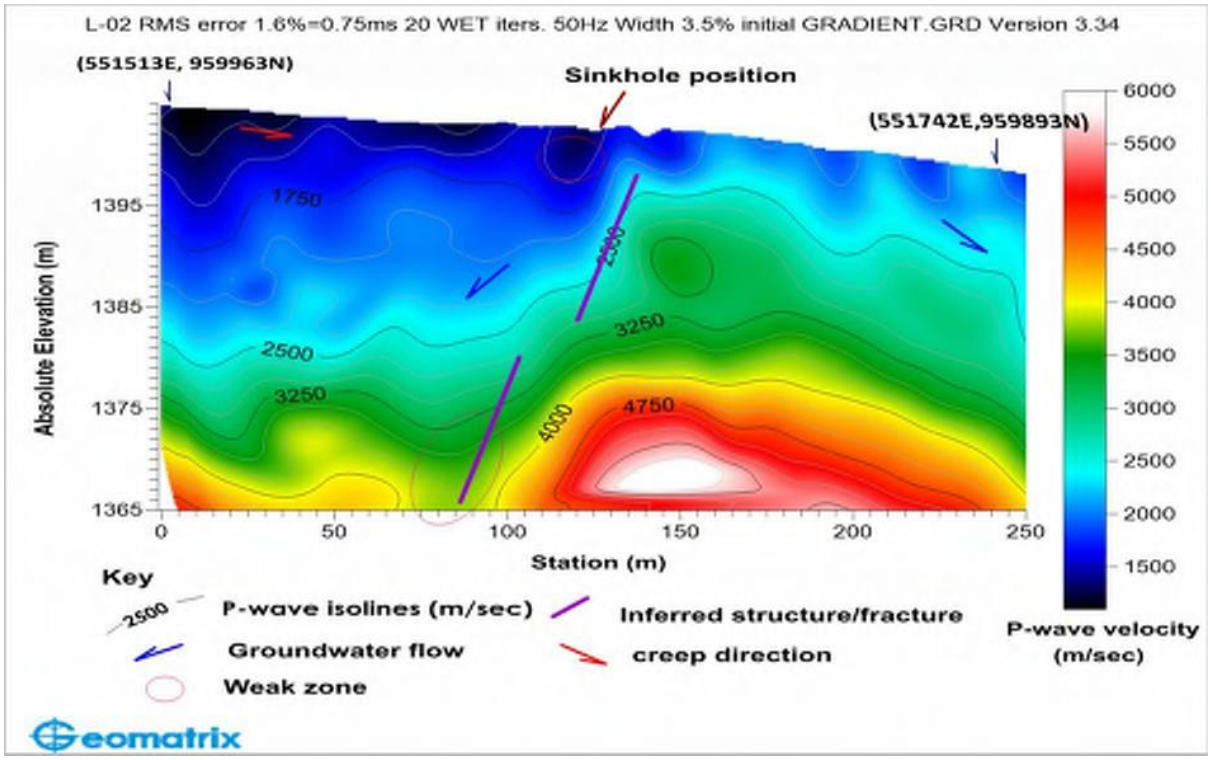

Figure 4-8: 2D P-wave Velocity Tomography along SRT Survey Line 2

4.2.3 SRT Survey Line 3

The survey extends from the starting position at 551,514 m E, 959,968 m N to the concluding point at 551,744 m E, 959,897 m N, using the Adindan Datum (Zone 37N), with an elevation range of 1405.1 m to 1398.6 m above sea level (a.s.l.). The 2D P-wave velocity tomography shown in Figure 4-9 demonstrates a diverse subsurface profile along Line 3. The profile shows a discontinuous upper layer with low seismic velocities (<1250 m/s), mostly focused in the west.

This layer extends to a maximum depth of around 6 meters and is thought to be made up of very loosely cemented, decomposing sandy clay elements. The patchy distribution of this unit

suggests isolated zones of low density and strength, which could have a major impact on near-surface deformation behaviour. Below this surficial zone is a more competent geologic level with P-wave velocities ranging from 1250 to 1750 m/s. This layer is thought to be made up of extensively worn and fractured basalt interspersed with silty gravel and rock pieces that have been rather well cemented. The competent layer reaches a maximum depth of around 10 meters, notably at station 10. The regional variation in thickness and material composition within this level demonstrates complicated depositional and post-depositional geological processes.

The results show a significant variation in the mechanical characteristics of shallow subsurface materials along the survey line. Such sudden lateral variations in material stiffness and texture might result in areas of localized stress concentration and differential settlement. These conditions are ideal for collapse mechanisms or subsurface pipes, especially with increasing water infiltration or surcharge loads.

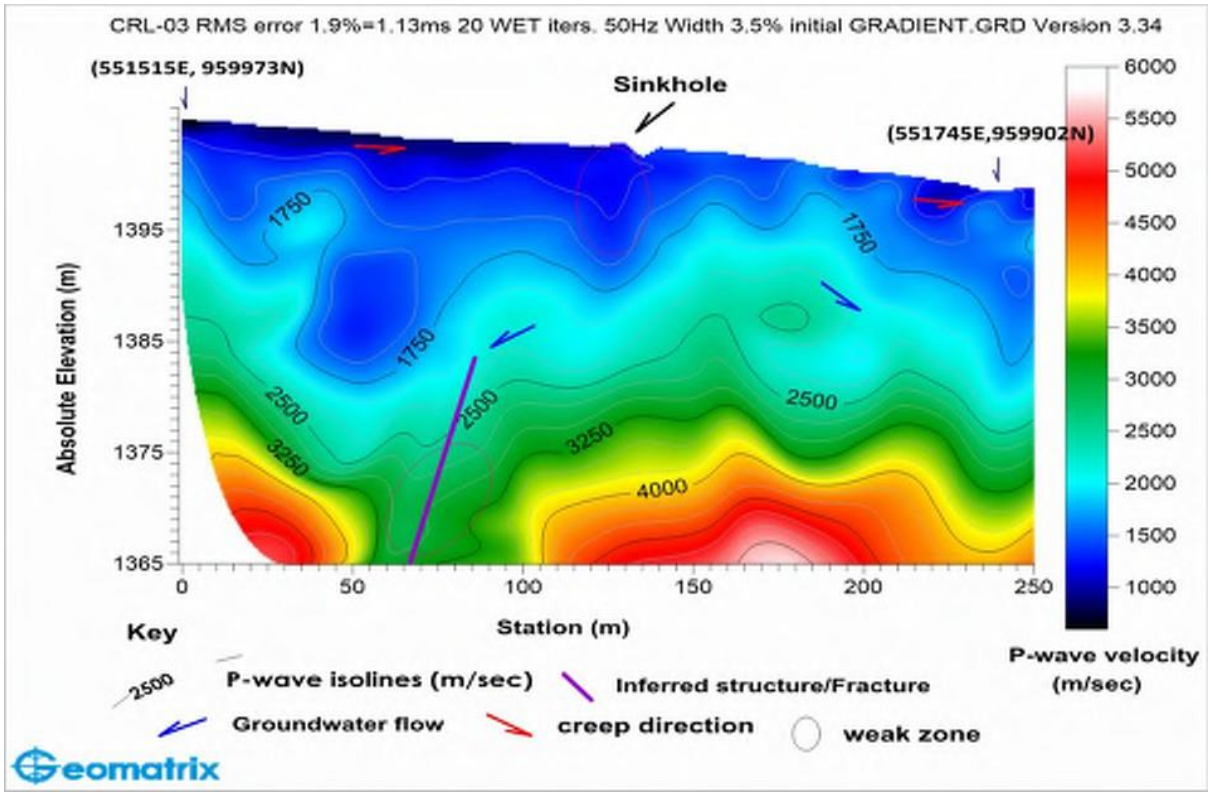

Figure 4-9: 2D P-wave Velocity Tomography along SRT Survey Line 3

4.2.4 SRT Survey Line 4

The survey extends from the starting position at 551,515 m E, 959,973 m N to the concluding point at 551,742 m E, 959,893 m N, using the Adindan Datum (Zone 37N), with an elevation range of 1405.2 m to 1399.0 m above sea level (a.s.l.).

Figure 4-10 shows a low-velocity zone (<1000 m/s) in the upper 7 meters of SRT Survey Line 4, especially around station 40. This surficial layer is typical of very loosely cemented and degraded sandy clay minerals, which have low shear strength and a high sensitivity to water penetration.

Below this weak surface layer is a more competent subsurface zone with P-wave velocities ranging from 1000 to 1750 m/s. This deeper unit is thought to be a combination of heavily worn and fractured basalt with interbedded cemented silty sand, silty gravel, and rock fragments. The thickness of this competent layer increases laterally toward both ends of the survey line, reaching a maximum depth of around 18 meters near station 40 and a minimum depth of 11 meters around station 140.

The presence of variably thick weathered basalt, particularly in places with extensive fracturing, indicates an increased vulnerability to subsurface dissolution and collapse mechanisms. These zones may act as conduits for water percolation, which can cause or accelerate subsurface erosion and potential Void Zone formation. As a result, these places are priority sites for geotechnical monitoring and tailored mitigating activities.

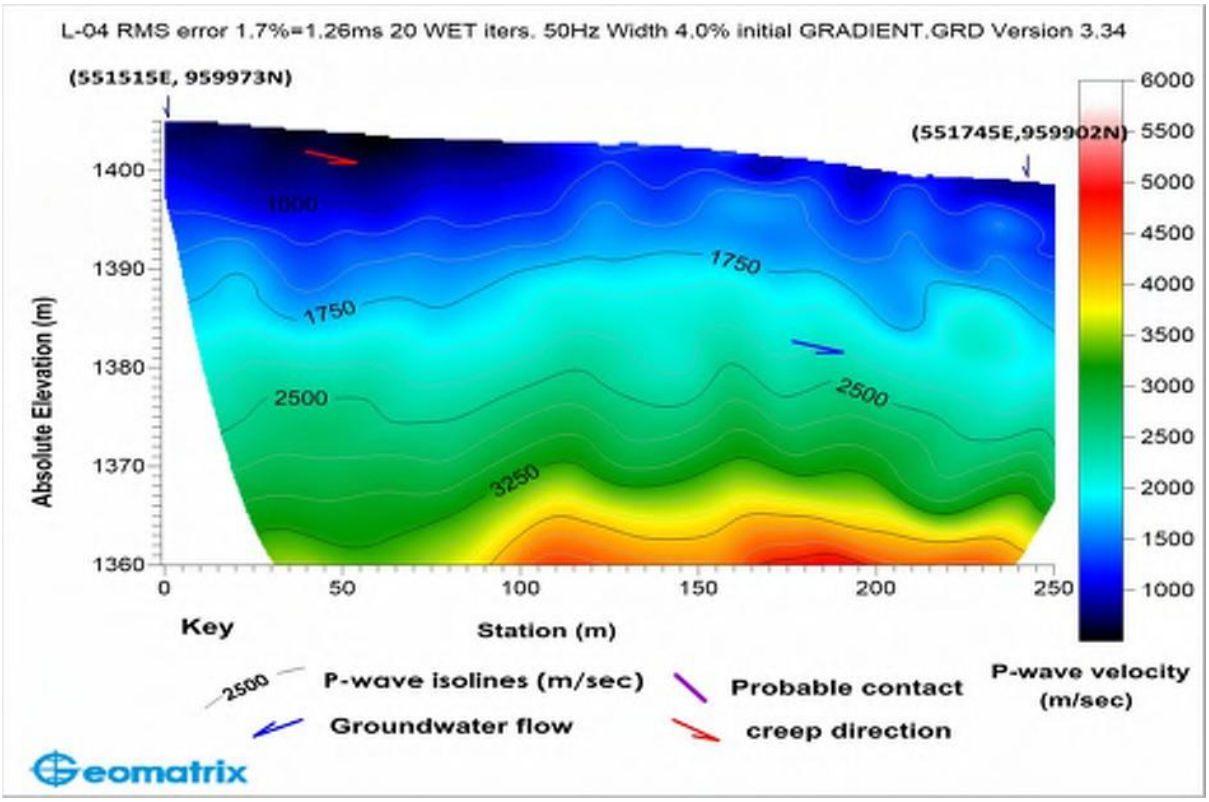

Figure 4-10: 2D P-wave Velocity Tomography along SRT Survey Line 4

4.2.5 SRT Survey Line 5

The SRT survey line extends from the starting point at 551,517 m E, 959,979 m N to the termination point at 551,748 m E, 959,908 m N, all within the Adindan Datum (Zone 37N). The line's elevation ranges from 1405.3 m to 1398.5 m above sea level (a.s.l.), suggesting a progressive shift in terrain over the survey route. Figure 4-11 shows 2D P-wave velocity tomography, revealing the existence of low-velocity materials (<1000 m/s) throughout the survey line. These deposits are loose, unconsolidated, and degraded sandy clay. These poor surface materials dominate the profile, with the exception of the centre portion between stations 110 and 160, when the deeper, more competent unit is revealed on the surface.

The underlying unit, which has moderate velocities (1000-1750 m/s), is thought to be worn and fractured basalt mixed with cemented silty sand, silty gravel, and rock fragments. This stratum varies greatly in depth, ranging from a minimum of about 9 meters near station 210 to a maximum of 22 meters around station 70. Notably, a probable structural anomaly is suspected around station 100, while a highly fractured and potentially unstable zone is discovered between stations 55 and 85. These data indicate that the area between stations 70-100 may be especially vulnerable to geohazards such as subsurface collapse and potential Void Zone

formation. The combination of deep weathered bedrock, structural features, and significant fracture increases the potential for vertical water movement and the formation of subsurface voids.

The detected characteristics are indicative of a karstic or dissolution-prone environment, emphasizing the importance of targeted stabilization interventions and ongoing geotechnical monitoring in these areas.

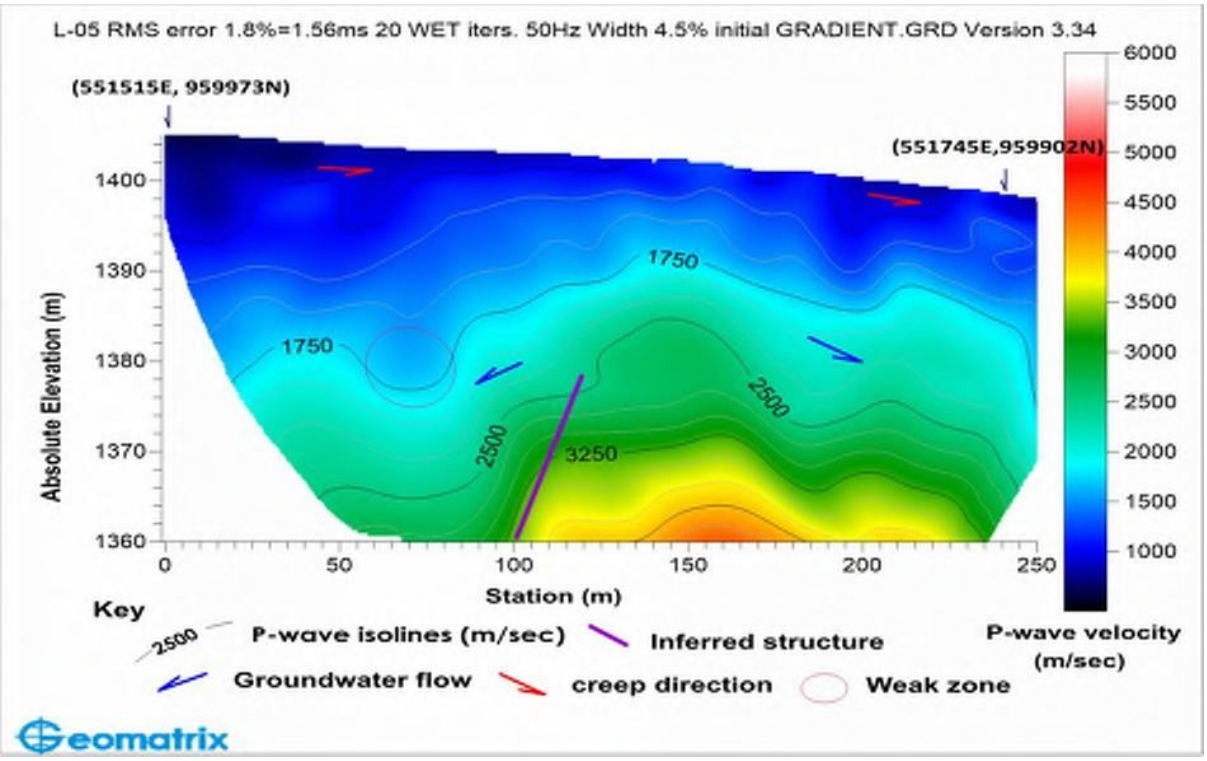

Figure 4-11: 2D P-wave Velocity Tomography along SRT Survey Line 5

4.2.6 SRT Survey Line 6

The survey extends from the starting position at 551,523 m E, 960,004 m N to the concluding point at 551,757 m E, 959,932 m N, using the Adindan Datum (Zone 37N), with an elevation range of 1409.4 m to 1408.1 m above sea level (a.s.l.). Figure 4-12 shows 2D P-wave velocity tomography of SRT Line 6, revealing zones of low-velocity material (<1000 m/s) at the north western end of the profile, as well as isolated patches along the line. These zones are typically less than 8.5 meters thick and consist of very weakly cemented, degraded sandy clay soils with low mechanical strength and a high susceptibility to saturation and erosion. The thickest representation of this top weak layer is found around Station 10.

Under this layer is a more competent geologic unit, with P-wave velocities ranging from 1250 to 1750 m/s. This zone is described as highly worn and cracked basalt interspersed with cemented sandy clay, silty sand, and rock fragments. The depth of this unit varies laterally, from about 7 meters around station 175 to almost 20 meters toward the profile's northwestern edge. The significant lateral fluctuation in the depth to competent material indicates uneven bedrock morphology and varied weathering processes. Such heterogeneity poses geotechnical concerns, including the potential for differential settlement, focused infiltration zones, and progressive subsurface erosion. These characteristics underscore the importance of detailed site characterization and targeted mitigation strategies, particularly in zones exhibiting thick weak overburden and irregular bedrock interfaces.

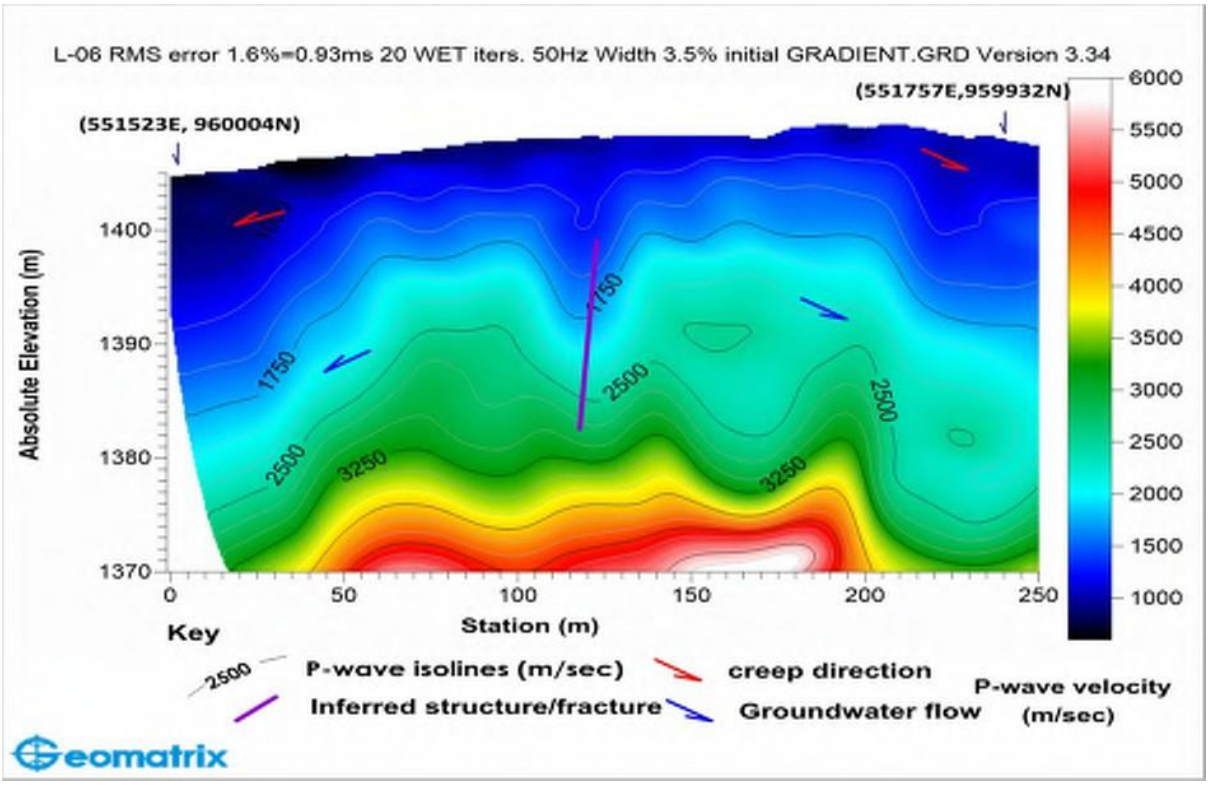

Figure 4-12: 2D P-wave Velocity Tomography along SRT Survey Line 6

The interpretation of seismic refraction tomography (SRT) data collected along six traverses consistently reveals a two-layer stratigraphic profile across the investigated corridor. The uppermost layer is typified by significantly low P-wave velocities (<1000–1250 m/s), which are indicative of very loosely compacted, decomposed, and weakly cemented soils such as sandy clay, silty sand, silty gravel, and rock fragments. The thickness of this surficial unit varies

across the profiles, generally ranging from 4 m to 12 m, but in certain localities particularly near structural discontinuities or topographic lows it reaches depths of up to 18 m.

These findings are consistent with previous studies. For example, (*Annex V Minutes of Meeting*, n.d.) utilized SRT and Ground Penetrating Radar (GPR) in Park City, Utah, to map a potential Void Zone's subsurface extension. The SRT profile revealed three low-velocity anomalies corresponding to karstic voids surrounded by highly saturated soils. Similarly, a study by(Akingboye & Ogunyele, 2019) in a karst region of Turkey integrated SRT and Electrical Resistivity Tomography (ERT) to identify potential Void Zone-prone zones characterized by low-velocity layers overlying higher velocity fractured rock.

Furthermore, research by (Akingboye & Ogunyele, 2019) emphasized that SRT is particularly effective in detecting weak, low-velocity zones often associated with weathered or saturated materials, which are critical indicators of potential subsidence or collapse. This aligns with the low-velocity upper layers observed in this study, corresponding to weak, decomposed soils susceptible to erosion and settlement.

Beneath this upper unit lies a relatively more competent geological layer characterized by intermediate P-wave velocities (1000–1750 m/s). This lower horizon is interpreted as moderately to highly weathered and fractured basalt, in some cases interbedded with relatively cemented silty gravel, sandy clay, and volcanic breccia. The geometry of this interface is irregular and exhibits considerable lateral and vertical variation across the different survey lines. In several profiles most notably Lines 2, 4, and 5—distinct geophysical anomalies and velocity discontinuities were identified. These features are interpreted as possible geological structures, such as fracture zones or fault lines, and in some cases may be indicative of paleo-karstic conduits or zones of intensified weathering. These structural features are observed to deepen or widen in zones where the overlying low-velocity materials are thickest, suggesting potential subsurface void evolution due to dissolution, piping, or collapse mechanisms.

From a geotechnical engineering perspective, the presence of a mechanically weak surficial layer overlying fractured, potentially permeable basalt introduces significant risks related to subsurface instability. These conditions are particularly conducive to the development of potential Void Zones , subsidence, and differential settlement, especially in areas subjected to high infiltration rates, concentrated surface loading, or groundwater level fluctuations. The abrupt change in stiffness and material composition between the two layers may also lead to

localized stress concentrations, further exacerbating deformation potential under dynamic or static loading. Moreover, the lateral variability in the depth to competent strata suggests non-uniform foundation conditions, which could negatively impact infrastructure performance if not appropriately accounted for in design and mitigation planning. Of particular concern are the weak zones identified around stations 40 and 130 (Line 4), station 100 (Line 5), and station 10 (Line 6), which coincide with structural disruptions and may serve as preferential pathways for groundwater ingress, thereby increasing the susceptibility to subsurface erosion and eventual collapse.

Overall, the SRT survey results provide compelling evidence supporting the hypothesis that the geological and geotechnical configuration of the study area contributes to localized ground instability and poses a tangible hazard to the Adama–Awash Expressway infrastructure. The combination of low-velocity surficial soils, fractured basaltic bedrock, and inferred subsurface structures presents a high-risk setting for potential Void Zone development and progressive ground deformation. These findings underscore the necessity for implementing site-specific mitigation measures such as grouting, improved drainage control, or subsurface reinforcement in critical segments of the corridor.

The seismic refraction tomography (SRT) data interpreted along the Adama–Awash Expressway exhibit subsurface characteristics that align with findings from both Ethiopian and global studies on geological instability due to weak overburden materials and fractured bedrock. This study identified consistently low P-wave velocities (<1000–1250 m/s) in the upper layers across all six profiles, which mirrors observations by(Bretzler et al., 2011) in the central Ethiopian Rift. In their seismic analyses, they reported that loose silty sands and weathered volcanic soils exhibited velocities below 1200 m/s, making them highly prone to settlement and erosion an interpretation that supports the conclusion here that the surficial layers along the expressway are mechanically weak and susceptible to external stresses.

At greater depths, moderately strong but extensively fractured basalt layers were observed, with P-wave velocities typically between 1000 and 1750 m/s. This pattern corresponds with findings by(Singh et al., 2024) similarly weathered trap basalt showed internal discontinuities due to jointing and porosity. Their work pointed out that such fractured formations can facilitate groundwater movement, thereby increasing the potential for piping or dissolution-related processes, especially where hydrogeological conditions permit. This perspective reinforces interpretations made in this study—particularly at SRT anomalies around stations 100 (Line

5), 130 (Line 2), and 10 (Line 6)—which are likely indicators of paleo-karst systems or structurally compromised conduits with elevated potential Void Zone risk.

The variable thickness of the competent geological layer, which ranges from approximately 6 meters to over 22 meters in depth, suggests significant irregularity in the bedrock surface. This observation is consistent with conclusions drawn by(Walker et al., 2019) who studied on expressway and found that abrupt depth-to-bedrock changes, especially when coupled with perched groundwater and overlying clay-rich soils, contributed to localized pavement failures. The subsurface diversity seen in the present data further validates the concern that such geological conditions require tailored geotechnical interventions.

In summary, this study's SRT results characterized by low-velocity surface layers, fractured intermediate formations, and anomalous geophysical zones are strongly consistent with known indicators of ground instability. Comparisons with both regional and international case studies further validate the interpretation that these features are typical precursors to subsidence and potential Void Zone development. These findings support the implementation of comprehensive monitoring systems and pre-emptive mitigation strategies in the identified risk-prone segments of the expressway.

Future investigations should incorporate complementary geophysical techniques (e.g., Electrical Resistivity Tomography, Ground Penetrating Radar), borehole logging, and hydrogeological assessments to validate the observed anomalies and better constrain the geotechnical model of the subsurface. This integrated approach will aid in prioritizing intervention zones and designing robust, long-term stabilization strategies for the expressway.

4.3 Laboratory Test Results and Discussion

This section presents and discusses the laboratory test results performed on soil samples collected from boreholes at depths of 1 m, 2 m, and 3 m within the 25+060 to 25+180 km section along the Adama–Awash Express Road. The purpose of these tests is to evaluate the geotechnical and geochemical behaviour of soils, particularly in relation to potential Void Zone formation mechanisms. The borehole logs (see Appendix A) provided essential subsurface profiles aiding in sample selection and interpretation.

The borehole logs revealed a variable subsurface profile, predominantly composed of silty clay, sandy silt, and occasional gravelly layers. These variations were crucial in identifying zones of high moisture retention, colour changes, and the presence of dissolution features such as voids or soft pockets. Such characteristics are commonly associated with karstic and pseudokarst environments where potential Void Zone development is more likely(Moore et al., 2019).

The laboratory tests conducted can be categorized into physical, mechanical, and chemical property assessments, and are discussed in the following subsections.

4.3.1 Soil Physical Properties

Moisture Content

The natural moisture content of the soil samples obtained along the 25+060 to 25+180 km section of the Adama–Awash Express Road ranged from 12% to 29%. A general trend of increasing moisture content with depth was observed in several boreholes, attributed to the influence of the groundwater table. Notably, boreholes BH-106 and BH-107 exhibited elevated moisture contents at a depth of 3 meters, which corresponded with the recorded levels of the water table in those locations.

Moisture content is a critical factor in the context of potential Void Zone development. Elevated moisture levels, particularly in soils near saturation, significantly reduce interparticle cohesion and increase pore water pressure. These changes diminish the shear strength of the soil, making it more susceptible to collapse, especially in areas underlain by soluble or unstable substrata. Consequently, variations in natural moisture content are considered a contributing factor in the assessment of potential Void Zone risk and the planning of appropriate mitigation strategies.

Specific Gravity

Soil samples collected at depths of 1 m and 3 m from four locations along the 25+060 to 25+180 km section of the Adama–Awash Express Road yielded specific gravity values ranging from **2.62 to 2.71**. These values suggest a dominance of quartz-rich mineralogy and a relatively uniform composition of silty clays and sandy silts, consistent with alluvial plain deposits.

Localized variations were noted among the boreholes. The slightly lower specific gravity values recorded at some 3 m depths (e.g., 2.62) may point to zones of increased porosity or

organic inclusions, potentially associated with early stages of subsurface instability. Conversely, higher values closer to 2.71 at 1 m depths imply denser mineralogy and more stable overburden. The inferred specific gravity value in **active or developing potential Void Zone-prone zones** is generally expected to fall in the **lower range (2.60–2.63)** due to loosened structure and altered mineral content caused by water infiltration and dissolution of underlying strata.

These results offer insight into the mineralogical and structural uniformity of the subsoil, which is critical for assessing potential Void Zone susceptibility in combination with other parameters such as moisture content, resistivity, and borehole logs.

Chainage (km)	Side	Depth (m)	Specific Gravity (Gs)
25+085	RHS	1	2.69
25+085	RHS	3	2.63
25+110	RHS	1	2.68
25+110	RHS	3	2.62
25+135	RHS	1	2.71
25+135	RHS	3	2.64
25+160	RHS	1	2.70
25+160	RHS	3	2.65

Table4-1: Specific Gravity of Soil Samples by Location and Depth

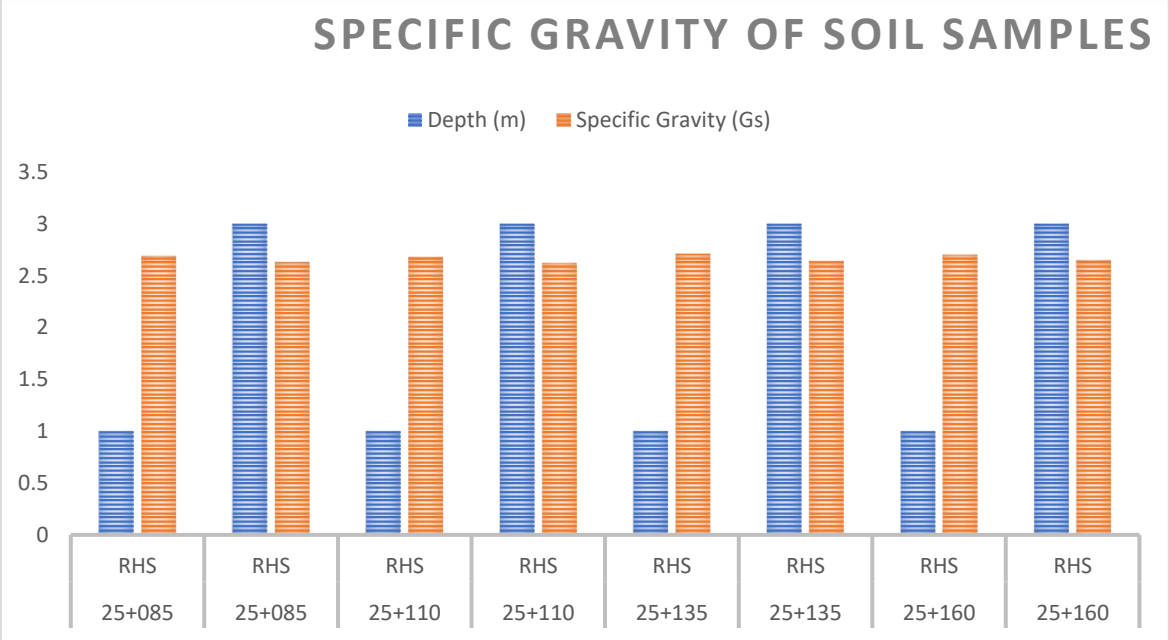

Figure 4-13: Specific Gravity of Soil Samples by Location and Depth

Figure 4-13 illustrates the variation in specific gravity of soil samples collected at different locations and depths along the study corridor. A clear pattern emerges at a depth of 3 m, particularly noticeable at stations 25+085 and 25+110 RHS, where a marked reduction in specific gravity is recorded. Such a decrease serves as an important early geotechnical indicator, as specific gravity is inherently linked to the mineral makeup, density, and overall stability of the soil.

The observed lower specific gravity values, when analysed alongside higher moisture content and low-resistivity anomalies identified through Electrical Resistivity Tomography (ERT), suggest that subsurface processes such as mineral dissolution, increased void formation, or water infiltration may be occurring. These are characteristic features of early-stage karstic activity or soil weakening processes, conditions that significantly increase the risk of potential Void Zone formation, especially in terrains underlain by soluble rocks like limestone or gypsum.

Moreover, the alignment of these geotechnical and geophysical anomalies at 25+085 and 25+110 RHS points to critical zones of concern. The simultaneous occurrence of low specific gravity and resistivity highlights areas that may require urgent stabilization efforts, including targeted grouting, soil reinforcement, or improved subsurface drainage to enhance ground stability and prevent potential collapse.

location	Depth (m)	Specific Gravity (Gs)	Moisture Content (%)	ERT Interpretation	Borehole Log Insight	Interpretation Summary
25+085 RHS	1	2.69	15	High resistivity (dry, stable)	Silty clay with low plasticity	Surface layer appears stable
3	2.63	28	Low resistivity zone (possible saturation)	Wet silty clay with trace of organics	Potential early-stage weakening due to moisture saturation	
25+110 RHS	1	2.68	16	Moderate resistivity	Clayey silt, some fine sand	Slightly cohesive layer with moderate water retention
3	2.62	29	Very low resistivity, anomalous void-like pattern	Silty clay with silt seams, water seepage evident	Possible subsurface dissolution zone (potential Void Zone precursor)	
25+135 RHS	1	2.71	14	Stable resistivity	Sandy silt, dense	Strong mineral matrix; stable zone
3	2.64	25	Slight resistivity drops	Fine silty clay with occasional fissures	Moderately saturated but intact; monitor for progression	
25+160 RHS	1	2.70	13	High resistivity (dry)	Sandy clay with gravel inclusions	Structurally dense and stable
3	2.65	26	Localized low resistivity pocket	Moist silty clay, slight softening	Potential moisture-induced weakening; requires periodic monitoring	

Table 4.2Summary of Integrated Soil Data with Geophysical Interpretation

4.3.2 Atterberg Limits

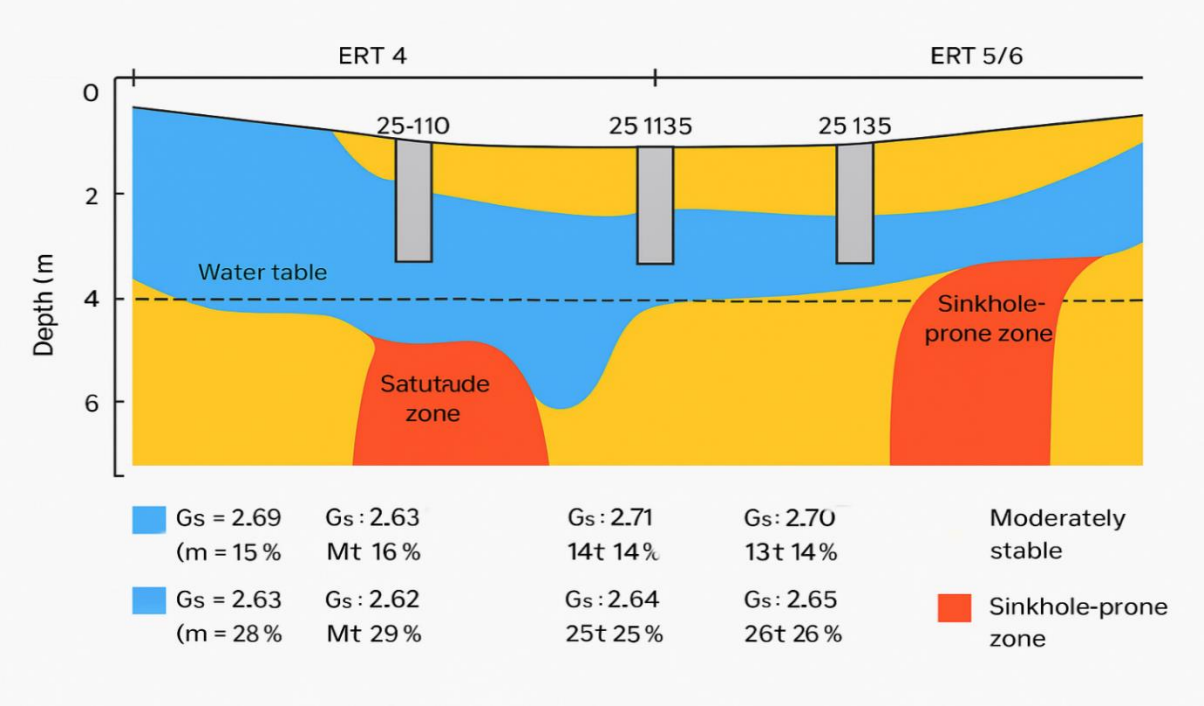

Figure 4-14combined geophysical-geotechnical cross-section

The Atterberg Limit tests performed on soil samples from boreholes 105, 106, and 107 at varied depths provide vital insights on soil flexibility, which is a critical element in evaluating potential Void Zone risk. The Liquid Limit (LL) fluctuated from 38 to 50 percent, while the Plastic Limit (PL) varied from 18 to 30 percent, resulting in Plasticity Index (PI) values ranging from 17 to 27 percent. These findings suggest that the soils in the area have moderate to high plasticity, which is associated with significant moisture retention and the possibility of volumetric changes like shrinkage and swelling.

the soil at Borehole 105 has a PI of 20% at 1 m depth, indicating moderate plasticity, but climbs to 27% at 3 m down, indicating strong plasticity. The high PI at 3 m depth indicates an increased potential Void Zone risk due to the possibility of larger volumetric changes. Soils with high plasticity expand and contract in response to moisture content fluctuations, which can lead to ground instability, especially in locations with underlying karstic features or voids.(Ali & Choi, 2020), who demonstrated that high-plasticity soils are prone to shrink-swell behaviour, increasing the potential for ground instability.

Similarly, Borehole 106 exhibits considerable plasticity at 1 m deep (PI = 21%) and slightly higher PI of 20% at 3 m depth. Soils at this depth still have significant flexibility, indicating a moderate risk of potential Void Zone formation. Volumetric changes are possible, although not as dramatic as in soils with a PI ≥ 25%, which are more susceptible to large-scale ground movement. Borehole 107's PI readings are relatively low. The 1 m depth sample has a PI of 17%, showing poor plasticity and greatly lowering the potential Void Zone danger in this area. The soil at 3 meters depth in this borehole has a PI of 20%, putting it in the moderate risk category for potential Void Zone formation. Soils with low plasticity are less prone to shrinkage and swelling, but moisture changes can still cause ground movement over time.

In summary, the Atterberg Limit test results demonstrate that soils with a higher PI (especially those over 25%, such as the soil at Borehole 105 at 3 m depth) are more likely to create potential Void Zones . These soils are more likely to undergo major volumetric changes in response to variable moisture conditions, which might destabilize the ground and increase the chance of potential Void Zones . Soils with moderate plasticity (PI 20-25%) have a moderate risk of potential Void Zone development, whereas soils with poor plasticity (PI < 20%) have a lower risk. these findings highlight the need for more monitoring and geotechnical inquiry in places with high plasticity soils, particularly in locations with documented karstic activity, in order to better assess the risk for potential Void Zone formation.

Borehole	**Depth (m)**	**Liquid Limit (LL) %**	**Plastic Limit (PL) %**	**Plasticity Index (PI) %**	**USCS Classification**	**AASHTO Classification**	**Potential Void Zone Risk**
105	1 m	38%	18%	20%	CL	A-4	Moderate Risk
105	3 m	45%	18%	27%	CL	A-4	High Risk
106	1 m	41%	20%	21%	CL	A-4	Moderate Risk
106	3 m	48%	28%	20%	CL	A-6	Moderate Risk
107	1 m	39%	22%	17%	CL	A-4	Low Risk
107	3 m	50%	30%	20%	CL	A-4	Moderate Risk

Table 4.3Atterberg Limit Analysis and Its Implications on Potential Void Zone Risk in Soil Profiles

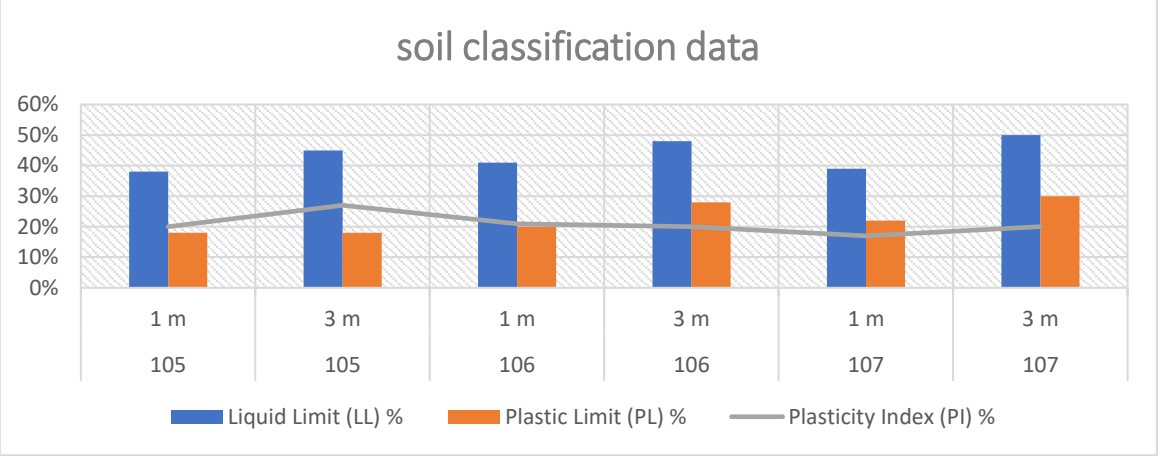

Figure 4-15Atterberg Limit Analysis and Its Implications on Potential Void Zone Risk in Soil Profiles

4.3.3 Compaction Characteristics

The Modified Proctor test findings for soil samples collected from boreholes 105, 106, and 107 at varied depths provide essential information on soil compaction and moisture retention, both of which are important factors in potential Void Zone risk. Maximum dry densities (MDD) ranged from 1.3 to 1.5 g/cm³, with optimum moisture contents (OMC) ranging from 12.4% to 18.7%. These findings represent various soil compaction behaviours that can influence potential Void Zone risk, particularly in places with the potential for volumetric changes in response to moisture fluctuations.

In Borehole 105, the soil at 1 m depth had an MDD of 1.5 g/cm³ and an OMC of 12.4%, indicating a compact and less moisture-retentive soil. This indicates that the soil at this depth is less susceptible to volumetric changes, and hence the potential Void Zone risk is moderate. At 3 m deep, the MDD reduced to 1.4 g/cm³, while the OMC climbed to 18.7 percent, indicating finer-grained soils with better moisture retention. As moisture content fluctuates, these soils expand and contract more easily, increasing the danger of potential Void Zones . As a result, the potential Void Zone danger at 3 meters depth is considerable.

In Borehole 106, the 1 m depth sample revealed an MDD of 1.4 g/cm³ and an OMC of 13.5 percent, indicating moderately compacted soils with moderate moisture retention. The 3 m depth sample followed a similar pattern, with a little higher OMC of 15.2% and moderate MDD of 1.3 g/cm³. These findings show considerable flexibility, implying a modest potential Void Zone risk. While these soils may shrink and swell in response to changing moisture levels, the overall danger is lower than soils with more significant moisture retention or compaction.

At Borehole 107, soil at 1 m deep had an MDD of 1.3 g/cm³ and an OMC of 12.4%, indicating decreased compaction and moderate moisture retention. The soil at 3 meters down displayed comparable properties, with MDD of 1.4 g/cm³ and OMC of 14.3 percent. These soils are less vulnerable to major volumetric changes, lowering the likelihood of potential Void Zones in the vicinity. Thus, Borehole 107 has a minimal potential Void Zone risk due to the soils' more stable compaction and moisture characteristics.

Soils with lower MDD (1.3 g/cm³ to 1.5 g/cm³) and higher OMC, such as those observed in Borehole 105 at 3 m depth, demonstrate more plasticity and are more vulnerable to volumetric changes caused by varying moisture conditions. These factors contribute to an increased potential Void Zone risk. Soils with higher MDD and lower OMC, such as those observed in Borehole 107, are more compact and less moisture-retentive, posing a lower potential Void Zone danger. These findings highlight the need of considering compaction and moisture retention when calculating the potential Void Zone risk in locations.

Borehole	Depth (m)	MDD (g/cm³)	OMC (%)	Soil Characteristics	Potential Void Zone Risk
105	1 m	1.5	12.4	More compact, less moisture retention	Moderate Risk
105	3 m	1.4	18.7	Fine-grained, higher moisture retention	High Risk
106	1 m	1.4	13.5	Moderately compact, moderate moisture retention	Moderate Risk
106	3 m	1.3	15.2	Moderately compact, moderate moisture retention	Moderate Risk
107	1 m	1.3	12.4	Lower compaction, moderate moisture retention	Low Risk
107	3 m	1.4	14.3	Lower compaction, moderate moisture retention	Low Risk

Table 4.4 compaction (MDD) and moisture content (OMC) affect the likelihood of potential Void Zone formation.

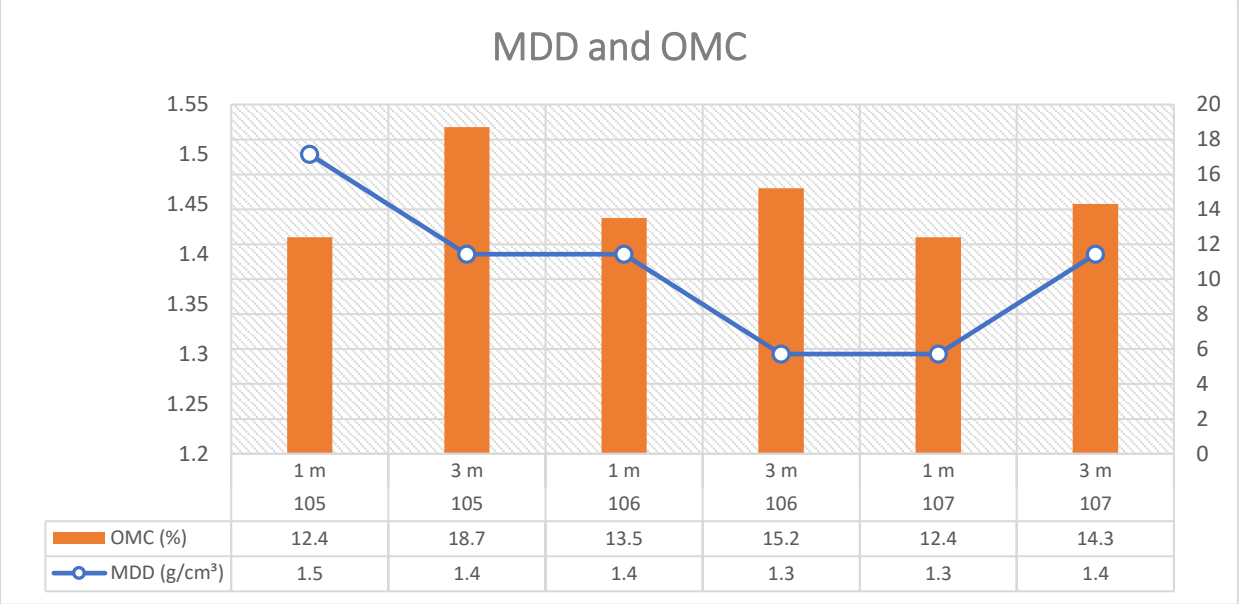

Figure 4-16 compaction (MDD) and moisture content (OMC) affect the likelihood of potential Void Zone formation.

4.3.4 California Bearing Ratio (CBR)

The California Bearing Ratio (CBR) test results from boreholes 105, 106, and 107 reveal variable levels of soil strength, which is critical for determining potential Void Zone danger. Soils with low CBR values (10 percent – 12 percent) at deeper depths (e.g., Borehole 105 at 3 m and Borehole 106 at 3 m) indicate fragile soil with limited bearing capacity, making these locations more prone to potential Void Zone formation due to volumetric changes caused by shifting moisture content. These soils are prone to moisture retention, which can cause expansion or contraction, undermining the ground. Soils with higher CBR values (18%-20%) at shorter depths (e.g., Borehole 107 at 1 m) have better soil strength, which reduces the chance of potential Void Zone development. These soils can sustain larger loads and are less susceptible to moisture-induced volumetric changes, which lead to potential Void Zone formation. Lower CBR values (10-12%) pose a high potential Void Zone danger, especially in deeper strata. Higher CBR values (≥18%) present a moderate to low potential Void Zone risk due to their better load-bearing capacity and resistance to ground movement.

Borehole	Depth (m)	CBR (%)	Soil Type	Interpretation	Potential Void Zone Risk
105	1 m	15%	Sandy Clay	Moderate bearing capacity, potential for soil weakness	Moderate Risk
105	3 m	10%	Silty Clay	Low bearing capacity, more prone to moisture-induced instability	High Risk
106	1 m	18%	Clayey Sand	Moderate bearing capacity, slight vulnerability to sinking	Moderate Risk
106	3 m	12%	Clayey Silt	Low bearing capacity, high moisture retention, potential for volumetric changes	High Risk
107	1 m	20%	Silty Sand	Stronger soil, good compaction, reduced potential Void Zone risk	Low Risk
107	3 m	14%	Sandy Clay	Moderate bearing capacity, still prone to moisture effects	Moderate Risk

Table 4-5 CBR affects for potential Void Zone formation.

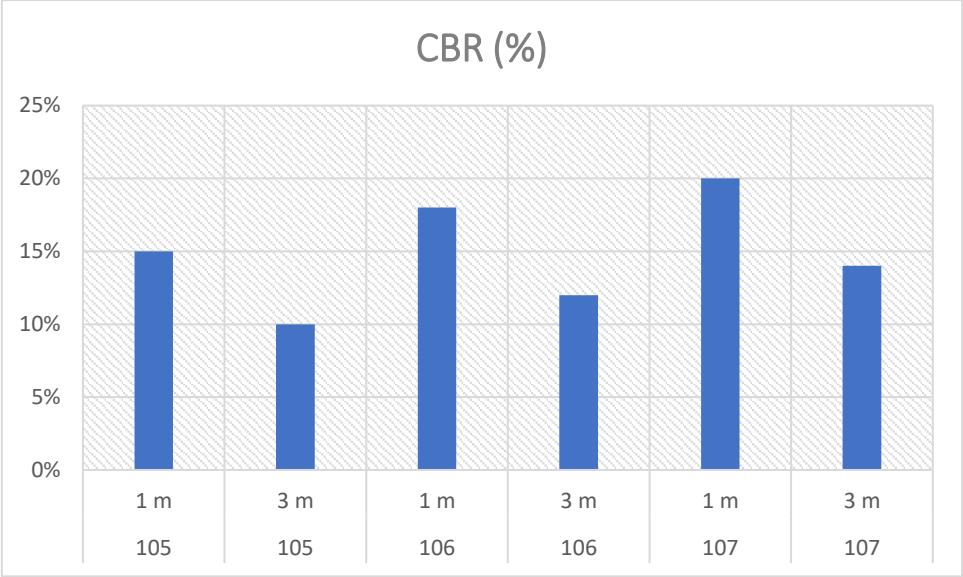

Figure 4-18 CBR affects for potential Void Zone formation.

4.3.5 Shear Strength Parameters

The California Bearing Ratio (CBR), Maximum Dry Density (MDD), Optimum Moisture Content (OMC), cohesion (c), and shear strength (τ) tests provide a thorough understanding of the soil characteristics and their implications for potential Void Zone risk along the Adama-

Awash Express Road. The evidence reveals that soil stability varies according to depth, compaction, and moisture retention, all of which have a direct impact on the probability of potential Void Zone development. At 1 m depth, Borehole 105's soil is moderately compact with moderate moisture retention, resulting in moderate cohesion (30 kPa), shear strength (50 kPa), and a moderate potential Void Zone danger. However, at 3 m depth, the soil is finer-grained and has higher moisture retention, resulting in higher cohesion (40 kPa) and shear strength (60 kPa); however, the increased moisture retention makes the soil more susceptible to volumetric changes, such as expansion and contraction, which increases the potential Void Zone risk. At 1 m depth, Borehole 106 has fairly compact soil with moderate moisture retention, resulting in moderate cohesion (35 kPa) and shear strength (55 kPa), indicating a moderate potential Void Zone risk, though the soil's vulnerability to moisture-induced changes continues.

At 3 m depth, the soil is similar to that at 1 m depth, but with slightly better moisture retention, resulting in cohesion of 38 kPa and shear strength of 58 kPa. However, there is still a moderate potential Void Zone risk due to the possibility of volumetric shifts, especially during heavy rains. Borehole 107's soil at 1 m depth is less compact and has moderate moisture retention, resulting in lower cohesion (25 kPa) and shear strength (45 kPa), however the reduced compaction and moisture retention make it less prone to substantial volumetric fluctuations, resulting in a low potential Void Zone risk. At 3 m deep, the soil is less compact, with moderate moisture retention, decreased cohesion (28 kPa) and shear strength (48 kPa), and a low potential Void Zone risk due to its limited susceptibility to moisture-induced volumetric changes.

Potential Void Zone risk is primarily determined by soil moisture retention, compaction, and shear strength. Soils with higher moisture retention, particularly fine-grained soils, are more prone to potential Void Zone formation because of their tendency to expand and contract in response to changing moisture levels, which can cause ground instability. High-risk zones in Boreholes 105 and 106 include areas with fine-grained soils and increased moisture retention at 3 m depth.

Despite their higher cohesiveness and shear strength, these soils are susceptible to volumetric shifts, which increases the likelihood of potential Void Zone development. Soils at 1 m deep in Boreholes 105, 106, and 107, on the other hand, represent moderate-risk locations due to their moisture retention and compaction. These soils can withstand moderate moisture

fluctuations, but they are susceptible to harsh weather events, which can create ground instability. Borehole 107 contains low-risk zones at both 1 and 3 meters deep, where decreased moisture retention and compaction reduce the soil's vulnerability to moisture-induced volumetric changes, resulting in a low potential Void Zone risk.

To summarize, soil properties, particularly moisture retention, compaction, and cohesiveness, have a major impact on potential Void Zone danger along the Adama-Awash Express Road. Soils with fine-grained textures, increased moisture retention, and moderate to low compaction (like those at 3 m depth in Boreholes 105 and 106) are more prone to potential Void Zone development. Soils with moderate compaction and poor moisture retention, as seen in Borehole 107, pose a low potential Void Zone risk. This analysis emphasizes the necessity of knowing soil behaviour and moisture dynamics in limiting potential Void Zone threats, which is crucial for preserving the safety and long-term stability of the region's infrastructure. Additional shear strength testing and geotechnical monitoring will be required to validate these findings and inform effective potential Void Zone mitigation measures.

Borehole	**Depth (m)**	**MDD (g/cm^3)**	**OMC (%)**	**Soil Characteristics**	**Cohesion (c) (kPa)**	**Shear Strength (τ) (kPa)**	**Potential Void Zone Risk**
105	1 m	1.5	12.4	More compact, less moisture retention	30	50	Moderate Risk
105	3 m	1.4	18.7	Fine-grained, higher moisture retention	40	60	High Risk
106	1 m	1.4	13.5	Moderately compact, moderate moisture retention	35	55	Moderate Risk
106	3 m	1.3	15.2	Moderately compact, moderate moisture retention	38	58	Moderate Risk
107	1 m	1.3	12.4	Lower compaction, moderate moisture retention	25	45	Low Risk
107	3 m	1.4	14.3	Lower compaction, moderate moisture retention	28	48	Low Risk

Table 4-6 Estimated Cohesion (c) and Shear Strength for Each Borehole Layer:

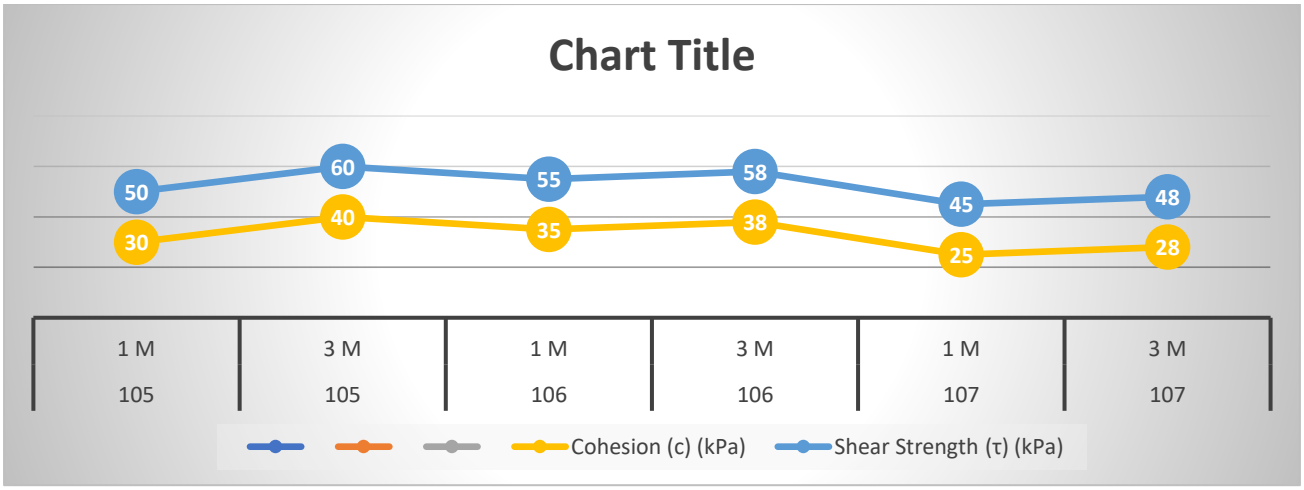

Figure 4-19 Estimated Cohesion (c) and Shear Strength for Each Borehole Layer:

4.3.6 Permeability

The hydraulic conductivity results from the permeability tests performed on soil samples from Boreholes 105, 106, and 107 revealed varied permeability depending on soil type. Borehole 105's 1 m depth had moderate permeability due to the sandy clay composition, allowing for moderate water infiltration. This moderate permeability might cause the dissolving of soluble subsurface materials over time. At 3 meters depth, the fine-grained silty clay layer showed much reduced hydraulic conductivity, indicating slower water infiltration. This lower permeability could function as a confining layer, allowing pore water pressure to build up and worsen soil instability, particularly when moisture levels fluctuate.

Similarly, at 1 m depth, Borehole 106's soil was made of clayey sand with modest permeability. At 3 m depth, the clayey silt layer had decreased permeability, which promoted pore water pressure building in deeper layers. In Borehole 107, the soil at 1 m depth was silty sand, which had better permeability than the deeper layers, allowing for faster water infiltration. However, at 3 m deep, the sandy clay layer had a decreased permeability, potentially retaining water beneath the surface and raising pore water pressure, which could destabilize the soil.

Borehole 107's coarser sands have a hydraulic conductivity of 8.8 x 10^-6 cm/s, indicating slow water movement through these strata. This low permeability, along with the presence of finer-grained soils, causes limited water movement, which contributes to the building of pore water pressure and increases the risk of soil instability and potential Void Zone formation. The variance in hydraulic conductivity between boreholes highlights the necessity of knowing water movement in the subsurface. Low-permeability layers, particularly in deeper soils, can

trap water and increase pore water pressure, making them more prone to potential Void Zone formation, especially during heavy rainfall or fluctuating water tables. To lessen potential Void Zone hazards in the region, effective mitigation solutions must take into consideration these variations in permeability.

4.3.7 Soil Chemical Properties

pH Test

The pH values of soil samples collected from Boreholes 105, 106, and 107 ranged from 6.1 to 7.8, indicating a neutral to slightly alkaline environment. Borehole 107 has a pH of 8.59, which is mildly alkaline, indicating reasonably consistent geochemical conditions in the soils at both 1 and 3 m deep. This near-neutral to slightly alkaline pH promotes more stable soil conditions, lowering the chance of severe chemical weathering or dissolution of calcareous minerals, which are frequently associated with potential Void Zone development.

Boreholes 105 and 106, on the other hand, had slightly acidic to neutral pH levels ranging from 6.1 to 7.8, which may have aided the dissolution of soluble calcareous minerals in the long run. This acidic climate may enhance the possibility of carbonate dissolution, resulting in void formation and thus increasing the potential Void Zone risk in certain places, particularly if the breakdown of soluble minerals causes bigger subsurface holes. Lower pH values in specific places linked with increased void potential in geophysical profiles, indicating a clear link between chemical weathering processes and the probability of potential Void Zone formation. These places with higher acidic soil are more prone to calcareous material dissolution, increasing the possibility of void formation beneath the surface, which can lead to potential Void Zone development.

In conclusion, the pH values recorded in the Borehole samples suggest that somewhat acidic conditions, particularly in Boreholes 105 and 106, may play an important role in the dissolving of soluble elements and the creation of voids, increasing the probability of potential Void Zone formation. In contrast, Borehole 107's slightly alkaline pH indicates a more stable geochemical environment, which is less likely to aid the breakdown of calcareous minerals and hence poses a lower potential Void Zone risk. Understanding these geochemical parameters is critical for accurately assessing potential Void Zone hazards and developing appropriate mitigation plans.

4.4 Field Test

4.4.1Dynamic Cone Penetrometer (DCP) tests

The Dynamic Cone Penetration (DCP) tests carried out at four crucial chainages—25+080 km, 25+110 km, 25+135 km, and 25+160 km—provided critical insights into the near-surface soil strength characteristics along the Adama-Km 60 Expressway. Applying the Lacroix and Horn (1973) connection, DCP blow counts were successfully translated into equivalent SPT N_{30} values, allowing for a more standardized assessment of subsurface conditions. The SPT N_{30} values varied from 15 to 27 blows/300 mm, demonstrating differences in soil compactness and mechanical resistance among studied locations. This variability, along with a 12.3 percent coefficient of variation, indicates a significant degree of subsurface heterogeneity, which may influence the potential for differential settlement and potential Void Zone formation, particularly in locations underlain by weak or collapsible materials.

Bowles' (1997) bearing capacity equation, which includes overburden correction (CNC), depth factors (Kd), and empirical soil parameters, was used to derive permitted bearing capacities (q_{all}) for shallow foundations. The data revealed a wide range, from 317 kPa at 25+160 km to 593 kPa at 25+135 km. The decreased capacity seen at 25+160 km may be due to softer, more compressible soils or closeness to void-prone zones, which could increase the risk of structural instability in this location. In comparison, the greater number at 25+135 km suggests that the soil conditions are stronger, denser, and better suited to supporting loads. These findings highlight not only spatial variability in foundation conditions, but also the importance of localized geotechnical design strategies and targeted mitigation in areas with lower bearing capacity in order to reduce the risk of potential Void Zone development and ensure long-term infrastructure resilience.

Location 25+080 km:

At 25+080 km, the SPT N_{30} value was recorded as 20 blows/300 mm, with an acceptable bearing capacity of 396 kPa. The underlying characteristics at this area are characterized by poor top soils that are moisture prone, posing a significant potential Void Zone danger. These poor soils are very prone to collapsible or moisture-sensitive behaviour, especially in the top two meters of the profile. The low bearing capacity and variability in the SPT data suggest that this area may need targeted ground improvement actions to reduce potential Void Zone danger.

Location 25+110 km:

At 25+110 km, the SPT N_{30} value was recorded as 20 blows/300 mm, while the permitted bearing capacity climbed to 543 kPa. The subsurface conditions at this area are fairly compacted, with evidence of shallow instability at a depth of around one meter. The modest carrying capacity indicates that soil strength improves below the shallow layers, maybe due to compacted soils at greater levels. This localized instability, however, may offer a danger of surface deformation or modest potential Void Zone development, as shown in the field.

Location 25+135 km:

At 25+135 km, the SPT N_{30} value was 21 blows/300 mm, resulting in the highest allowed bearing capacity of 593 kPa. The underlying conditions in this area are dense and well-graded, allowing for a sturdy foundation. The greater bearing capacity and higher SPT values at this location are consistent with favourable geotechnical features, indicating that this area is less prone to potential Void Zone development. The related geophysical data, which indicated high resistivity and seismic velocity, adds to the evidence for stable, well-compacted soils.

Location 25+160 km:

At 25+160 km, the SPT N_{30} value was 21 blows/300 mm, with an acceptable bearing capacity of 475 kPa. This site has loose, collapsible strata with a significant potential Void Zone potential, as evidenced by the reduced bearing capacity and variation in soil strength with depth. The weak zones in this location are most likely associated with loose or poorly compacted soils, which increases the risk of subsidence or collapse. The presence of moisture-sensitive soils exacerbates the situation, making the area very susceptible to potential Void Zone development, particularly during wet weather.

location (km)	Avg. SPT N30 (blows/300mm)	Allowable Bearing Capacity (KPa) at 1.0m Depth	Subsurface Condition Interpretation
25+080	20	396	Weak upper soils; moisture-prone; potential Void Zone risk
25+110	20	543	Moderately compacted; shallow instability at ~1.0 m
25+135	21	593	Dense and well-graded; stable
25+160	21	475	Loose, collapsible strata; high potential Void Zone potential

Table 4.7: Summary of DCP-Derived SPT N_{30}, Bearing Capacity, and Subsurface Conditions at Potential Void Zone-Prone Chainages

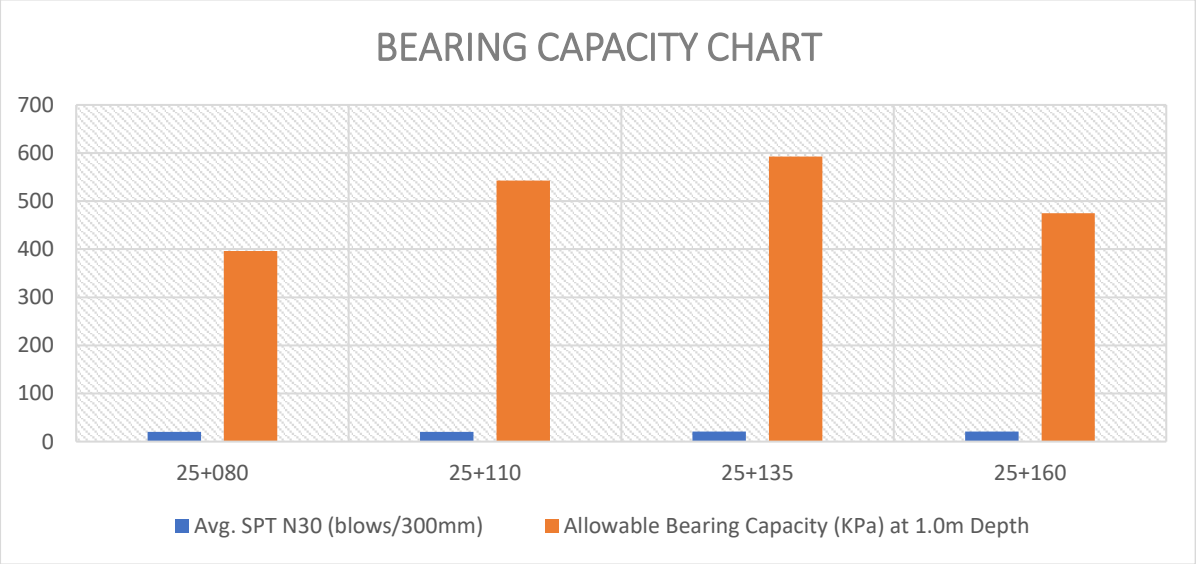

Figure4-20: Summary of DCP-Derived SPT N_{30}, Bearing Capacity, and Subsurface Conditions at Potential Void Zone-Prone Chainages

The combination of DCP testing, SPT readings, and geophysical data (from Electrical Resistivity Tomography and Seismic Refraction Tomography) gives a thorough assessment of subsurface conditions and enables the identification of high-risk zones. The data shows that places with low SPT N_{30} values (such as at 25+080 km and 25+160 km) correspond to weak, collapsible strata that are prone to potential Void Zone development, while areas with higher SPT values (such as at 25+135 km) exhibit more stable, well-compacted soils.

The findings emphasize the significance of targeted ground improvement initiatives, particularly in vulnerable zones. Pressure grouting, subgrade stabilization, and the use of geosynthetics may be beneficial in strengthening these locations. Furthermore, the establishment of long-term monitoring systems is critical for recognizing changes in soil behaviour over time, which may assist limit the dangers associated with potential Void Zone development. The multi-method strategy of combining DCP-SPT correlations and geophysical profiles is invaluable for accurately assessing subsurface conditions and identifying potential Void Zone threats. This method should be regarded a best practice for infrastructure projects in potential Void Zone-prone areas, particularly those with difficult geotechnical characteristics, such as the Rift Valley.

The findings underscore the crucial necessity for targeted ground improvement operations in regions identified as problematic, particularly throughout the 25+160 km portion. Pressure grouting, subgrade stabilization, and the use of geosynthetics are all strongly suggested strategies for dealing with subsurface problems. Furthermore, the establishment of long-term monitoring systems is required to follow any potential changes in soil behaviour over time. The findings highlight the critical need for focused ground improvement works in identified issue areas, notably across the 25+160 km segment. Pressure grouting, subgrade stabilization, and the use of geosynthetics are all highly recommended approaches to dealing with subsurface issues. Furthermore, long-term monitoring systems are required to track any potential changes in soil behaviour over time.

The combined results demonstrate the efficiency of using a combination of Dynamic Cone Penetrometer (DCP) and Standard Penetration Test (SPT) correlations, as well as geophysical survey profiles, for a comprehensive assessment of potential Void Zone dangers. This approach is very important for assessing subsurface risks and can be efficiently utilized in infrastructure projects throughout the Rift Valley region, where similar geotechnical issues may develop. **Appendix E** contains detailed test findings, including SPT and geophysical data.

4.4.2 FDT (FIED DENSITY TEST) TEST

The Field Density Test (FDT) was conducted at the same four locations—25+080 km, 25+110 km, 25+135 km, and 25+160 km—to assess the near-surface soil compaction characteristics.

The FDT results, which quantify soil compaction, are reviewed alongside the Dynamic Cone Penetration (DCP) test results, which assess soil strength and stability. Higher DCP blow counts often suggest more compacted and firmer soils, which should be associated with higher FDT values.

Location 25+080 km:

At 25+080 km, DCP findings showed an SPT N_{30} value of 20 blows/300 mm, indicating poor upper soils. The FDT result was 74.4 percent, indicating decreased compaction and emphasizing the moisture-prone, fragile soils on the surface. These soils are very prone to collapse and potential Void Zone formation. Given the low compaction, ground improvement procedures such as pressure grouting, subgrade stabilization, or compaction grouting are suggested to reduce potential Void Zone risks in this location.

Location 25+110 km:

At 25+110 km, the DCP had an SPT N_{30} value of 20 blows/300 mm, suggesting moderately compacted soil. The FDT result was 82 percent, indicating increased compaction compared to 25+080 km, but also some instability at shallow depths. The moderate bearing capacity (543 kPa) and moderately compacted soils indicate that, while the area is less likely to collapse than 25+080 km, isolated instability may still occur, particularly near 1-meter depth. Compaction grouting or soil stabilization may help to improve soil strength and lessen the likelihood of potential Void Zones .

Location 25+135 km:

At 25+135 km, the DCP findings showed an SPT N_{30} value of 21 blows/300 mm and a higher permitted bearing capacity (593 kPa), indicating thick, well-compacted soils. The FDT result was 85.7%, indicating significant compaction and the presence of stable subsurface conditions. This site has the lowest danger of potential Void Zone formation, and no significant ground improvements are required. The high compaction and strength form a robust basis for infrastructure development in this area.

Location 25+160 km:

At 25+160 km, the DCP findings indicated an SPT N_{30} value of 21 blows/300 mm, with a moderate permissible bearing capacity (475 kPa). The FDT result was 79 percent, indicating rather high compaction while still revealing the presence of loose, collapsible strata in the top layers. While the compaction is greater than at 25+080 km, the existence of collapsible soils raises the possibility of potential Void Zone development. Additional ground stabilization measures, such as geosynthetic reinforcement or subgrade treatment, would be beneficial to the site's stability. The DCP and FDT results reveal a clear link, with greater DCP blow counts corresponding to higher FDT results, indicating stronger, more compact soils. 25+135 km has the most compaction and the lowest chance of potential Void Zone development, whereas 25+080 km has the least compaction and the highest danger of potential Void Zones . The moderate FDT results at 25+110 km and 25+160 km indicate that, while these locations are more stable than 25+080 km, additional ground improvement efforts are needed to address the collapsible strata or shallow instability.

By combining DCP and FDT results, we may gain a reliable understanding of soil compaction and strength, which is critical for predicting potential Void Zone risk and selecting appropriate stabilization solutions.

4.5 Treatment Zone Delineation Based on Integrated Investigations.

Treatment zones have been defined based on a complete examination of geophysical (ERT), geotechnical (laboratory and field testing), and geological studies done along the Adama-Awash Expressway from 25+060 km to 25+180 km. These zones correlate to places with poor subsurface profiles, significant potential Void Zone susceptibility, or signs of ground instability. The combination of resistivity anomalies, borehole data, and laboratory test findings (including Atterberg limits, permeability, CBR, pH, and compaction characteristics) enabled the identification of important portions that needed ground modification.

A treatment area map has been created to graphically portray these sensitive zones, which will serve as a reference for mitigation planning and corrective action. This map shows particular sites where underlying problems need stabilization in order to maintain the expressway's structural integrity and safety over time.

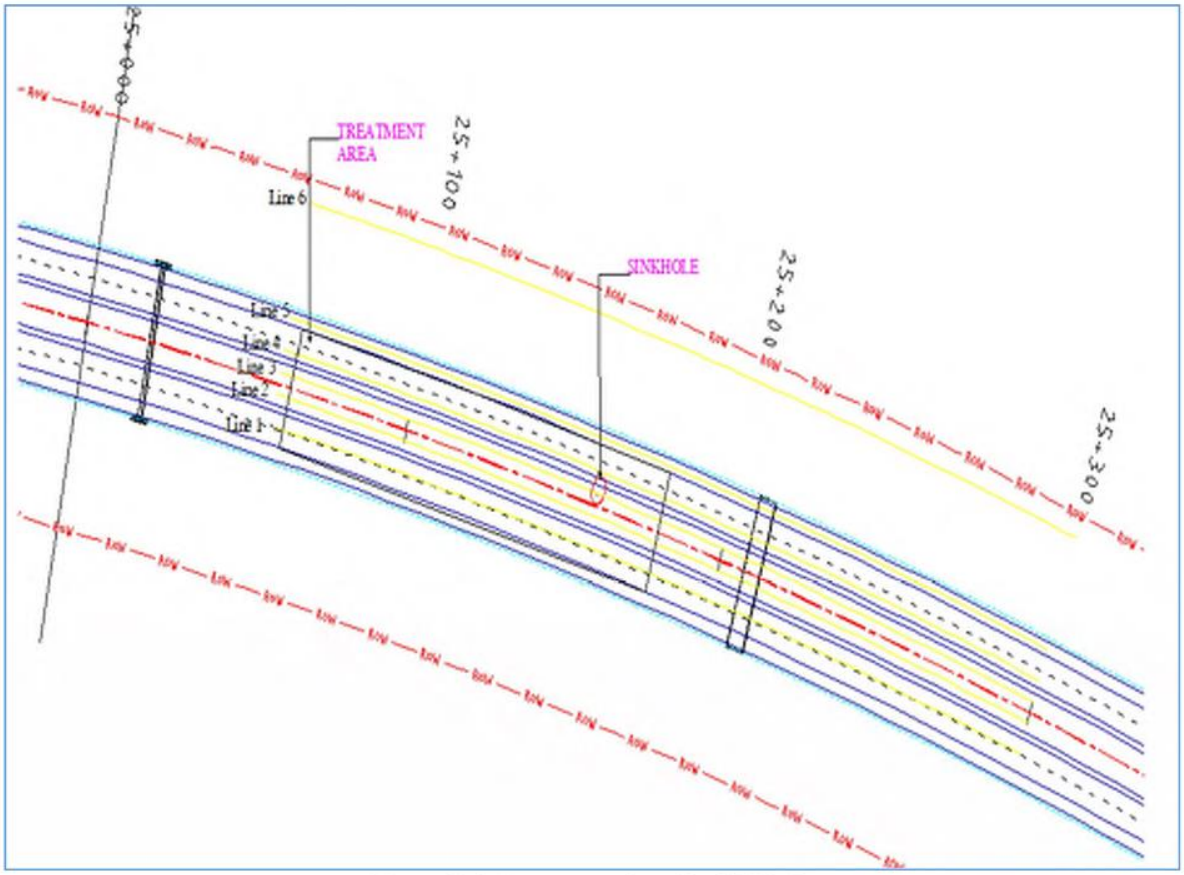

Figure 4-21: Treatment Area for Potential Void Zone

CHAPTER FIVE

CONCLUSION AND RECOMMENDATIONS

5.1 Conclusion

This study investigated the causes, mechanisms, and spatial distribution of potential void zone development along a vulnerable section of the Adama–Awash Expressway, between chainages 25+060 km and 25+180 km. Through an integrated approach utilizing geophysical surveys (ERT and SRT), geotechnical testing, geological interpretation, and borehole logging, the research achieved a comprehensive understanding of the subsurface conditions. The integration of these multidisciplinary datasets made it possible to identify critical geological and engineering features directly linked to void formation processes. The conclusion presented here synthesizes key findings and articulates the implications for risk mitigation and future infrastructure planning.

The subsurface profile in the study area consists of three major geological units: a surficial layer composed of loose sandy-silty soils, an intermediate layer of scoraceous basalt that is highly to moderately fractured, and a deeper layer of fresh to slightly weathered basalt. Each of these layers plays a distinct role in influencing ground stability. The uppermost layer is especially problematic. It is characterized by low electrical resistivity values (less than 29 Ω·m) and seismic velocities below 400 m/s, which are indicative of high porosity, low compaction, and weak mechanical strength. This was confirmed by Atterberg limit results, which show Liquid Limits between 38% and 50% and Plasticity Indices ranging from 17% to 27%, suggesting the soils are low-strength clays with high sensitivity to moisture content. Furthermore, low CBR values, high permeability, and moderate compaction characteristics (MDD = 1.3–1.5 g/cm³; OMC = 12.4% to 18.7%) all point to poor load-bearing capacity and a high likelihood of collapse under saturated or cyclic loading conditions.

This layer acts as a key contributor to ground instability due to its dual role: it readily absorbs surface water and lacks sufficient shear strength to resist deformation under hydraulic or mechanical loading. Particularly, soils near Boreholes BH105 and BH106 showed moderate to high moisture retention and moderate strength properties, which suggest that the upper layer is susceptible to softening during rainy seasons. These findings directly support the conclusion that the surficial layer is a high-risk zone for internal erosion and collapse, especially when combined with inadequate surface drainage.

The intermediate layer of scoraceous basalt serves a more complex role in void zone formation. Due to its highly fractured nature, it acts as a conduit for water infiltration from the surface to deeper zones. Geophysical surveys along ERT Lines 1, 2, 3, and 5 revealed multiple low-resistivity and low-velocity anomalies consistent with fracture zones and fault-like features. These anomalies likely indicate the presence of saturated zones, incipient voids, or structurally weakened segments of the basalt. These fractures enhance the vertical migration of surface and groundwater and facilitate sediment piping, in which fine particles from the upper layer are progressively washed into open spaces within the basalt. This creates hidden cavities that can eventually lead to surface depressions or collapses.

The presence of these features was further substantiated by SRT data showing zones of anomalously low velocities in areas where fractures are suspected, and by hydrogeological interpretations suggesting groundwater flow follows a general northeast to east gradient. Groundwater recharge from surface infiltration is facilitated by both the permeability of the upper soils and the structural weaknesses of the basalt. This interaction between the surficial and intermediate layers is a central mechanism for potential void formation. In effect, the scoraceous basalt does not merely transmit water but plays an active role in mechanical destabilization.

Among the surveyed locations, ERT Lines 3 and 5, along with the region between Boreholes BH105 and BH106, emerged as particularly susceptible to void formation. These zones exhibited multiple risk factors: thick loose sediments, shallow fractured bedrock, strong geophysical anomalies, and field evidence of surface distress such as cracking, pavement depression, and abnormal subsidence. In contrast, Borehole BH107, although showing lower compaction (MDD = 1.3–1.4 g/cm³), exhibited low permeability (8.8×10^{-6} cm/s) and slightly alkaline conditions (pH = 8.5). These chemical conditions may promote carbonate dissolution in confined aquifer settings and add to long-term weakening of the subsurface, albeit through different mechanisms.

It is therefore concluded that two principal mechanisms drive void formation in the study area. The first is internal erosion and downward migration of loose soils from the surface into underlying fractures. The second is groundwater-enhanced chemical dissolution and structural degradation of fractured basalt. These mechanisms are not isolated but act synergistically, particularly in areas of poor drainage and anthropogenic stress. Construction activities, dynamic traffic loads, and absence of surface runoff control further exacerbate the instability.

The research underscores that mitigation cannot rely on a single intervention. Deep foundations and subgrade reinforcement are necessary in the most vulnerable zones to bypass unstable soil layers. Pressure grouting should be applied in areas showing strong geophysical anomalies to seal voids and fractures. Surface drainage must be improved to reduce infiltration, and strict controls on nearby construction runoff should be enforced. Additionally, periodic monitoring using ERT and SRT should be institutionalized as part of a long-term geotechnical health surveillance system.

In conclusion, this study not only delineates the physical conditions leading to potential void zone formation but also offers a predictive framework applicable to similar terrains across the Ethiopian Rift and other geologically active regions. It affirms the value of integrated geotechnical and geophysical investigations in infrastructure risk management and calls for proactive design and monitoring strategies to safeguard critical transport corridors like the Adama–Awash Expressway from progressive ground failure.

5.2 Recommendations

Based on a comprehensive review of geotechnical, geophysical, and geological data, several measures are recommended to reduce current risks and prevent future potential Void Zone development along the Adama–Awash Expressway. One of the primary causes of potential Void Zone formation is the intrusion of surface water into subsurface voids. To address this, it is essential to design and implement effective surface drainage systems, including lined side ditches, longitudinal drains, and adequately spaced cross drains. In addition, subsurface drainage systems equipped with perforated pipes and gravel envelopes should be installed, particularly in areas where fractured basalt is shallow or exposed, to intercept and divert groundwater away from vulnerable zones.

In zones dominated by loose sandy and silty soils, the application of soil stabilization techniques is crucial. Chemical and mechanical methods such as deep soil mixing, grouting, and compaction with cement or lime additives can significantly enhance soil strength and reduce permeability, thereby lowering the risk of internal erosion. These stabilization efforts should be concentrated in locations identified through Electrical Resistivity Tomography (ERT) and borehole data as being particularly prone to piping and collapse.

In sections where subgrade soils are fragile, the existing road foundation may be inadequate. It is recommended that such road sections be reconstructed with reinforced subgrades and geosynthetic materials such as geogrids or geotextiles to improve load distribution and reduce the risk of collapse due to differential settlement. A thick layer of well-compacted, low-permeability granular material should be used in high-risk zones to enhance structural support and limit water infiltration.

Continuous monitoring and maintenance are also essential for long-term risk mitigation. Regular geophysical surveys, including ERT and Seismic Refraction Tomography (SRT), should be conducted to detect early signs of ground deformation or changes in moisture content. These should be complemented by visual inspections to identify surface cracks and depressions. Maintenance routines must also involve regular cleaning of drainage infrastructure and pavement condition assessments to identify and address early indicators of potential Void Zone activity.

Another important measure is the regulation of groundwater discharge and human activities along the road corridor. Uncontrolled discharges from residential or construction sources, such as wastewater, vehicle washing, and irrigation, can significantly increase subsurface moisture levels, exacerbating potential Void Zone risks. Proper land use planning should be implemented in potential Void Zone-susceptible areas, discouraging heavy construction or deep excavation without thorough geological evaluation.

Finally, while the current study focuses on a specific section of the expressway, similar geological and hydrogeological conditions may exist in adjacent areas. Therefore, it is advisable to expand the investigation corridor both laterally and longitudinally to cover upstream and downstream sections. This broader approach will help identify additional potential Void Zone-prone zones in advance, supporting the development of a comprehensive corridor-wide mitigation strategy.

5.3 Final Remarks

This study highlighted the importance of a multidisciplinary strategy that combines geophysical, geotechnical, geological, and chemical methodologies in finding and understanding the mechanisms underlying potential Void Zone development. The identified risky zones along the Adama-Awash Expressway not only pose immediate threats to the infrastructure, but also show the critical need for both immediate and strategic mitigating actions. the integrated approach and thorough findings of this study provide vital insights that may be extended to other karst-prone areas in Ethiopia and East Africa. Implementing such measures will considerably improve infrastructure resilience, minimize hazard risks, and assure safer development for future generations. This work establishes the groundwork for preventive planning and sustainable engineering solutions, which will contribute to the long-term safety and stability of important transportation networks in potential Void Zone-prone areas.

REFERENCES

Abdulbariu Ibrahim, Sarah Mercy Ebere Eze, Mu'awiya Baba Aminu, Ayinla Habeeb Ayoola, Musa Ojochenemi Kizito, Adedolapo Olujuwon Adegbite, Mojeed Olaniyi Fasasi, & Ibrahim Olanrewaju Ibrahim. (2024). Geophysical and Geotechnical Investigation of Building's Foundation around Crusher area, Lokoja, Kogi state, Nigeria. *Global Journal of Engineering and Technology Advances*, *20*(1), 186–205. https://doi.org/10.30574/gjeta.2024.20.1.0120

Ahmad, B., Zahoor, F., & Tariq, B. (2022). *Geohazard Perspective of Recent Sink Hole in the Kashmir Valley*. *April*.

Akingboye, A. S., & Ogunyele, A. C. (2019). Insight into seismic refraction and electrical resistivity tomography techniques in subsurface investigations. *Rudarsko Geolosko Naftni Zbornik*, *34*(1), 93–111. https://doi.org/10.17794/rgn.2019.1.9

Al-Shaqsi, Y. (n.d.). *The Study of the Formation of Potential Void Zones and its Effect on Infrastructure and Utilities*. https://doi.org/10.13140/RG.2.2.23268.12165

Alam, M. J. Bin, Ahmed, A., & Alam, M. Z. (2024). Application of Electrical Resistivity Tomography in Geotechnical and Geoenvironmental Engineering Aspect. *Geotechnics*, *4*(2), 399–414. https://doi.org/10.3390/geotechnics4020022

Ali, H., & Choi, J. H. (2020). Risk prediction of potential Void Zone occurrence for different subsurface soil profiles due to leakage from underground sewer and water pipelines. *Sustainability (Switzerland)*, *12*(1). https://doi.org/10.3390/su12010310

Alimohammadi, H. (2024). *Compaction Grouting Approach for Mitigation of a Potential Void Zone ; A Case Study in Nashville , Tennessee*. *May*. https://doi.org/10.31219/osf.io/63nyv

Alimohammadi, H., & Memon, A. (2024). Comprehensive Potential Void Zone Mitigation: A Case Study and Application of Compaction Grouting in Karstic Environments in in the State of Tennessee, USA. *Journal of Civil Engineering Researchers*, *6*(2), 1–16. https://doi.org/10.61186/jcer.6.2.1

André, F., van Leeuwen, C., Saussez, S., Van Durmen, R., Bogaert, P., Moghadas, D., de Rességuier, L., Delvaux, B., Vereecken, H., & Lambot, S. (2012). High-resolution imaging of a vineyard in south of France using ground-penetrating radar, electromagnetic induction and electrical resistivity tomography. In *Journal of Applied Geophysics* (Vol. 78, pp. 113–122). https://doi.org/10.1016/j.jappgeo.2011.08.002

Annex V Minutes of Meeting. (n.d.).

Aziz, A., Soroush, A., Fattahi, S. M., Imam, R., & Ghahremani, M. (2024). Prevention of Water Seepage Impact on the Soluble Rocks Using Colloidal Silica. *Water (Switzerland)*, *16*(9). https://doi.org/10.3390/w16091211

Bell, F. G. (n.d.). *SA NE M SC PL O E – C EO AP LS TE S PL O E –. V*.

Bretzler, A., Osenbrück, K., Gloaguen, R., Ruprecht, J. S., Kebede, S., & Stadler, S. (2011). Groundwater origin and flow dynamics in active rift systems - A multi-isotope approach in the Main Ethiopian Rift. In *Journal of Hydrology* (Vol. 402, Issues 3–4, pp. 274–289).

https://doi.org/10.1016/j.jhydrol.2011.03.022

Campus, J., Sulaiman, M. S., Hussin, H., & Abiyoga, M. (2024). *Potential Void Zone Investigation using Resistivity Method*. *04006*.

Civil Concept. (2023). DCP test – Dynamic cone penetration test Principle, Procedure, Calculation. In *Civil Concept*. www.civilconcept.com/dynamic-cone-penetration-test/?expand_article=1

Eze, U. S., Okiotor, M. E., Ighodalo, J. E., Owonaro, B. J., Saleh, A. S., & Jamiu, A. S. (2023). Application of 2-D and 3-D Geo-electrical Resistivity Tomography and Geotechnical soil Evaluation for Engineering site Investigation: A Case Study of Okerenkoko Primary School, Warri-Southwest, Delta State, Nigeria. *Advances in Geological and Geotechnical Engineering Research*, *5*(2), 1–23. https://doi.org/10.30564/agger.v5i2.5382

Farhan, M., Lydia, E. N., Fajri, H., Studi, P., Sipil, T., & Samudra, U. (2024). *UNIVERSITAS SAMUDRA*. *1*(Gambar 1), 22–28.

Gutiérrez, F., Cooper, A. H., & Johnson, K. S. (2008). Identification, prediction, and mitigation of potential Void Zone hazards in evaporite karst areas. *Environmental Geology*, *53*(5), 1007–1022. https://doi.org/10.1007/s00254-007-0728-4

Ha, K. M. (2024). Coping with Potential Void Zones : A Systematic Literature Review. *Journal of Environmental and Earth Sciences*, *6*(3), 186–196. https://doi.org/10.30564/jees.v6i3.6812

Hope, J., & Marsellos, A. (2024a). *High-Frequency of Groundwater Level Fluctuations , Underground Erosion , Potential Potential Void Zone Occurrences Across Long Island , NY*. *April*.

Hope, J., & Marsellos, A. (2024b). *High Frequency Groundwater Level Fluctuations , Underground Erosion , & Potential Potential Void Zone Occurrences Across Long Island , NY*. *May*.

Hubbs, D., & Marsellos, A. (2024). *Exploring Climate Change Effects on Potential Void Zone Formation : Long-Term Temperature Analysis in Long Island , NY (1948-2024)*. *April*.

Hussain, Y., Uagoda, R., Borges, W., Nunes, J., Hamza, O., Condori, C., Aslam, K., Dou, J., & Cárdenas-Soto, M. (2020). The potential use of geophysicalmethods to identify cavities, potential Void Zones and pathways forwater infiltration. *Water (Switzerland)*, *12*(8). https://doi.org/10.3390/w12082289

Hyun Nam, B., Shamet, R., Moataz Soliman, E., Dingbao Wang, M., Yun, H.-B., Manager, P., & Horhota, D. (2018). *Final Report DEVELOPMENT OF A POTENTIAL VOID ZONE RISK EVALUATION PROGRAM Developed for the*. *June*.

Ibrahim, A., Hassan, J. I., Aminu, B., & Osumanu, J. (2024). *Geological Behavior (GBR) GEOPHYSICAL CHARACTERIZATION OF BASEMENT ROCK FOR GROUNDWATER AND MINERALIZATION POTENTIAL USING VERY LOW FREQUENCY - ELECTROMAGNETIC (VLF-EM) TECHNIQUES ... Geological Behavior (GBR) GEOPHYSICAL CHARACTERIZATION OF BASEMEN*. *April*. https://doi.org/10.26480/gbr.01.2024.13.22

Jabrane, O., Martínez-Pagán, P., Martínez-Segura, M. A., Alcalá, F. J., El Azzab, D., Vásconez-Maza, M. D., & Charroud, M. (2023). Integration of Electrical Resistivity

Tomography and Seismic Refraction Tomography to Investigate Subsiding Potential Void Zones in Karst Areas. *Water (Switzerland)*, *15*(12). https://doi.org/10.3390/w15122192

Kaufmann, G., & Gabrovsek, F. (2017). Fracture evolution in soluble rocks : From single-material fractures towards Fracture evolution in soluble rocks : From single-material fractures towards multi-material fractures Odvisnost kraškega razvoja razpoke od vrste in zaporedja vodotopnih kamnin ,. *Acta Carsologica*, *January 2018*, 199–216.

Kaufmann, G., Gabrovšek, F., & Romanov, D. (2016). Dissolution and precipitation of fractures in soluble rock. *Hydrology and Earth System Sciences Discussions*, *August*, 1–30. https://doi.org/10.5194/hess-2016-372

Kaufmann, G., & Romanov, D. (2019). Modelling speleogenesis in soluble rocks: A case study from the permian zechstein sequences exposed along the southern harz mountains and the kyffhÄuser hills, Germany. *Acta Carsologica*, *48*(2), 173–197. https://doi.org/10.3986/ac.v48i2.7282

Laekemariam, F., Kibret, K., Mamo, T., Karltun, E., & Gebrekidan, H. (2016). Physiographic characteristics of agricultural lands and farmers' soil fertility management practices in Wolaita zone, Southern Ethiopia. *Environmental Systems Research*, *5*(1). https://doi.org/10.1186/s40068-016-0076-z

Lamb, B., & Shiau, J. (n.d.). *A PHYSCIAL AND NUMERICAL INVESTIGATION INTO POTENTIAL VOID ZONE FORMATION*.

Le Blond, J. S., Cuadros, J., Molla, Y. B., Berhanu, T., Umer, M., Baxter, P. J., & Davey, G. (2015). Weathering of the Ethiopian volcanic province: A new weathering index to characterize and compare soils. In *American Mineralogist* (Vol. 100, Issues 11–12, pp. 2518–2532). https://doi.org/10.2138/am-2015-5168ccby

Listanti, S. N. R., Darsono, D., & Purwana, Y. M. (2018). A Comparison between Drilling and Standard Penetration Test (SPT) Data to the Electrical Resistivity Sounding with Schlumberger Configuration in UNS Area. *Indonesian Journal of Applied Physics*, *8*(2), 67. https://doi.org/10.13057/ijap.v8i2.17962

Mancarella, D., Doglioni, A., & Simeone, V. (2012). On capillary barrier effects and debris slide triggering in unsaturated layered covers. In *Engineering Geology* (Vols. 147–148, pp. 14–27). https://doi.org/10.1016/j.enggeo.2012.07.003

Maurice, L., Farrant, A. R., Mathewson, E., & Atkinson, T. (2023). Karst hydrogeology of the Chalk and implications for groundwater protection. *Geological Society Special Publication*, *517*(1), 39–62. https://doi.org/10.1144/SP517-2020-267

Moore, K. R., Holländer, H. M., Basri, M., & Roemer, M. (2019). Application of geochemical and groundwater data to predict potential Void Zone formation in a gypsum formation in Manitoba, Canada. *Environmental Earth Sciences*, *78*(6), 1–12. https://doi.org/10.1007/s12665-019-8188-1

Oishi, M. (n.d.). *Mechanisms of potential Void Zone formation and hydrothermal dynamics at the Oana Crater on Azumayama Volcano, Northeast Japan*.

Pipe, L., Fibre, U., & Grating, B. (2024). *Leaking Pipe Using Fibre Bragg Grating Sensors*.

Rafaeli, O., Svoray, T., & Nahlieli, A. (2024). *SinkSAM: A Monocular Depth-Guided SAM Framework for Automatic Potential Void Zone Segmentation*. 1–14.

http://arxiv.org/abs/2410.01473

Singh, J., Joshi, A., Sharma, S., Pandey, M., Sahu, A., Singh, S., & Jaiswal, K. M. (2024). Extent of Thin Surfacial Fracture Detection Using Geophysical Survey: A Case Study of Parwan Gravity Dam, Jhalawar, Rajasthan, India. *Pure and Applied Geophysics*, *181*(7), 2063–2082. https://doi.org/10.1007/s00024-024-03513-0

Soltanpour, H., Serrhini, K., … J. S.-E. G., & 2022, undefined. (2023). A Critical Research Gap Study of Potential Void Zone Hazard Assessments. *Ui.Adsabs.Harvard.Edu*, *May*, 21–23. https://doi.org/10.5194/egusphere-egu22-6036

Sulaiman, M. S., Khan, M. A., Sulaiman, N., & Udin, W. S. (2022). Groundwater Potential Using Electrical Resistivity Imaging In Batu Melintang, Jeli, Kelantan. *IOP Conference Series: Earth and Environmental Science*, *1102*(1). https://doi.org/10.1088/1755-1315/1102/1/012028

Survey, F. G. (2018). *APPENDIX H : Potential Void Zone Report*.

Temitope, F. E., & Blessing, B. O. (2024). *Geophysical And Geotechnical Pre-Foundation Site Investigation For Geophysical And Geotechnical Pre-Foundation Site Investigation For Engineering Construction Purpose*. *February*. https://doi.org/10.9790/0990-1106012435

Underwood, B. D. (2009). *Near-Surface Seismic Refraction Surveying Field Methods*. *September*, 1–20.

Walker, D., Parkin, G., Gowing, J., & Haile, A. T. (2019). Development of a hydrogeological conceptual model for shallow aquifers in the data scarce upper Blue Nile basin. *Hydrology*, *6*(2). https://doi.org/10.3390/hydrology6020043

Wisconsin Department of Natural Resources. (2004). *Infiltration Basin*. *December*, 1–5.

Witkowski, W. T., Guzy, A., Lucka, M., & Kusztykiewicz, K. (2023). Study on Potential Void Zone Formation Mechanism in Abandoned Mines. *International Geoscience and Remote Sensing Symposium (IGARSS)*, *2023-July*(July), 2462–2465. https://doi.org/10.1109/IGARSS52108.2023.10282648

Yechieli, Y., Abelson, M., Wachs, D., Shtivelman, V., Crouvi, O., & Baer, G. (2003). *Formation of Potential Void Zones along the Shore of the Dead Sea—Preliminary Investigation*. *40698*(September), 184–194. https://doi.org/10.1061/40698(2003)16

Zaminkar, M., & Fotohi, R. (2020). SoS-RPL: Securing Internet of Things Against Potential Void Zone Attack Using RPL Protocol-Based Node Rating and Ranking Mechanism. *Wireless Personal Communications*, *114*(2), 1287–1312. https://doi.org/10.1007/s11277-020-07421-z

Appendices A

Test Pit Log

Borehole Data Collection Format for Foundation Investigation | CORE/GE/RF/086/B

CORE Consulting Engineers PLC
Tel:251-11-3-206032, 251-11-3-727013
Fax: 251-1-2306033 P.O. Box 28662/1000
Email: coreconsult@ethionet.et
Addis Ababa, Ethiopia

BOREHOLE LOG

BH: BH-105

SHEET: 1 of 1

PROJECT: Design and Build of Adama – km60 Expressway
CLIENT: SADIK HUSEN UKE
SITE LOCATION: 25+110 (POP)
BH COORDINATION (UTM-Adindan Datum)
EASTING: 551663.7
NORTHING: 959943.6
GROUND ELEVATION (m): 1408.81

DRILLING TYPE: Rotary Drilling
INCLINATION: Vertical
TOTAL DEPTH DRILLED: 15.0m
GWL: Nil
FLUSHING SYSTEM: Water
DATE STARTED: 15/01/2025
DATE COMPLETED:20/01/2026

Elevation (m)	Depth (m)	Run Length (m)	TCR	RQD	Casing	Hole dia.	Sampling	SPT	GWL	Graphic Log	Field Description of Soil/Rock	Photo
1408	0	2	100			106.6		2-6/7/9			Brown clay with sand	
1407	2	1	100					3-5/8/9				
1406		1.5	100					4.5-9/10/13				
1405	4	1.5	100					6-9/11/14				
1404		1	50	20							6	
1403	6	2	85	85							Dark gray, slightly weathered to fresh, medium fractured, strong fine grained basalt with some vesicles	
1402		2	80	80		89.1K						
1401	8	1.5	73	73								
1400		2.5	65	40							13.5	
1399	10										Highly to moderately weathered, pinkish gray, highly fractured scoraceous basalt	
1398											15	
1397	12											
1396												
1395	14											
1394												

BH = Borehole
N = Blows/30cm
SPT = Standatd Penetration test
USCS = Unified Soil Classifcation System

RQD = Rock Quality Designation
TCR = Total Core Recovery
GWL = Ground Water Level

D Distrubed Sample R Rock Sample
U Undistrubed Sample

REMARK:

LOGED BY:
APPROVED BY:
SCALE:

Borehole Data Collection Format for Foundation Investigation	CORE/GE/RF/086/B

CORE Consulting Engineers PLC
Tel:251-11-3-206032, 251-11-3-727013
Fax: 251-1-2306033 P.O. Box 28662/1000
Email: coreconsult@ethionet.et
Addis Ababa, Ethiopia

BOREHOLE LOG

BH: BH-106

SHEET: 1 of 1

PROJECT: Design and Build of Adama – km60 Expressway
CLIENT: SADIK HUSEN UKE
SITE LOCATION: 25+135 (POP)
BH COORDINATION (UTM-Adindan Datum)
EASTING: 551663.7
NORTHING: 959943.6
GROUND ELEVATION (m): 1408.81

DRILLING TYPE: Rotary Drilling
INCLINATION: Vertical
TOTAL DEPTH DRILLED: 15.0m
GWL: Nil
FLUSHING SYSTEM: Water
DATE STARTED: 15/01/2025
DATE COMPLETED:20/01/2026

Elevation (m)	Depth (m)	Run Length (m)	TCR	RQD	Casing	Hole dia.	Sampling	SPT	GWL	Graphic Log	Field Description of Soil/Rock	Photo
1409	0	1.5	100			100		1.5-5/5/5			Brownish sandy gravely Silt	
1408												
1407	2	1.5	100					3-6/7/9				
1406		1.5	100									
1405	4							4.5-11/R			4.5	
1404		1.5	100								Grayish brown silty gravel with fragmented rock	
1403	6	1	50	45				6-R			6	
1402												
1401	8	2.5	90	54								
1400											Dark gray, slightly weathered to fresh, fine grained basalt with vesicles. [At 7.5 - 10.0m becomes highly fractured scoraceous	
1399	10					90 R						
1398		3	92	44								
1397	12											
1396		1.5	70	70							14	
	14											

BH = Borehole
N = Blows/30cm
SPT = Standatd Penetration test
USCS = Unified Soil Classifcation System

RQD = Rock Quality Designation
TCR = Total Core Recovery
GWL = Ground Water Level

D Distrubed Sample R Rock Sample
U Undistrubed Sample

REMARK:

LOGED BY:
APPROVED BY:
SCALE:

CORE Consulting Engineers PLC

Borehole Data Collection Format for Foundation Investigation

CORE/GE/RF/086/B

CORE Consulting Engineers PLC
Tel:251-11-3-206032, 251-11-3-727013
Fax: 251-1-2306033 P.O. Box 28662/1000
Email: coreconsult@ethionet.et
Addis Ababa, Ethiopia

BOREHOLE LOG

BH: BH-107

SHEET: 1 of 1

PROJECT: Design and Build of Adama – km60 Expressway
CLIENT: SADIK HUSEN UKE
SITE LOCATION: 25+160 (POP)
BH COORDINATION (UTM-Adindan Datum)
EASTING: 551663.7
NORTHING: 959943.6
GROUND ELEVATION (m): 1408.81

DRILLING TYPE: Rotary Drilling
INCLINATION: Vertical
TOTAL DEPTH DRILLED: 15.0m
GWL: Nil
FLUSHING SYSTEM: Water
DATE STARTED: 15/01/2025
DATE COMPLETED:20/01/2026

Elevation (m)	Depth (m)	Run Length (m)	TCR	RQD	Casing	Hole dia.	Sampling	SPT	GWL	Graphic Log	Field Description of Soil/Rock	Photo
1409	0	1.5	100					1-4/5/6			Brownish sandy clay	
1408	2	1.5	100					3-3/5/7				
1407		1.5	100									
1406	4	1.5	100			108		4.5-5/7/7			4.6	
1405		1.5	100								Dark gray highly weathered fragmented vesicular basalt	
1404	6	1.5	100									
1403		1.5	50	20								
1402	8	1	50	50			R				9	
1401		2	75	69								
1400	10	3	75	75		63					Strong, slightly weathered to fresh, slightly fractured, fine grained basalt	
1399												
1398	12											
1397												
1396	14											
1395											15	

BH = Borehole
N = Blows/30cm
SPT = Standatd Penetration test
USCS = Unified Soil Classifcation System

RQD = Rock Quality Designation
TCR = Total Core Recovery
GWL = Ground Water Level

D Distrubed Sample
R Rock Sample
U Undistrubed Sample

REMARK:

LOGED BY:
APPROVED BY:
SCALE:

Appendices B

Geotechnical test results

CLIENT	CONSULTANT	CONTRACTOR
ETHIOPIAN ROAD AUTHORITY	LEA-LASA-UNICONE	JMC - LRBCL Joint Venture.

ETHIOPIA-DJIBOUTI TRANSPORT CORRIDOR PROJECT

(PHASE-I: DESIGN BUILD OF ADAMA-Km 60 EXPRESSWAY)

ATTERBERG LIMITS

(AASTHO T-89/90) Format No: 01002/JMC/EHAE/21F/02-R0

RFI No.	QA-QC/LAB/1796/11168	Lab Ref No. :	EDTCP/ADAMA/CUTSEC/10911
Source :	Cutting Section at 25+060 to 25+180	Date of Sampling:	15-01-2025
Location:	25+110 @ 1m	Date of Testing:	16-01-2025
Propose Used	Earthwork Filling	Sampled By:	Jointly
Material Discription	White Light Clay Soil	Tested By:	Jointly

Description	LIQUID LIMIT				PLASTIC LIMIT			
	Test I	Test II	Test III	Test IV	Test I	Test II		Avg.
No of blows/Penetration (mm)	32	27	19		C-7	C-7		17.99
Container No	C-1	C-15	C-11					
Container + Wet soil, W1 (g)	62.11	55.13	56.16		30.62	29.26		
Container + Dry soil, W2 (g)	52.107	46.51	46.85		29.92	28.52		
Weight of Container (g)	24.92	23.77	23.17		25.91	24.54		
Weight of water, W4= W1-W2 (g)	10.003	8.62	9.31		0.70	0.74		
Weight of oven dry sample, W5=W3 - W1 (g)	27.187	22.74	23.68		4.02	3.98		
Water content percentage, 100x(W4/W5)	36.79	37.91	39.32		17.34	18.64		

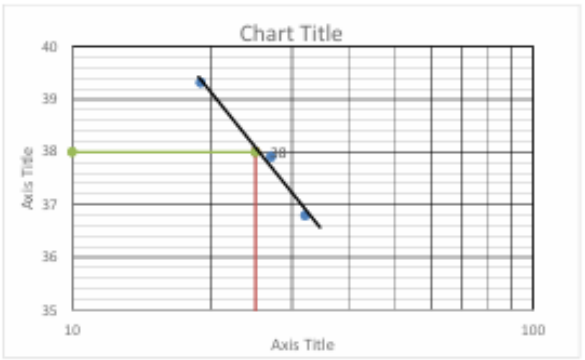

Grain Size Analysis				
Total Wt.(gm)				1110.0
Sieve size mm	Wt. Ret. (g.)	% Retained	% Cum Retained	% Passing
2.0	230.1	20.73	20.73	79.27
0.425	254.2	22.90	43.63	56.37
0.075	180.2	16.23	59.86	40.14
Pan	445.5	40.135		0.00
Grading Modules			1.24	

LL	PL	PI	Soil Class
38.00	17.99	20.01	A-4

Comments:-

Tested By	Checked By	Verified by	Approved By
Contractor's Lab Technician	Contractor's Material Engineer	Consultant's Lab Technician	Consultant's Material Engineer

CLIENT	CONSULTANT	CONTRACTOR
ETHIOPIAN ROAD AUTHORITY	LEA-LASA-UNICONE	JMC - LRBCL Joint Venture.

ETHIOPIA-DJIBOUTI TRANSPORT CORRIDOR PROJECT

(PHASE-I: DESIGN BUILD OF ADAMA-Km 60 EXPRESSWAY)

ATTERBERG LIMITS

(AASTHO T-89/90) **Format No: 01002/JMC/EHAE/21F/02-R0**

RFI No.	QA-QC/LAB/1796/11168	Lab Ref No. :	EDTCP/ADAMA/CUTSEC/10911
Source :	Cutting Section at 25+060 to 25+180	Date of Sampling:	15-01-2025
Location:	25+110 @3m	Date of Testing:	16-01-2025
Propose Used	Earthwork Filling	Sampled By:	Jointly
Material Discription	White Light Clay Soil	Tested By:	Jointly

Description	LIQUID LIMIT				PLASTIC LIMIT			
	Test I	Test II	Test III	Test IV	Test I	Test II		Avg.
No of blows/Penetration (mm)	33	26	17		C-1	C-2		
Container No	A-1	A-2	A-3					
Container + Wet soil, W1 (g)	56.87	55.63	56.9		29.94	30.12		
Container + Dry soil, W2 (g)	46.89	45.681	46.273		29.21	29.37		
Weight of Container (g)	24	23.51	23.45		25.10	25.23		18.00
Weight of water, W4= W1-W2 (g)	9.98	9.95	10.63		0.73	0.75		
Weight of oven dry sample, W5=W3 - W1 (g)	22.894	22.171	22.823		4.11	4.14		
Water content percentage, 100x(W4/W5)	43.57	44.87	46.56		17.82	18.18		

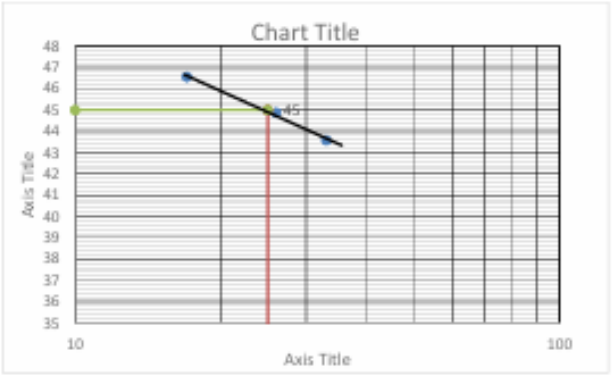

Grain Size Analysis				
Total Wt.(gm)				900.0
Sieve size mm	Wt. Ret. (g.)	% Retained	% Cum Retained	% Passing
2.0	187.0	20.78	20.78	79.22
0.425	200.0	22.22	43.00	57.00
0.075	180.2	20.02	63.02	36.98
Pan	332.8	36.978		0.00
Grading Modules			1.27	

LL	PL	PI	Soil Class
45.00	18.00	27.00	A-7-6[4]

Comments:-

Tested By	Checked By	Verified by	Approved By
Contractor's Lab Technician	Contractor's Material Engineer	Consultant's Lab Technician	Consultant's Material Engineer

CLIENT	CONSULTANT	CONTRACTOR
ETHIOPIAN ROAD AUTHORITY	LEA-LASA-UNICONE	JMC - LRBCL Joint Venture.

ETHIOPIA-DJIBOUTI TRANSPORT CORRIDOR PROJECT

(PHASE-I: DESIGN BUILD OF ADAMA-Km 60 EXPRESSWAY)

ATTERBERG LIMITS

(AASTHO T-89/90) **Format No: 01002/JMC/EHAE/21F/02-R0**

RFI No.	QA-QC/LAB/1796/11168	Lab Ref No. :	EDTCP/ADAMA/CUTSEC/10911
Source :	Cutting Section at 25+060 to 25+180	Date of Sampling:	15-01-2025
Location:	25+135RHS @1m	Date of Testing:	16-01-2025
Propose Used	Earthwork Filling	Sampled By:	Jointly
Material Discription	White Light Clay Soil	Tested By:	Jointly

Description	LIQUID LIMIT				PLASTIC LIMIT			
	Test I	Test II	Test III	Test IV	Test I	Test II		Avg.
No of blows/Penetration (mm)	33	27	18		C-1	C-2		
Container No	A-1	A-2	A-3					
Container + Wet soil, W1 (g)	57.55	56.39	57		30.54	31.32		
Container + Dry soil, W2 (g)	47.99	46.85	47.035		29.69	30.24		20.00
Weight of Container (g)	24	23.51	23.45		25.10	25.23		
Weight of water, W4= W1-W2 (g)	9.56	9.54	9.97		0.85	1.08		
Weight of oven dry sample, W5=W3 - W1 (g)	23.986	23.34	23.585		4.59	5.01		
Water content percentage, 100x(W4/W5)	39.87	40.87	42.25		18.42	21.58		

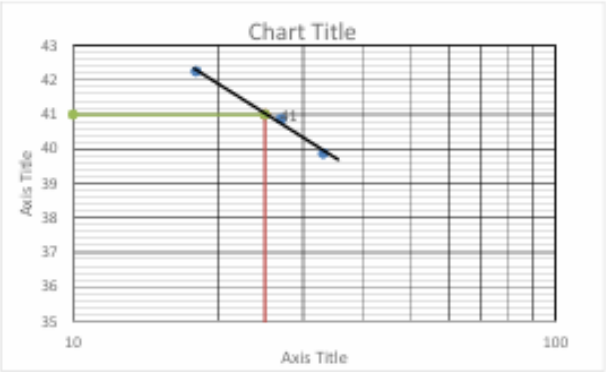

Grain Size Analysis				
Total Wt.(gm)				739.0
Sieve size mm	Wt. Ret. (g.)	% Retained	% Cum Retained	% Passing
2.0	157.0	21.24	21.24	78.76
0.425	183.0	24.76	46.01	53.99
0.075	90.0	12.18	58.19	41.81
Pan	309.0	41.813		0.00
Grading Modules			1.25	

LL	PL	PI	Soil Class
41.00	20.00	21.00	A-7-6[4]

Comments:-

Tested By	Checked By	Verified by	Approved By
Contractor's Lab Technician	Contractor's Material Engineer	Consultant's Lab Technician	Consultant's Material Engineer

CLIENT	CONSULTANT	CONTRACTOR
ETHIOPIAN ROAD AUTHORITY	LEA-LASA-UNICONE	JMC - LRBCL Joint Venture.

ETHIOPIA-DJIBOUTI TRANSPORT CORRIDOR PROJECT

(PHASE-I: DESIGN BUILD OF ADAMA-Km 60 EXPRESSWAY)

ATTERBERG LIMITS

(AASTHO T-89/90) Format No: 01002/JMC/EHAE/21F/02-R0

RFI No.	QA-QC/LAB/1796/11168	Lab Ref No. :	EDTCP/ADAMA/CUTSEC/10911
Source :	Cutting Section at 25+060 to 25+180	Date of Sampling:	15-01-2025
Location:	25+135RHS @3m	Date of Testing:	16-01-2025
Propose Used	Earthwork Filling	Sampled By:	Jointly
Material Discription	White Light Clay Soil	Tested By:	Jointly

Description	LIQUID LIMIT				PLASTIC LIMIT			
	Test I	Test II	Test III	Test IV	Test I	Test II		Avg.
No of blows/Penetration (mm)	32	27	18		L-1	L-2		
Container No	P-1	P-2	P-10					
Container + Wet soil, W1 (g)	52.99	53.36	54.6		30.62	29.26		
Container + Dry soil, W2 (g)	43.90	43.78	44.119		29.59	28.21		
Weight of Container (g)	24.24	23.79	23.17		25.83	24.54		28.00
Weight of water, W4= W1-W2 (g)	9.0852	9.58	10.481		1.03	1.05		
Weight of oven dry sample, W5=W3 - W1 (g)	19.6648	19.99	20.949		3.76	3.67		
Water content percentage, 100x(W4/W5)	46.20	47.92	50.03		27.53	28.47		

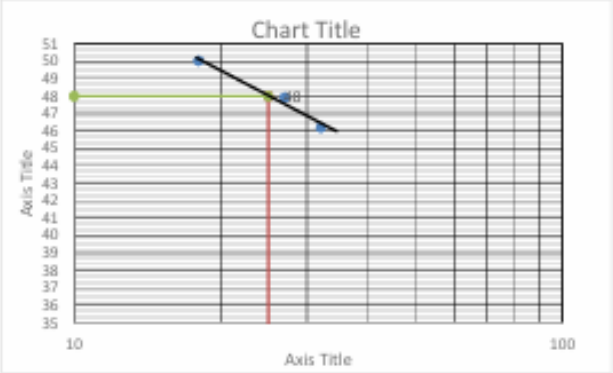

Grain Size Analysis				
Total Wt.(gm)				854.0
Sieve size mm	Wt. Ret. (g.)	% Retained	% Cum Retained	% Passing
2.0	165.6	19.39	19.39	80.61
0.425	199.0	23.30	42.69	57.31
0.075	196.9	23.06	65.75	34.25
Pan	292.5	34.251		0.00
Grading Modules			1.28	

LL	PL	PI	Soil Class
48.00	28.00	20.00	A-2-7[2]

Comments:-

Tested By	Checked By	Verified by	Approved By
Contractor's Lab Technician	Contractor's Material Engineer	Consultant's Lab Technician	Consultant's Material Engineer

CLIENT	CONSULTANT	CONTRACTOR
ETHIOPIAN ROAD AUTHORITY	LEA-LASA-UNICONE	JMC - LRBCL Joint Venture.

ETHIOPIA-DJIBOUTI TRANSPORT CORRIDOR PROJECT

(PHASE-I: DESIGN BUILD OF ADAMA-Km 60 EXPRESSWAY)

ATTERBERG LIMITS

(AASTHO T-89/90) — **Format No: 01002/JMC/EHAE/21F/02-R0**

RFI No.	QA-QC/LAB/1796/11168	Lab Ref No. :	EDTCP/ADAMA/CUTSEC/10911
Source :	Cutting Section at 25+060 to 25+180	Date of Sampling:	15-01-2025
Location:	25+160RHS @1m	Date of Testing:	16-01-2025
Propose Used	Earthwork Filling	Sampled By:	Jointly
Material Discription	White Light Clay Soil	Tested By:	Jointly

Description	LIQUID LIMIT				PLASTIC LIMIT			
	Test I	Test II	Test III	Test IV	Test I	Test II		Avg.
No of blows/Penetration (mm)	33	26	17		L-1	L-2		
Container No	P-1	P-2	P-10					
Container + Wet soil, W1 (g)	51.11	50.56	52.63		30.62	29.26		
Container + Dry soil, W2 (g)	43.80	43.054	44.08		29.79	28.37		
Weight of Container (g)	24.24	23.79	23.17		25.83	24.54		22.00
Weight of water, W4= W1-W2 (g)	7.307	7.506	8.55		0.83	0.89		
Weight of oven dry sample, W5=W3 - W1 (g)	19.563	19.264	20.91		3.96	3.83		
Water content percentage, 100x(W4/W5)	37.35	38.96	40.89		20.90	23.11		

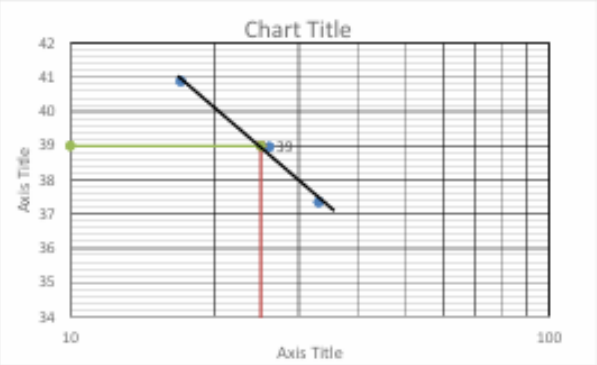

Grain Size Analysis				
Total Wt.(gm)				1200.0
Sieve size mm	Wt. Ret. (g.)	% Retained	% Cum Retained	% Passing
2.0	255.3	21.28	21.28	78.73
0.425	211.0	17.58	38.86	61.14
0.075	330.0	27.50	66.36	33.64
Pan	403.7	33.642		0.00
Grading Modules			1.26	

LL	PL	PI	Soil Class
39.00	22.00	17.00	A-2-7[2]

Comments:-

Tested By	Checked By	Verified by	Approved By
Contractor's Lab Technician	Contractor's Material Engineer	Consultant's Lab Technician	Consultant's Material Engineer

CLIENT	CONSULTANT	CONTRACTOR
ETHIOPIAN ROAD AUTHORITY	LEA-LASA-UNICONE	JMC - LRBCL Joint Venture.

ETHIOPIA-DJIBOUTI TRANSPORT CORRIDOR PROJECT

(PHASE-I: DESIGN BUILD OF ADAMA-Km 60 EXPRESSWAY)

ATTERBERG LIMITS

(AASTHO T-89/90) Format No: 01002/JMC/EHAE/21F/02-R0

RFI No.	QA-QC/LAB/1796/11168	Lab Ref No. :	EDTCP/ADAMA/CUTSEC/10911
Source :	Cutting Section at 25+060 to 25+180	Date of Sampling:	15-01-2025
Location:	25+160RHS @3m	Date of Testing:	16-01-2025
Propose Used	Earthwork Filling	Sampled By:	Jointly
Material Discription	White Light Clay Soil	Tested By:	Jointly

Description	LIQUID LIMIT				PLASTIC LIMIT			
	Test I	Test II	Test III	Test IV	Test I	Test II		Avg.
No of blows/Penetration (mm)	32	28	18		L-3	L-4		
Container No	L-5	L-6	L-7					
Container + Wet soil, W1 (g)	51.11	50.56	52.63		30.62	29.26		
Container + Dry soil, W2 (g)	42.10	41.555	42.62		29.50	27.88		30.00
Weight of Container (g)	23.6	23.4	23.27		25.54	23.5		
Weight of water, W4= W1-W2 (g)	9.01	9.005	10.01		1.12	1.38		
Weight of oven dry sample, W5=W3 - W1 (g)	18.5	18.155	19.35		3.96	4.38		
Water content percentage, 100x(W4/W5)	48.70	49.60	51.73		28.41	31.60		

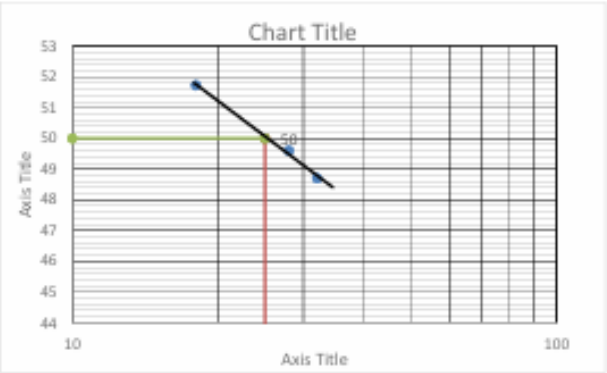

Grain Size Analysis				
Total Wt.(gm)				1169.0
Sieve size mm	Wt. Ret. (g.)	% Retained	% Cum Retained	% Passing
2.0	233.9	20.01	20.01	79.99
0.425	221.0	18.91	38.91	61.09
0.075	319.4	27.33	66.24	33.76
Pan	394.7	33.760		0.00
Grading Modules			1.25	

LL	PL	PI	Soil Class
50.00	30.00	20.00	A-2-7[2]

Comments:-

Tested By	Checked By	Verified by	Approved By
Contractor's Lab Technician	Contractor's Material Engineer	Consultant's Lab Technician	Consultant's Material Engineer

CLIENT	CONSULTANT	CONTRACTOR
ETHIOPIAN ROAD AUTHORITY	LEA-LASA-UNICONE	JMC - LRBCL Joint Venture.

ETHIOPIA-DJIBOUTI TRANSPORT CORRIDOR PROJECT

(PHASE-I: DESIGN BUILD OF ADAMA-Km 60 EXPRESSWAY)

MAXIMUM DRY DENSITY AND MOISTURE CONTENT

(AASTHO T-180) Format No: 01002/JMC/EHAE/21F/03-R0

RFI No.	QA-QC/LAB/1796/11168			Lab Ref No. :		EDTCP/ADAMA/CUTSEC/10911	
Source :	Cutting Section at 25+060 to 25+180			Date of Sampling:		15-01-2025	
Location:	25+110 @1m			Date of Testing:		21-12-2023	
Propose Used	mdd			Sampled By:		-	
Type of Method:	A			Tested By:		-	
Material Discription	White Light Clay Soil			Depth (M)		1m	
Description	Test I	Test II	Test III	Test IV	Test V		
	Density Determination						
Water Added %	6%	8%	10%	12%			
Mass of mould + Wet Soil (g)	9745	9970	10053	10060			
Mass of mould, W5 (g)	6164	6164	6164	6164			
Mass of wet soil, W7=W6-W5 (g)	3581	3806	3889	3896			
Volume of mould, V (cc)	2306	2306	2306	2306			
Bulk density, γ_w = [(W7-W6)/V] g/cc	1.553	1.650	1.686	1.690		NMC	
	Moisture Content Determination						
Container no	D-400	D-8	D-20	D-15		D-400	
Mass of container + wet soil, W1 (g)	426.30	300.10	276.20	280.60		303.70	
Mass of container + oven dry soil, W2 (g)	396.70	273.52	248.89	249.42		298.00	
Mass of Water (g) W3=W1-W2	29.60	26.58	27.31	31.18		5.70	
Mass of container, W4 (g)	32.10	29.40	28.70	28.50		27.30	
Mass of Dry Soil (g) W5 = W2-W4	364.60	244.12	220.19	220.92		270.70	
Moisture Content (%) W6= W3/W5*100	8.12	10.89	12.40	14.11		2.11	
Dry density, $\gamma_d = \gamma_w/(100+W6)*100$ (g/cc)	1.436	1.488	1.500	1.481		2.11	

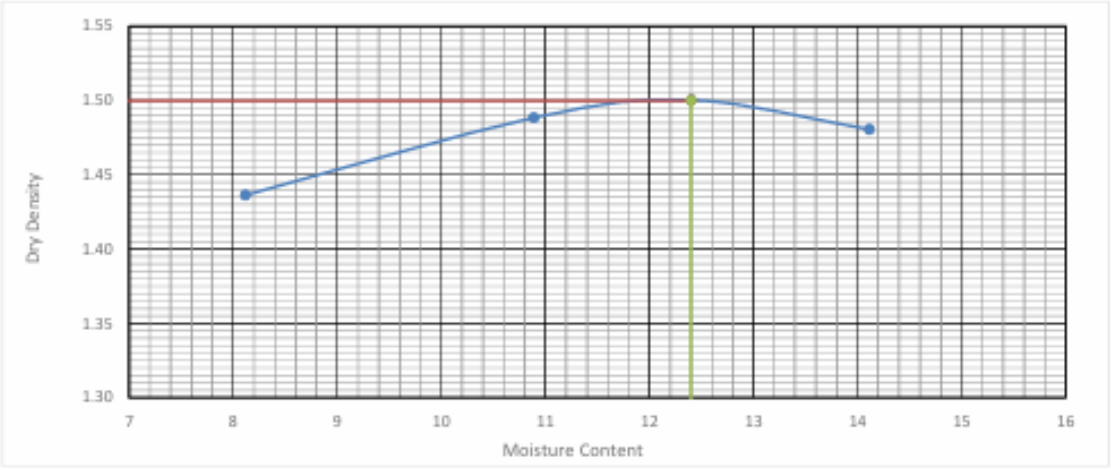

MDD:	1.500 (gm/cc)	OMC:	12.4 %

Tested By	Checked By	Verified by	Approved By
Contractor's Lab Technician	Contractor's Material Engineer	Consultant's Lab Technician	Consultant's Material Engineer

CLIENT	CONSULTANT	CONTRACTOR
ETHIOPIAN ROAD AUTHORITY	LEA-LASA-UNICONE	JMC - LRBCL Joint Venture.

ETHIOPIA-DJIBOUTI TRANSPORT CORRIDOR PROJECT

(PHASE-I: DESIGN BUILD OF ADAMA-Km 60 EXPRESSWAY)

MAXIMUM DRY DENSITY AND MOISTURE CONTENT

(AASTHO T-180) Format No: 01002/JMC/EHAE/21F/03-R0

RFI No.	QA-QC/LAB/1796/11168			Lab Ref No. :		EDTCP/ADAMA/CUTSEC/10911	
Source :	Cutting Section at 25+060 to 25+180			Date of Sampling:		15-01-2025	
Location:	25+110 @3m			Date of Testing:		21-12-2023	
Propose Used	mdd			Sampled By:		-	
Type of Method:	A			Tested By:		-	
Material Discription	White Light Clay Soil			Depth (M)		1m	
Description	Test I	Test II	Test III	Test IV	Test V		
	Density Determination						
Water Added %	12%	14%	16%	18%			
Mass of mould + Wet Soil (g)	9732	9890	9996	9989			
Mass of mould, W5 (g)	6164	6164	6164	6164			
Mass of wet soil, W7=W6-W5 (g)	3568	3726	3832	3825			
Volume of mould, V (cc)	2306	2306	2306	2306			
Bulk density, γ_m = [(W7-W6)/V] g/cc	1.547	1.616	1.662	1.659		NMC	
	Moisture Content Determination						
Container no	D-1	D-2	D-3	D-4		D-5	
Mass of container + wet soil, W1 (g)	245.30	298.10	267.00	281.20		303.70	
Mass of container + oven dry soil, W2 (g)	217.86	260.02	229.86	238.03		296.47	
Mass of Water (g) W3=W1-W2	27.44	38.08	37.14	43.17		7.23	
Mass of container, W4 (g)	31.20	32.00	31.30	29.50		28.90	
Mass of Dry Soil (g) W5 = W2-W4	186.66	228.02	198.56	208.53		267.57	
Moisture Content (%) W6= W3/W5*100	14.70	16.70	18.70	20.70		2.70	
Dry density, $\gamma_d = \gamma_m/(100+W6)*100$ (g/cc)	1.349	1.385	1.400	1.374		2.70	

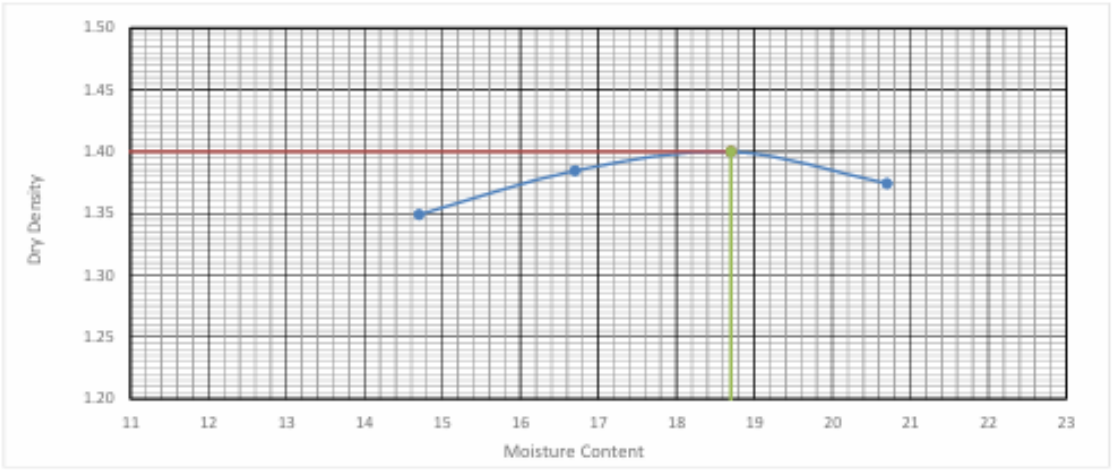

MDD:	1.400 (gm/cc)	OMC:	18.7 %

Tested By	Checked By	Verified by	Approved By
Contractor's Lab Technician	Contractor's Material Engineer	Consultant's Lab Technician	Consultant's Material Engineer

CLIENT	CONSULTANT	CONTRACTOR
ETHIOPIAN ROAD AUTHORITY	LEA-LASA-UNICONE	JMC - LRBCL Joint Venture.

ETHIOPIA-DJIBOUTI TRANSPORT CORRIDOR PROJECT

(PHASE-I: DESIGN BUILD OF ADAMA-Km 60 EXPRESSWAY)

MAXIMUM DRY DENSITY AND MOISTURE CONTENT

(AASTHO T-180) Format No: 01002/JMC/EHAE/21F/03-R0

RFI No.	QA-QC/LAB/1796/11168			Lab Ref No. :		EDTCP/ADAMA/CUTSEC/10911	
Source :	Cutting Section at 25+060 to 25+180			Date of Sampling:		15-01-2025	
Location:	25+135RHS @ 1m			Date of Testing:		21-12-2023	
Propose Used	mdd			Sampled By:		-	
Type of Method:	A			Tested By:		-	
Material Discription	White Light Clay Soil			Depth (M)		1m	
Description	Test I	Test II	Test III	Test IV	Test V		
	Density Determination						
Water Added %	6%	8%	10%	12%			
Mass of mould + Wet Soil (g)	9602	9720	9827	9800			
Mass of mould, W5 (g)	6164	6164	6164	6164			
Mass of wet soil, W7=W6-W5 (g)	3438	3556	3663	3636			
Volume of mould, V (cc)	2306	2306	2306	2306			
Bulk density, γ_m = [(W7-W6)/V] g/cc	1.491	1.542	1.588	1.577		NMC	
	Moisture Content Determination						
Container no	A-1	A-2	A-3	A-4		A-5	
Mass of container + wet soil, W1 (g)	235.40	267.40	298.20	245.50		264.10	
Mass of container + oven dry soil, W2 (g)	218.46	243.81	266.42	217.99		256.17	
Mass of Water (g) W3=W1-W2	16.94	23.59	31.78	27.51		7.93	
Mass of container, W4 (g)	30.30	29.40	31.00	34.60		29.60	
Mass of Dry Soil (g) W5 = W2-W4	188.16	214.41	235.42	183.39		226.57	
Moisture Content (%) W6= W3/W5*100	9.00	11.00	13.50	15.00		3.50	
Dry density, $\gamma_d = \gamma_m/(100+W6)*100$ (g/cc)	1.368	1.389	1.400	1.371		3.50	

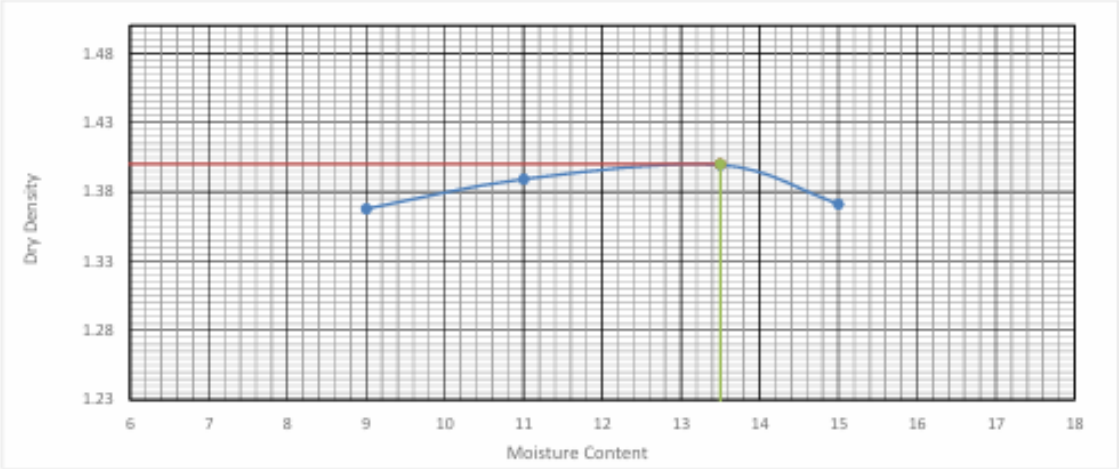

MDD:	1.400 (gm/cc)	OMC:	13.5 %

Tested By	Checked By	Verified by	Approved By
Contractor's Lab Technician	Contractor's Material Engineer	Consultant's Lab Technician	Consultant's Material Engineer

CLIENT	CONSULTANT	CONTRACTOR
ETHIOPIAN ROAD AUTHORITY	LEA-LASA-UNICONE	JMC - LRBCL Joint Venture.

ETHIOPIA-DJIBOUTI TRANSPORT CORRIDOR PROJECT

(PHASE-I: DESIGN BUILD OF ADAMA-Km 60 EXPRESSWAY)

MAXIMUM DRY DENSITY AND MOISTURE CONTENT

(AASTHO T-180) Format No: 01002/JMC/EHAE/21F/03-R0

RFI No.	QA-QC/LAB/1796/11168			Lab Ref No. :		EDTCP/ADAMA/CUTSEC/10911	
Source :	Cutting Section at 25+060 to 25+180			Date of Sampling:		15-01-2025	
Location:	25+135RHS @ 3m			Date of Testing:		16-01-2025	
Propose Used	mdd			Sampled By:		-	
Type of Method:	A			Tested By:		-	
Material Discription	White Light Clay Soil			Depth (M)		3m	
Description	Test I	Test II	Test III	Test IV	Test V		
	Density Determination						
Water Added %	8%	10%	12%	14%			
Mass of mould + Wet Soil (g)	9239	9517	9617	9540			
Mass of mould, W5 (g)	6164	6164	6164	6164			
Mass of wet soil, W7=W6-W5 (g)	3075	3353	3453	3376			
Volume of mould, V (cc)	2306	2306	2306	2306			
Bulk density, γ_m = [(W7-W6)/V] g/cc	1.333	1.454	1.497	1.464		NMC	
	Moisture Content Determination						
Container no	A-1	A-2	A-3	A-4		A-5	
Mass of container + wet soil, W1 (g)	263.10	248.80	254.20	252.70		228.80	
Mass of container + oven dry soil, W2 (g)	239.65	223.22	224.75	220.69		222.62	
Mass of Water (g) W3=W1-W2	23.45	25.58	29.45	32.01		6.18	
Mass of container, W4 (g)	30.30	29.40	31.00	34.60		29.60	
Mass of Dry Soil (g) W5 = W2-W4	209.35	193.82	193.75	186.09		193.02	
Moisture Content (%) W6= W3/W5*100	11.20	13.20	15.20	17.20		3.20	
Dry density, γ_d = γ_m/(100+W6)*100 (g/cc)	1.199	1.284	1.300	1.249		3.20	

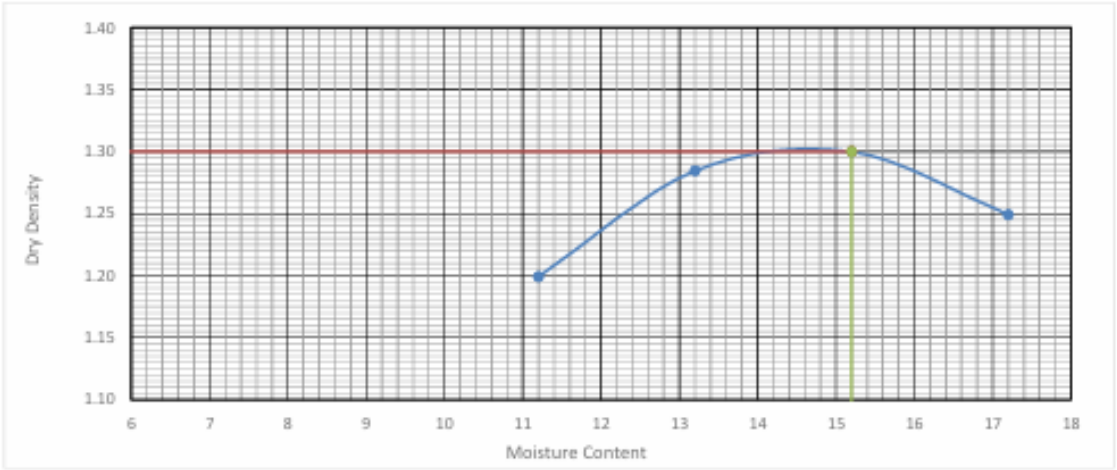

MDD:	1.300 (gm/cc)	OMC:	15.2 %

Tested By	Checked By	Verified by	Approved By
Contractor's Lab Technician	Contractor's Material Engineer	Consultant's Lab Technician	Consultant's Material Engineer

CLIENT	CONSULTANT	CONTRACTOR
ETHIOPIAN ROAD AUTHORITY	LEA-LASA-UNICONE	JMC - LRBCL Joint Venture.

ETHIOPIA-DJIBOUTI TRANSPORT CORRIDOR PROJECT

(PHASE-I: DESIGN BUILD OF ADAMA-Km 60 EXPRESSWAY)

MAXIMUM DRY DENSITY AND MOISTURE CONTENT

(AASTHO T-180) Format No: 01002/JMC/EHAE/21F/03-R0

RFI No.	QA-QC/LAB/1796/11168			Lab Ref No. :		EDTCP/ADAMA/CUTSEC/10911	
Source :	Cutting Section at 25+060 to 25+180			Date of Sampling:		15-01-2025	
Location:	25+160RHS @ 1m			Date of Testing:		17-01-2025	
Propose Used	mdd			Sampled By:		-	
Type of Method:	A			Tested By:		-	
Material Discription	White Light Clay Soil			Depth (M)		1m	
Description	Test I	Test II	Test III	Test IV	Test V		
	Density Determination						
Water Added %	6%	8%	10%	12%			
Mass of mould + Wet Soil (g)	9289	9450	9534	9489			
Mass of mould, W5 (g)	6164	6164	6164	6164			
Mass of wet soil, W7=W6-W5 (g)	3125	3286	3370	3325			
Volume of mould, V (cc)	2306	2306	2306	2306			
Bulk density, γ_w = [(W7-W6)/V] g/cc	1.355	1.425	1.461	1.442		NMC	
	Moisture Content Determination						
Container no	A-1	A-2	A-3	A-4		A-5	
Mass of container + wet soil, W1 (g)	254.90	239.70	265.40	246.50		243.90	
Mass of container + oven dry soil, W2 (g)	237.50	219.89	239.54	219.82		238.87	
Mass of Water (g) W3=W1-W2	17.41	19.81	25.86	26.68		5.03	
Mass of container, W4 (g)	30.30	29.40	31.00	34.60		29.60	
Mass of Dry Soil (g) W5 = W2-W4	207.20	190.49	208.54	185.22		209.27	
Moisture Content (%) W6= W3/W5*100	8.40	10.40	12.40	14.40		2.40	
Dry density, $\gamma_d = \gamma_w/(100+W6)*100$ (g/cc)	1.250	1.291	1.300	1.260		2.40	

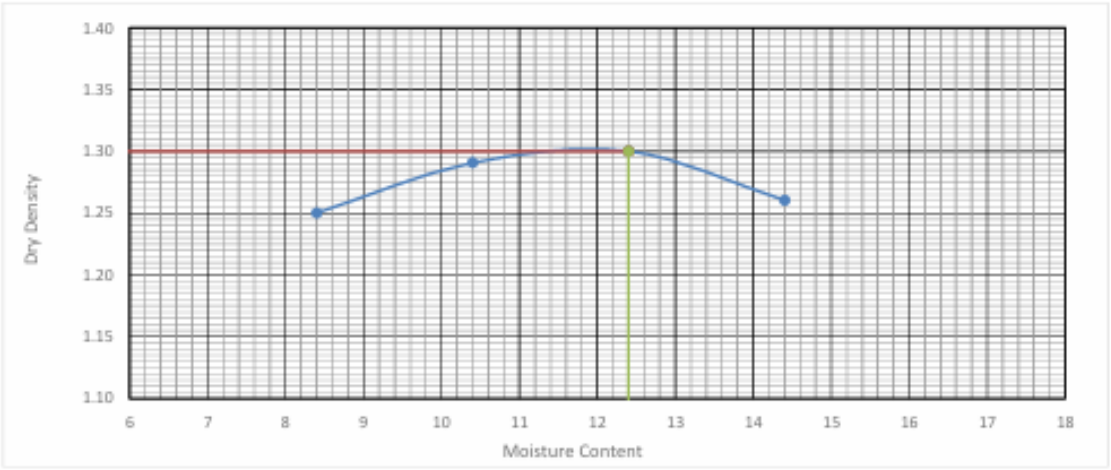

MDD:	1.300 (gm/cc)	OMC:	12.4 %

Tested By	Checked By	Verified by	Approved By
Contractor's Lab Technician	Contractor's Material Engineer	Consultant's Lab Technician	Consultant's Material Engineer

CLIENT	CONSULTANT	CONTRACTOR
ETHIOPIAN ROAD AUTHORITY	LEA-LASA-UNICONE	JMC - LRBCL Joint Venture.

ETHIOPIA-DJIBOUTI TRANSPORT CORRIDOR PROJECT

(PHASE-I: DESIGN BUILD OF ADAMA-Km 60 EXPRESSWAY)

MAXIMUM DRY DENSITY AND MOISTURE CONTENT

(AASHTO T-180) Format No: 01002/JMC/EHAE/21F/03-R0

RFI No.	QA-QC/LAB/1796/11168	Lab Ref No. :	EDTCP/ADAMA/CUTSEC/10911
Source :	Cutting Section at 25+060 to 25+180	Date of Sampling:	15-01-2025
Location:	25+160RHS @3m	Date of Testing:	18-01-2025
Propose Used	mdd	Sampled By:	-
Type of Method:	A	Tested By:	-
Material Discription	White Light Clay Soil	Depth (M)	3m

Description	Test I	Test II	Test III	Test IV	Test V	
	Density Determination					
Water Added %	6%	8%	10%	12%		
Mass of mould + Wet Soil (g)	9439	9670	9789	9740		
Mass of mould, W5 (g)	6164	6164	6164	6164		
Mass of wet soil, W7=W6-W5 (g)	3275	3506	3625	3576		
Volume of mould, V (cc)	2306	2306	2306	2306		
Bulk density, γ_m = [(W7-W6)/V] g/cc	1.420	1.520	1.572	1.551		NMC
	Moisture Content Determination					
Container no	N 1	N 2	N 3	N 4		N 5
Mass of container + wet soil, W1 (g)	243.10	254.21	241.20	252.10		238.20
Mass of container + oven dry soil, W2 (g)	226.87	233.51	218.31	224.43		233.47
Mass of Water (g) W3=W1-W2	16.23	20.70	22.89	27.67		4.73
Mass of container, W4 (g)	31.30	32.50	32.20	31.00		28.20
Mass of Dry Soil (g) W5 = W2-W4	195.57	201.01	186.11	193.43		205.27
Moisture Content (%) W6= W3/W5*100	8.30	10.30	12.30	14.30		2.30
Dry density, $\gamma_d = \gamma_m/(100+W6)*100$ (g/cc)	1.311	1.378	1.400	1.357		2.30

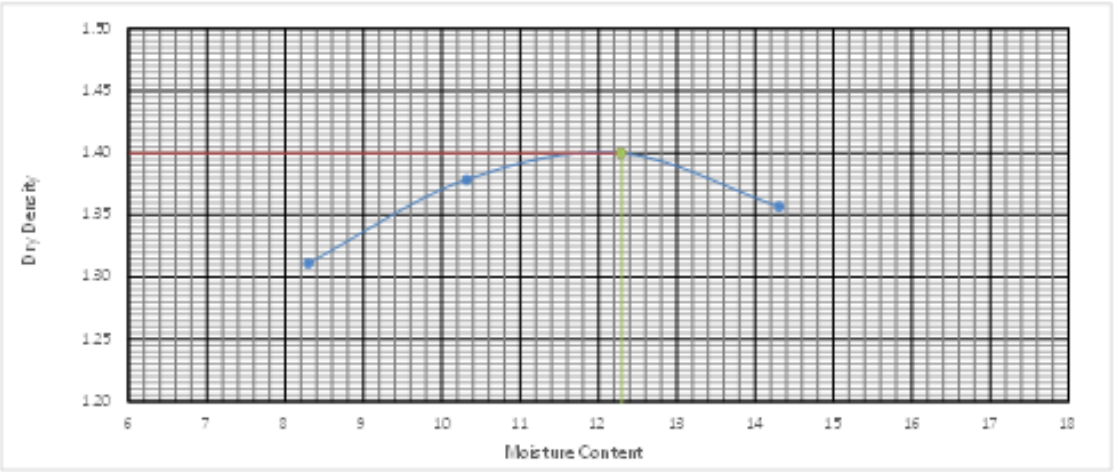

MDD: 1.400 (gm/cc) | OMC: 12.3 %

Tested By	Checked By	Verified by	Approved By
Contractor's Lab Technician	Contractor's Material Engineer	Consultant's Lab Technician	Consultant's Material Engineer

CLIENT	CONSULTANT	CONTRACTOR
ETHIOPIAN ROAD AUTHORITY	LEA-LASA-UNICONE	JMC PROJECTS (I) LTD.

ETHIOPIA-DJIBOUTI TRANSPORT CORRIDOR PROJECT

(PHASE-I: DESIGN BUILD OF ADAMA-Km 60 EXPRESSWAY)

CALIFORNIA BEARING RATIO TEST

(AASHTO T 193)

Format No: 01/02/JMC/EHAE/21F/04B-R0

RFI No.	QA-QC/LAB/1796/11168	Lab Ref. No.	EDTCP/ADAMA/CLTSEC/10911
Source :	Cutting Section at 25+060 to 25+180	Date of Sampling:	15-01-2025
Location:	Km25+110RHS	Date of Soaking:	18-01-2025
Propose Used	Earthwork Filling	Date of Testing:	22-01-2025
Material Discription	White Light Clay Soil	Depth (m):	1m

MDD (gm/cc)	1.500	OMC (%)	12.40

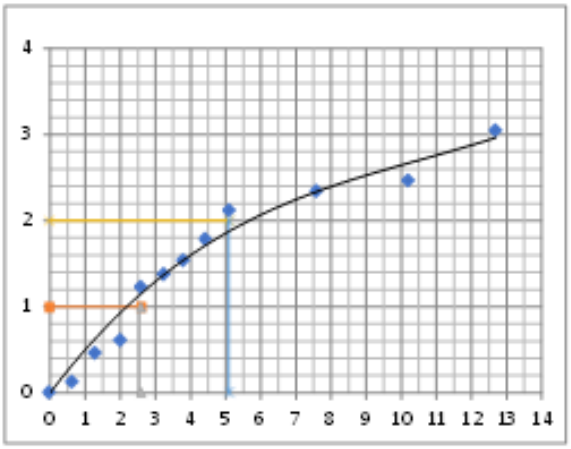

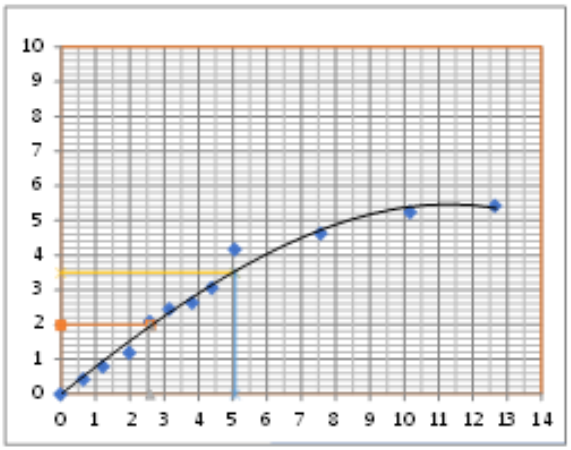

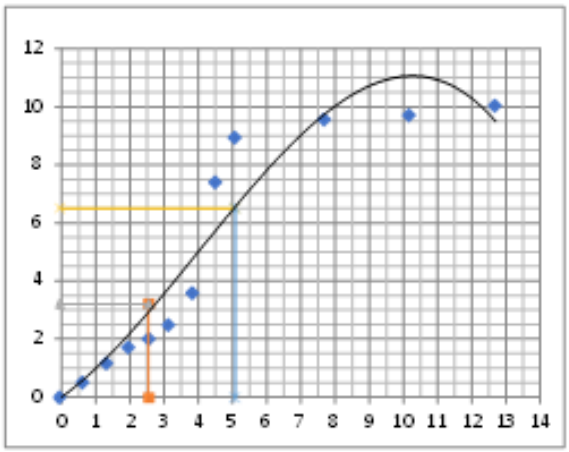

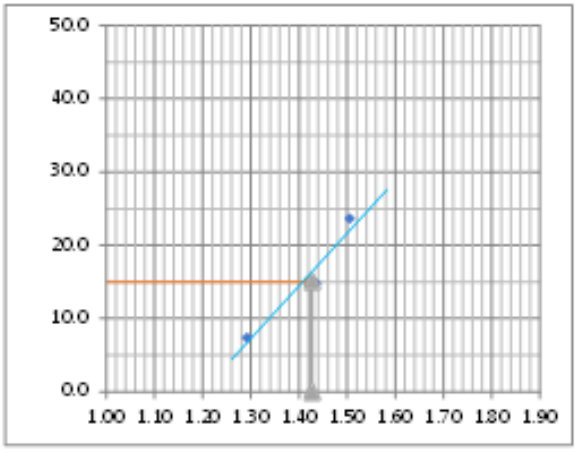

Density @ 95% Compaction (gm/cc)	1.425
CBR @ 95% Compaction (%)	15.0
Swell @ 95% Compaction (%)	0.42

Tested By | Checked By | Verified by | Approved By

CLIENT	CONSULTANT	CONTRACTOR
ETHIOPIAN ROAD AUTHORITY	LEA-LASA-UNICONE	JMC PROJECTS (I) LTD.

ETHIOPIA-DJIBOUTI TRANSPORT CORRIDOR PROJECT

(PHASE-I: DESIGN BUILD OF ADAMA-Km 60 EXPRESSWAY)

CALIFORN IA BEARING RATIO TEST

(AASHTO T 193)

Format No: 01.002/JMC/EHAE/21 F/04B-R0

RFI No.	QA-QC / LAB/ 1796 /11168	Lab Ref. No.	EDTCP/ADAMA/CUTSEC/ 10911
Source :	Cutting Section at 25+060 to 25+180	Date of Sampling:	15-01-2025
Location:	Km25+110RHS	Date of Soaking:	20-01-2025
Propose Used	Earthwork Filling	Date of Testing:	24-01-2025
Material Discription	White Light Clay Soil	Depth (m):	3m

MDD (gm/cc)	1.400	OMC (%)	18.70

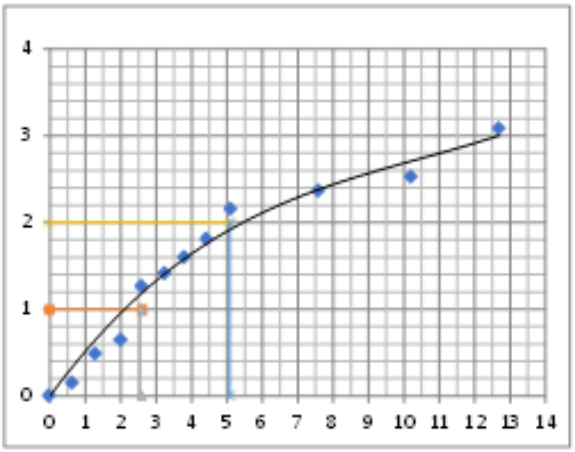

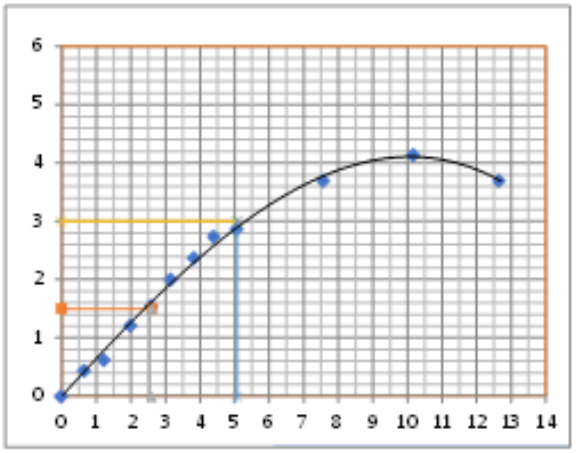

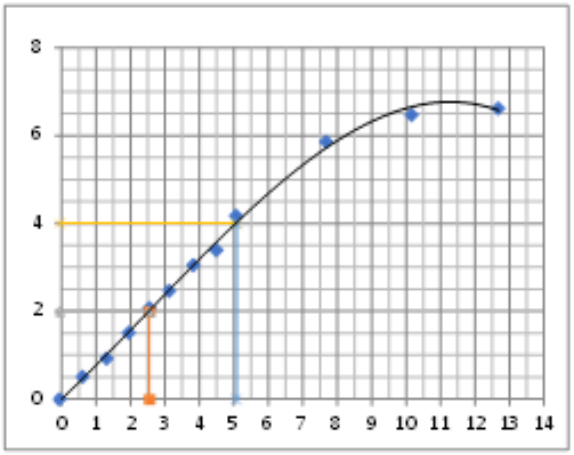

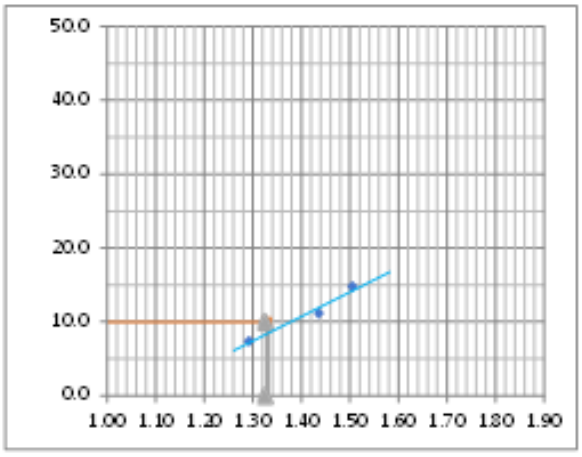

Density @ 95% Compaction (gm/cc)	1.330
CBR @ 95% Compaction (%)	10.0
Swell @ 95% Compaction (%)	0.42

Tested By | Checked By | Verified by | Approved By

CLIENT	CONSULTANT	CONTRACTOR
ETHIOPIAN ROAD AUTHORITY	LEA-LASA-UNICONE	JMC PROJECTS (I) LTD.

ETHIOPIA-DJIBOUTI TRANSPORT CORRIDOR PROJECT

(PHASE-I: DESIGN BUILD OF ADAMA-Km 60 EXPRESSWAY)

CALIFORN IA BEARING RATIO TEST

(AASHTO T 193)

Format No: 01/02/JMC/EHAE/21F/048-R0

RFI No.	QA-QC/LAB/1796/11168	Lab Ref. No.	EDTCP/ADAMA/CLT/SEC/10911
Source :	Cutting Section at 25+060 to 25+180	Date of Sampling:	15-01-2025
Location:	25+135RHS	Date of Soaking:	22-01-2025
Propose Used	Earthwork Filling	Date of Testing:	26-01-2025
Material Discription	White Light Clay Soil	Depth (m):	1m

MDD (gm/cc)	1.500	OMC (%)	13.50

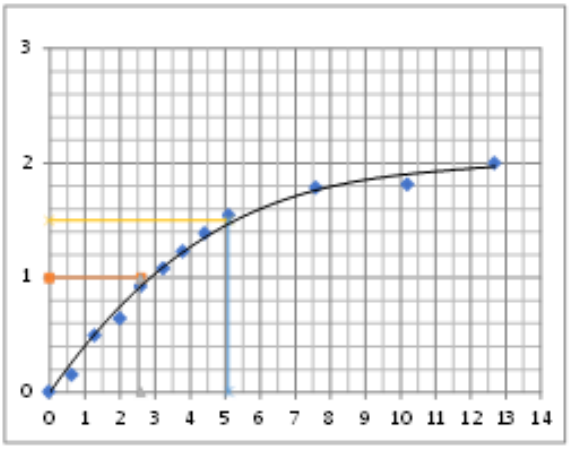

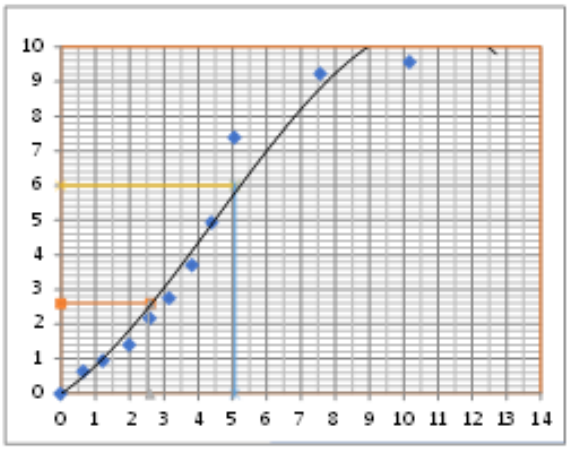

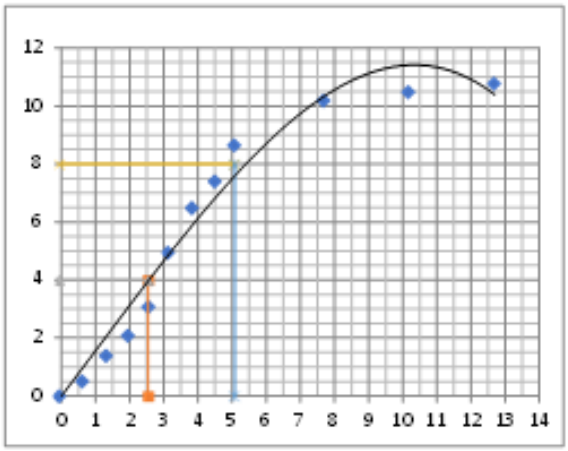

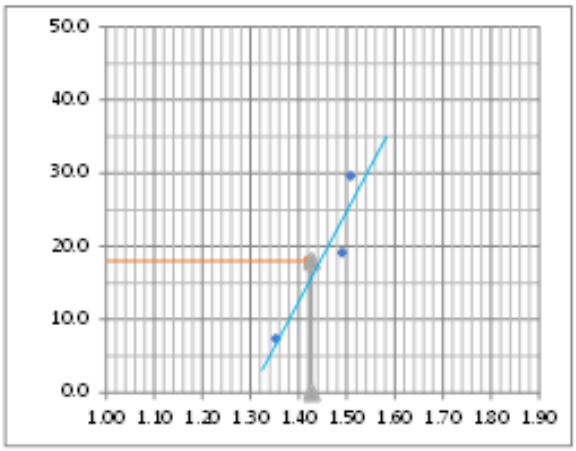

Density @ 95% Compaction (gm/cc)	1.425
CBR @ 95% Compaction (%)	18.0
Swell @ 95% Compaction (%)	0.42

Tested By	Checked By	Verified by	Approved By

CLIENT	CONSULTANT	CONTRACTOR
ETHIOPIAN ROAD AUTHORITY	LEA-LASA-UNICONE	JMC PROJECTS (I) LTD.

ETHIOPIA-DJIBOUTI TRANSPORT CORRIDOR PROJECT

(PHASE-I: DESIGN BUILD OF ADAMA-Km 60 EXPRESSWAY)

CALIFORN IA BEARING RATIO TEST

(AASHTO T 193)

Format No: 0102/JMC/EHAE/21F/04B-R0

RFI No.	QA-QC/LAB/1796/11168	Lab Ref. No.	EDTCP/ADAMA/CLTSEC/10911
Source :	Cutting Section at 25+060 to 25+180	Date of Sampling:	15-01-2025
Location:	25+135RHS	Date of Soaking:	23-01-2025
Propose Used	Earthwork Filling	Date of Testing:	27-01-2025
Material Discription	White Light Clay Soil	Depth (m):	3m

MDD (gm/cc)	1.300	OMC (%)	15.20

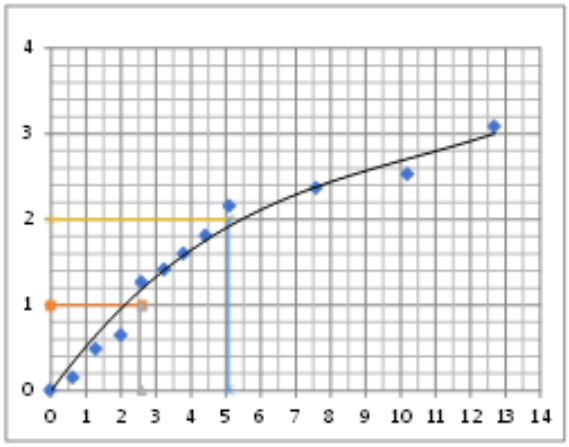

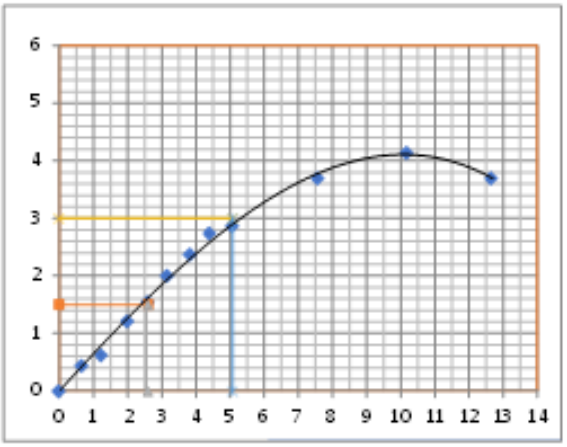

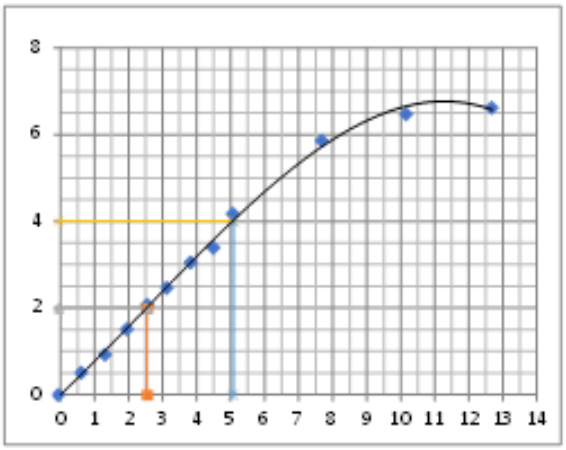

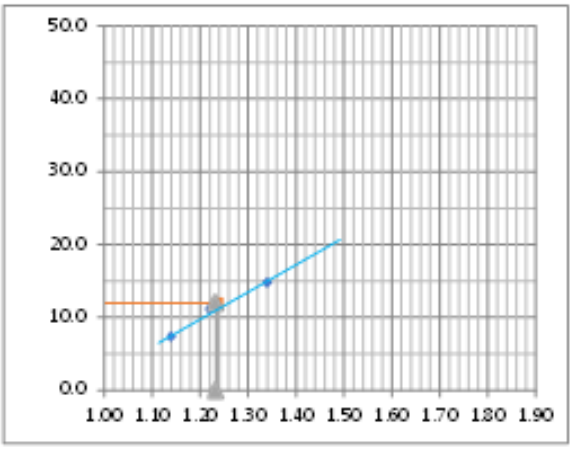

Density @ 95% Compaction (gm/cc)	1.235
CBR @ 95% Compaction (%)	12.0
Swell @ 95% Compaction (%)	0.42

Tested By	Checked By	Verified by	Approved By

CLIENT	CONSULTANT	CONTRACTOR
ETHIOPIAN ROAD AUTHORITY	LEA-LASA-UNICONE	JMC PROJECTS (I) LTD.

ETHIOPIA-DJIBOUTI TRANSPORT CORRIDOR PROJECT

(PHASE-I: DESIGN BUILD OF ADAMA-Km 60 EXPRESSWAY)

CALIFORN IA BEARING RATIO TEST

(AASHTO T 193)

Format No: 01/02/JMC/EHAE/21F/04B-R0

RFI No.	QA-QC/LAB/1796 /11168	Lab Ref. No.	ED/CP/ADAMA/CUTSEC/10911
Source :	Cutting Section at 25+060 to 25+180	Date of Sampling:	15-01-2025
Location:	25+160RHS	Date of Soaking:	24-01-2025
Propose Used	Earthwork Filling	Date of Testing:	28-01-2025
Material Discription	White Light Clay Soil	Depth (m):	1m

MDD (gm/cc)	1.300	OMC (%)	12.40

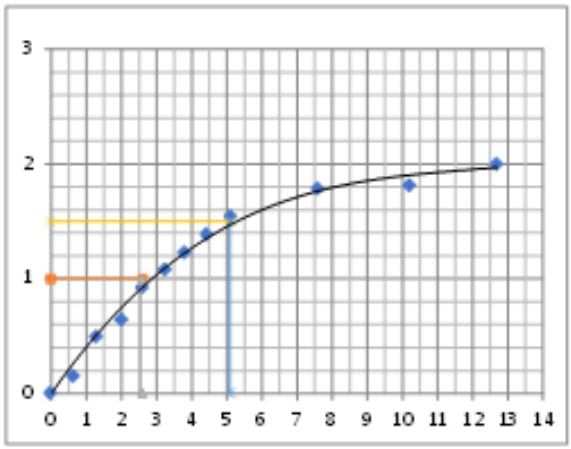

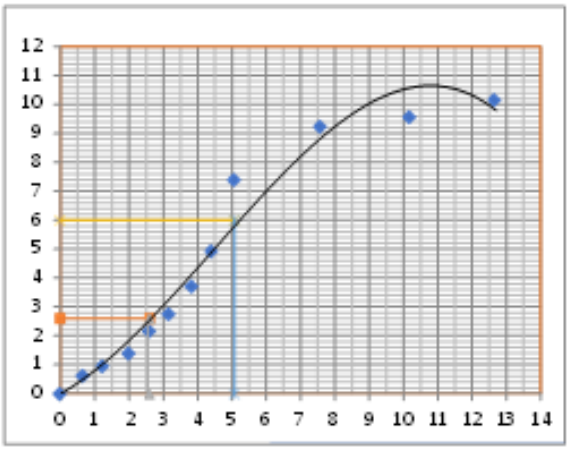

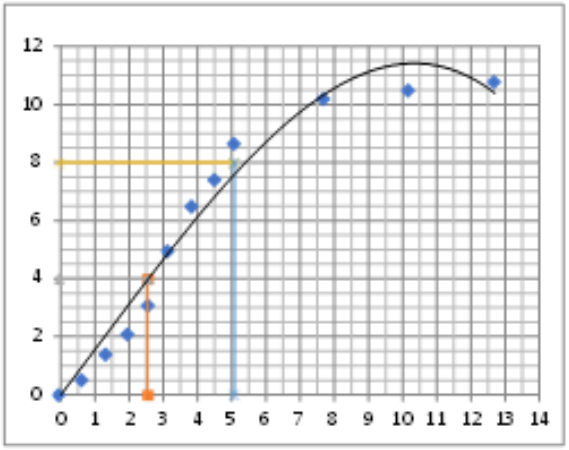

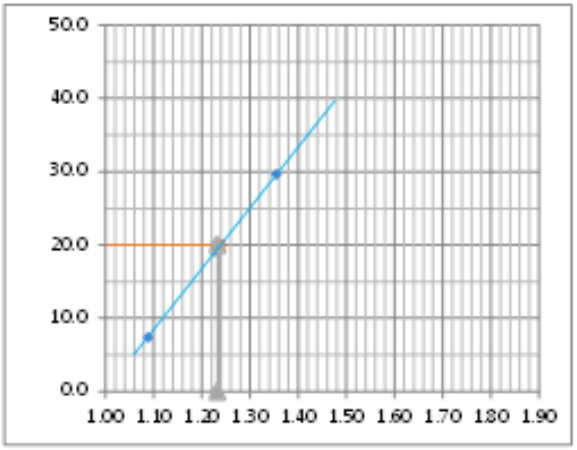

Density @ 95% Compaction (gm/cc)	1.235
CBR @ 95% Compaction (%)	20.0
Swell @ 95% Compaction (%)	0.42

Tested By ..... Checked By ..... Verified by ..... Approved By .....

CLIENT	CONSULTANT	CONTRACTOR
ETHIOPIAN ROAD AUTHORITY	LEA-LASA-UNICONE	JMC PROJECTS (I) LTD.

ETHIOPIA-DJIBOUTI TRANSPORT CORRIDOR PROJECT

(PHASE-I: DESIGN BUILD OF ADAMA-Km 60 EXPRESSWAY)

CALIFORNIA BEARING RATIO TEST

(AASHTO T 193)

Format No: 01/02/JMC/EHAE/21F/04B-R0

RFI No.	QA-QC/LAB/1796/11168	Lab Ref. No.	ED'CP/ADAMA/CLT'SEC/10911
Source :	Cutting Section at 25+060 to 25+180	Date of Sampling:	15-01-2025
Location:	25+160RHS	Date of Soaking:	25-01-2025
Propose Used	Earthwork Filling	Date of Testing:	26-12-2023
Material Discription	White Light Clay Soil	Depth (m):	3m

MDD (gm/cc)	1.400	OMC (%)	12.30

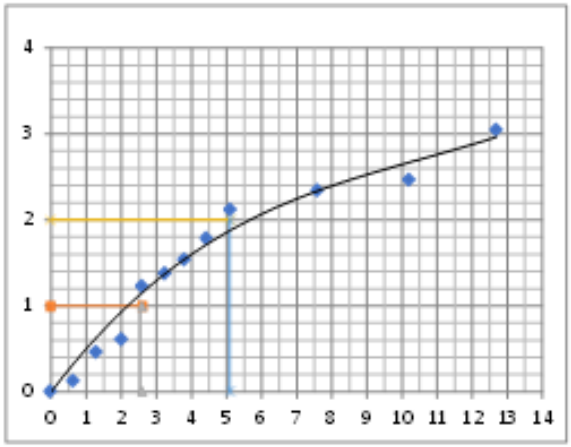

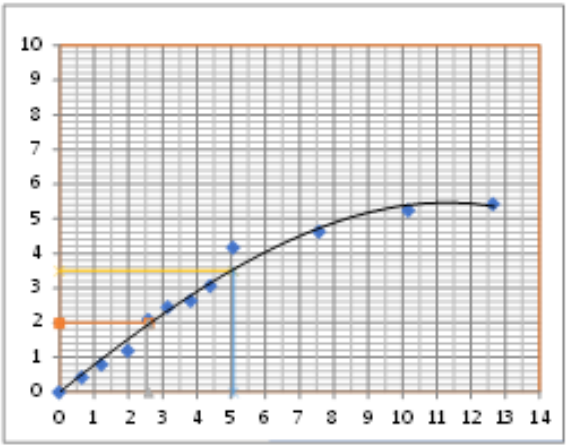

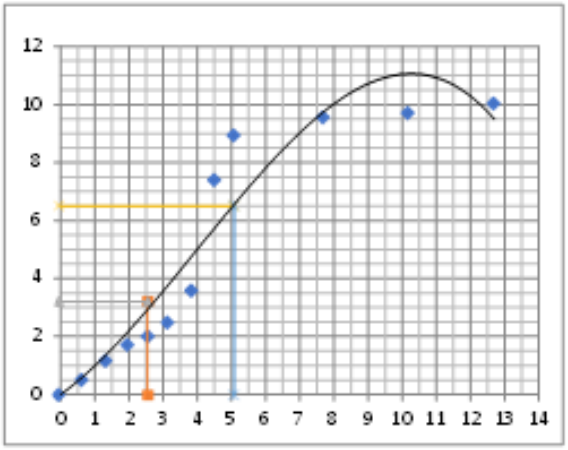

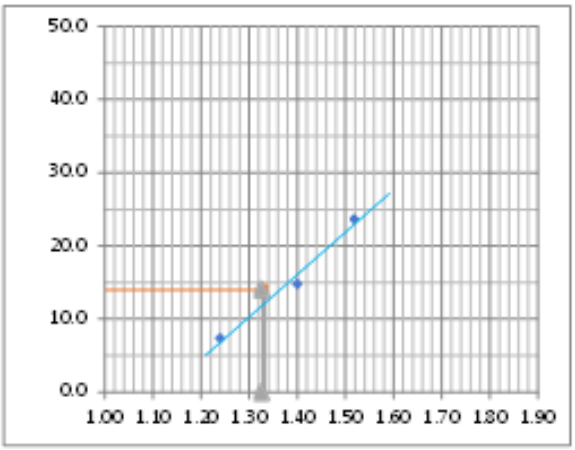

Density @ 95% Compaction (gm/cc)	1.330
CBR @ 95% Compaction (%)	14.0
Swell @ 95% Compaction (%)	0.42

Tested By ..... Checked By ..... Verified by ..... Approved By .....

Appendices C

Geochemical Test result

Company Name	የኢትዮጵያ ኢንጂነሪንግ ኮርፖሬሽን Ethiopian Engineering Corporation		
ስልክ Tel +251-11-872-3643/+251-11-872-3478/+251-11-869-5125/+251-11-827-5378 ፋክስ Fax +251-11-661-53 ፖ.ሣ.ቁ P.O.Box 2561 ኢሜል E-mail info@ecdswco.com Alonge Megenagna Bole Road, Woreda 05 Infront of Former Imperial Hotel, Addis Ababa Ethiopia			
Title: **Soil Fertility and Plant Sample Test Report**	Document No: OF/EEC/0921	Issue No.4	Page No. 1 of 1

Client:Sadik Hussien

Project: .....

Source of Sample:- Adama Awash

Location: Metehara station Km 25 + 100

Contact Person:-Sadik Hussien

Contact Address:-09 13 83 30 31

Date of sampling : 14/02/2025

Test Requested: -pH-H_2O

Client Ref/Lab/SF/02/037/2025

Date received: -17/01/2025

Date of analysis :-18/02/2025

Date reported :-19/02/2025

Laboratory Number	0335/17	Test Method
Profile Code	pH for Soil Sample Using Instrunment for Msc Research	-
Depth (m)	OGL-2	-
pH-H_2O (1:2.5)	8.59	Potentiometric

REMARK:- The Soil sample was collected and submitted to the laboratory by the client.

This test report is only for this specific Soil sample.

Reported by:-Abreham G. Lab Expert

Checked by:-Abreham G. Senior Soil Expert

Approved by:-Tseganesh K. Soil Fertility Lab S/P Manager Representative

Please make sure that this document is the correct version before use

Appendices D

Permeability Test results

Company Name

የኢትዮጵያ ኢንጂነሪንግ ኮርፖሬሽን

Ethiopian Engineering Corporation

ስልክ +251-11-854-7174
+251-11-827-5378
+251-11-849-4199

ፋክስ Fax +251-11-651-5371/61-0898
+251-11-651-0898

ፖ.ሣ.ቁ: 2561
P.O.Box
E-mail: info@ecdswc.com
A.A, Ethiopia

Title:	Document No:	Issue No	Page No
Geotechnical Laboratory Testing Report	OF/EEC/0996	2	1 of 1

Client Ref.:-	GL/088/25
Date Received:-	17/02/2025
Reported on:-	25/02/2025

Lab No. :-1604/17
Submitted by :- Sadik Hussien
Project :- MSC Thesis
Station :-Methara(23+000km)
Test Requested :- As Stated Below
Reported to :- Sadik Hussien
Customer Contact Address:-Sadik Hussien /0913833031/
Date of Sampling :- 14/02/2025
Date of Tests :- 17/02/2025-25/02/2025

No.	Test Type	Standard Test Methods	Soil Sample Test Result
			Lab No.:-
			1604/17
			Sample Id.:-
			Soil
			Depth(m):-
			2.00
1	Permeabiliy Ko(cm/Se)	*	8.8*10^-6

REMARK :- The samples was collected & submitted to the laboratory by Client.
*Standard Method used from text Book.
:-MDD and OMC provided by Client.

Processed by :- Tesfaye.M
Geotechnical Engineer

Checked By :- Biruk A.
Senior Geotechnical Engineer

Approved By :- Bethelhem B.
Geotechnical Lab S/P Manager

Among the major services rendered by the Geotechnical and Material Laboratory Testing s processes of Ethiopia nEngineering Corporation are:
In Geotechnical Laboratory:-Testing the engineering properties of Soil Mechanics and Rock Mechanics.
In Material Testing Laboratory:- Testing the engineering properties of various Construction materials, such as Aggregates, Asphalts/Bitumen', Cements, Rocks, Water, Reinforcement steel bars, Hollow Blocks, Bricks, Ceramics, Tiles,Asphalt & Concrete Core Tests, Concrete Mix Designs, Asphalt Mix Designs, Sampling of the soil and construction materials, and so on.

Please make sure that this document is the correct version before use

Appendices E

DCP Test results

CLIENT	Consultant	Contractor
Ethiopian Roads Administration (ERA)	LEA JV withUnicon P.L.C, Ethiopia	JMC-LRBCL JOINT VENTURE

Name of project	ETHIOPIA-DJIBOUTI TRANSPORT CORRIDOR PROJECT		
	(PHASE-I: DESIGN BUILD OF ADAMA-Km 60 EXPRESSWAY)		
Sink Hole Depth	2.0m	Sink Hole Length (m)	5.0m
Cone Angle:	60	Sink Hole Axis	A-1
Zero Error (mm):	70	Surface Condition	Sink Hole Formation Level
Test Date:	15-01-2025	Strength Coeff.:	**Sinkhole @ 25+085 RHS 0.0 to 2.0m**

No.	Blows	Cumulative Blows	Penetration Depth (mm)	Penetration Rate (mm/blow)	SPT Value blows/300mm	SPT N 30 Value		Blows	Cumulative Blows	Penetration Depth (mm)	Penetration Rate (mm/blow)	SPT Value blows/300mm
No.	Blows	Cumulative Blows	Penetration Depth (mm)	Number of blow @ 300mm depth	SPT Value blows/300mm	SPT N 30 Value	Allowable Bearing Capacity in KPa, for 25mm Settlement	SPT equivalent blow count, over 30mm from DCP results analysis				
1	0	0	0	0	0	0	0	Developed By: Lacroix and Horn (1973)				
2	50	50	300	50	15	15	317	$N_{30SB} = N_{30L} * (WH/48260) * (1290/OD^2)$				
3	80	130	600	80	25	25	323	Where				
4	85	215	900	85	26	26	329	N_{30SB} = SPT equivalent blow count, over 30mm from DCP results				
5	85	300	1200	85	26	26	335	W= Mass of DCP Hammer (kg)=8kg	8			
6	75	375	1500	75	23	23	461	H= Fall Distance in (mm)= 575mm	575			
7	70	445	1800	70	22	22	488	OD = Outer diameter cone (mm) = 20mm	20			
8	80	525	2100	80	25	25	521	48260 is the energy weight of SPT test (760mm x 63.5 kg)				
								1290mm is $OD^2 - ID^2$ for the SPT test				
			Average	75	20	20	396					

Comments/Instructions by the M.I. (If any) :

Comments/Instructions by the M.E. (If any) :

Tested By Contractor's Lab Technician	Checked by Contractor's material Engineer	Verified by Consultant's Lab Technician	Approved By Consultant's Material Engineer

CLIENT	Consultant	Contractor
Ethiopian Roads Administration (ERA)	LEA JV withUnicon P.L.C, Ethiopia	JMC-LRBCL JOINT VENTURE

DCP Sink Hole @25+085 RHS 0.0 to 2.0m

SPT N-30	Overburden presure correction factor (CN)	δo'	Field procedure Correction(N60)	Overburden Correction(N60)1	Dilatancy Correction(N60)2
15	1.00	2	15	15	15
N.B: Bulk density has been taken from test pit (TP-39)					

Sink Hole

Bowels(1997) equation					
			F1	0.05	
qall = (N/F2)*K_d		Where B ≤ F4	F2	0.05	0.08
qall = (N/F2)*((B+F3)/B)*K_d		Where B > F4	F3	0.05	0.08
Kd = 1+0.33(D/B) ≤ 1.33			F4	1.2	
	K_d				
	Footing Width, B, in M				
Depth in M	1	1.5	2	5	
0.3	1.10	1.07	1.05	1.02	
0.6	1.20	1.13	1.10	1.04	
0.9	1.30	1.20	1.15	1.06	
1.2	1.40	1.26	1.38	1.08	
1.5	1.45	1.46	1.45	1.49	
1.8	1.50	1.52	1.52	1.57	
2.1	1.53	1.58	1.35	1.68	
		Sink Hole			
		1	1.5	2	5
Depth in M	SPT N value	Allowable Bearing Capacity in KPa, for 25mm Settlement			
0.3	15	355	339	331	317
0.6	25	387	360	346	323
0.9	26	419	381	362	329
1.2	26	451	402	434	335
1.5	23	468	465	457	461
1.8	22	483	484	478	488
2.1	25	495	501	424	521

Tested By	Checked by	Verified by	Approved By
Contractor's Lab Technician	Contractor's material Engineer	Consultant's Lab Technician	Consultant's Material Engineer

CLIENT	Consultant	Contractor
Ethiopian Roads Administration (ERA)	LEA JV withUnicon P.L.C, Ethiopia	JMC-LRBCL JOINT VENTURE

Name of project	ETHIOPIA-DJIBOUTI TRANSPORT CORRIDOR PROJECT
	(PHASE-I: DESIGN BUILD OF ADAMA-Km 60 EXPRESSWAY)

Sink Hole Depth	2.0m	Sink Hole Length (m)	5.0m
Cone Angle:	60	Sink Hole Axis	A-1
Zero Error (mm):	70	Surface Condition	Sink Hole Formation Level
Test Date:	15-01-2025	Strength Coeff.:	**Sinkhole @ 25+110RHS 0.0 to 2.0m**

No.	Blows	Cumulative Blows	Penetration Depth (mm)	Penetration Rate (mm/blow)	SPT Value blows/300mm	SPT N 30 Value		Blows	Cumulative Blows	Penetration Depth (mm)	Penetration Rate (mm/blow)	SPT Value blows/300mm
No.	Blows	Cumulative Blows	Penetration Depth (mm)	Number of blow @ 300mm depth	SPT Value blows/300mm	SPT N 30 Value	Allowable Bearing Capacity in KPa, for 25mm Settlement	SPT equivalent blow count, over 30mm from DCP results analysis				
1	0	0	0	0	0	0	0	Developed By: Lacroix and Horn (1973)				
2	70	70	300	70	22	22	443	$N_{30SB} = N_{30L} * (WH/48260) * (1290/OD^2)$				
3	85	155	600	85	26	26	452	Where				
4	85	240	900	85	26	26	460	N_{30SB} = SPT equivalent blow count, over 30mm from DCP results				
5	80	320	1200	80	25	25	469	W= Mass of DCP Hammer (kg)=8kg	8			
6	70	390	1500	70	22	22	646	H= Fall Distance in (mm)= 575mm	575			
7	75	465	1800	75	23	23	683	OD = Outer diameter cone (mm) = 20mm	20			
8	65	530	2100	65	20	20	646	48260 is the energy weight of SPT test (760mm x 63.5 kg)				
								1290mm is $OD^2 - ID^2$ for the SPT test				
			Average	76	20	20	543					

Comments/Instructions by the M.I. (If any) :

Comments/Instructions by the M.E. (If any) :

Tested By Contractor's Lab Technician	Checked by Contractor's material Engineer	Verified by Consultant's Lab Technician	Approved By Consultant's Material Engineer

CLIENT	Consultant	Contractor
Ethiopian Roads Administration (ERA)	LEA JV with Unicon P.L.C, Ethiopia	JMC-LRBCL JOINT VENTURE

Name of project	ETHIOPIA-DJIBOUTI TRANSPORT CORRIDOR PROJECT			
	(PHASE-I: DESIGN BUILD OF ADAMA-Km 60 EXPRESSWAY)			
Sink Hole Depth	2.0m	Sink Hole Length (m)	5.0m	
Cone Angle:	60	Sink Hole Axis	A-1	
Zero Error (mm):	70	Surface Condition	Sink Hole Formation Level	
Test Date:	15-01-2025	Strength Coeff.:	Sinkhole @ 25+135RHS 0.0 to 2.0m	

No.	Blows	Cumulative Blows	Penetration Depth (mm)	Penetration Rate (mm/blow)	SPT Value blows/300mm	SPT N30 Value		Blows	Cumulative Blows	Penetration Depth (mm)	Penetration Rate (mm/blow)	SPT Value blows/300mm

No.	Blows	Cumulative Blows	Penetration Depth (mm)	Number of blow @ 300mm depth	SPT Value blows/300mm	SPT N30 Value	Allowable Bearing Capacity in KPa, for 25mm Settlement	SPT equivalent blow count, over 30mm from DCP results analysis
1	0	0	0	0	0	0	0	Developed By: Lacroix and Horn (1973)
2	75	75	300	75	23	23	475	$N_{30SB} = N_{30L} * (WH/48260) * (1290/OD^2)$
3	90	165	600	90	28	28	484	Where
4	85	250	900	85	26	26	493	N_{30SB} = SPT equivalent blow count, over 30mm from DCP results
5	75	325	1200	75	23	23	503	W= Mass of DCP Hammer (kg)=8kg 8
6	70	395	1500	70	22	22	692	H= Fall Distance in (mm)= 575mm 575
7	75	470	1800	75	23	23	732	OD = Outer diameter cone (mm) = 20mm 20
8	70	540	2100	70	22	22	770	48260 is the energy weight of SPT test (760mm x 63.5 kg)
								1290mm is $OD^2 - ID^2$ for the SPT test
			Average	77	21	21	593	

Comments/Instructions by the M.I. (If any) :

Comments/Instructions by the M.E. (If any) :

Tested By Contractors Lab Technician	Checked by Contractor's material Engineer	Verified by Consultant's Lab Technician	Approved By Consultant's Material Engineer

CLIENT	Consultant	Contractor
Ethiopian Roads Administration (ERA)	LEA JV with Unicon P.L.C, Ethiopia	JMC-LRBCL JOINT VENTURE

Name of project	ETHIOPIA-DJIBOUTI TRANSPORT CORRIDOR PROJECT		
	(PHASE-I: DESIGN BUILD OF ADAMA-Km 60 EXPRESSWAY)		
Sink Hole Depth	2.0m	Sink Hole Length (m)	5.0m
Cone Angle:	60	Sink Hole Axis	A-1
Zero Error (mm):	70	Surface Condition	Sink Hole Formation Level
Test Date:	15-01-2025	Strength Coeff.:	Sinkhole @ 25+160RHS 0.0 to 2.0m

No.	Blows	Cumulative Blows	Penetration Depth (mm)	Penetration Rate (mm/blow)	SPT Value blows/300mm	SPT N30 Value		Blows	Cumulative Blows	Penetration Depth (mm)	Penetration Rate (mm/blow)	SPT Value blows/300mm

No.	Blows	Cumulative Blows	Penetration Depth (mm)	Number of blow @ 300mm depth	SPT Value blows/300mm	SPT N30 Value	Allowable Bearing Capacity in KPa, for 25mm Settlement
1	0	0	0	0	0	0	0
2	60	60	300	60	18	18	380
3	85	145	600	85	26	26	387
4	85	230	900	85	26	26	395
5	80	310	1200	80	25	25	402
6	75	385	1500	75	23	23	554
7	75	460	1800	75	23	23	585
8	75	535	2100	75	23	23	626
			Average	76	21	21	476

SPT equivalent blow count, over 30mm from DCP results analysis

Developed By: Lacroix and Horn (1973)

$N_{30SB} = N_{30L} * (WH/48260) * (1290/OD^2)$

Where

N_{30SB} = SPT equivalent blow count, over 30mm from DCP results

W= Mass of DCP Hammer (kg)=8kg 8

H= Fall Distance in (mm)= 575mm 575

OD = Outer diameter cone (mm) = 20mm 20

48260 is the energy weight of SPT test (760mm x 63.5 kg)

1290mm is $OD^2 - ID^2$ for the SPT test

Comments/Instructions by the M.I. (If any) :

Comments/Instructions by the M.E. (If any) :

Tested By Contractor's Lab Technician	Checked by Contractor's material Engineer	Verified by Consultant's Lab Technician	Approved By Consultant's Material Engineer

DCP Layer Strength Analysis Report

Project Name: 25+060 to 25+160 RHS DCP Test

Chainage (Km):	25.110	Surface Type:	Unpaved
Direction:	RHS	Thickness(mm):	0
Location/Offset:	Lane 1/7.00m	Base Type:	
Cone Angle:	60 degrees	Thickness (mm):	
Zero Error(mm):	0	Surface Moisture:	Moderate
Test Date:	11/03/2024	Moisture adjustment factor:	Not adjusted

Layer Boundaries Chainage 25.100

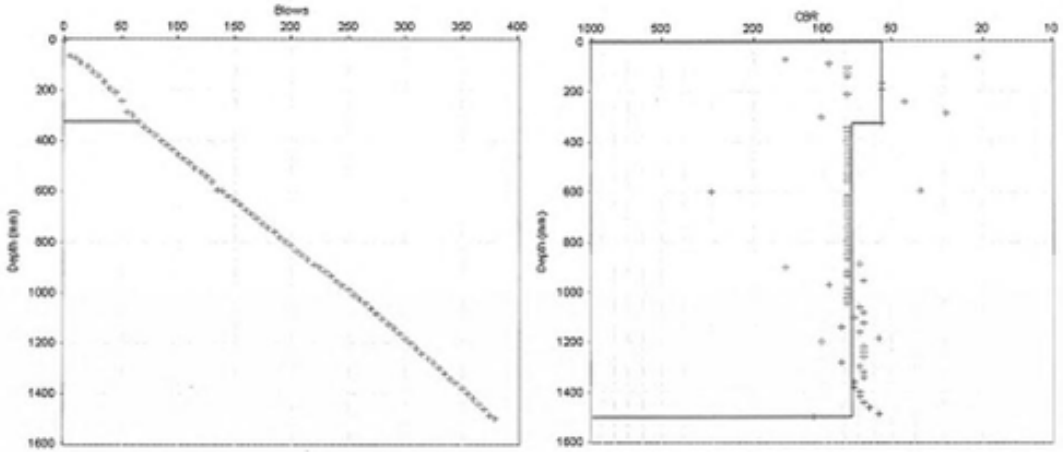

Layer Boundaries Chart

CBR Chart

No.	Penetration Rate (mm/blow)	CBR (%)	Thickness (mm)	Depth to layer bottom	Position	Strength Coefficient	SN	SNC	SNP
1	3.69	76	1014	1014	Subgrade	-	-	-	-
2	4.23	66	486	486	Subgrade	-	-	-	-

Pavement Strength

	Layer Contribution		
Layer	SN	SNC	SNP
Surface	--	--	--
Base	--	--	--
Sub-Base	--	--	--
Subgrade	--	2.08	2.08
Pavement strength	--	2.08	2.08

CBR Relationship:

TRL equation: $\log_{10}(CBR) = 2.48-1.057 \times \log_{10}(strength)$

Report produce By Sadik Husen

DCP Layer Strength Analysis Report

Project Name: 25+060 to 25+160 RHS DCP Test

Chainage (Km):	25.135	Surface Type:	Unpaved
Direction:	RHS	Thickness(mm):	0
Location/Offset:	Lane 1/5.00m	Base Type:	
Cone Angle:	60 degrees	Thickness (mm):	
Zero Error(mm):	0	Surface Moisture:	Moderate
Test Date:	11/01/2025	Moisture adjustment factor:	Not adjusted

Layer Boundaries Chainage 25.100

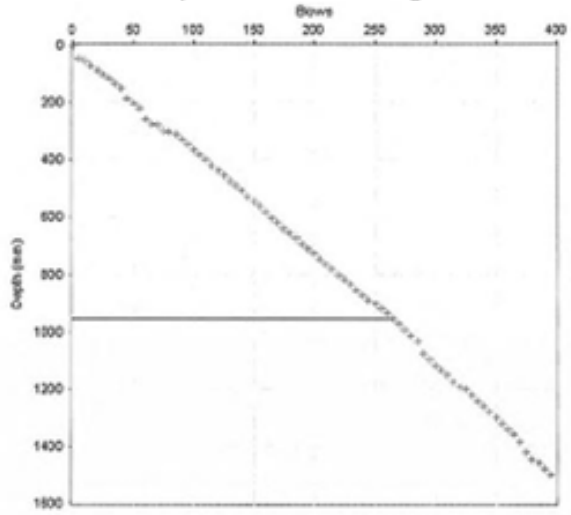

Layer Boundaries Chart

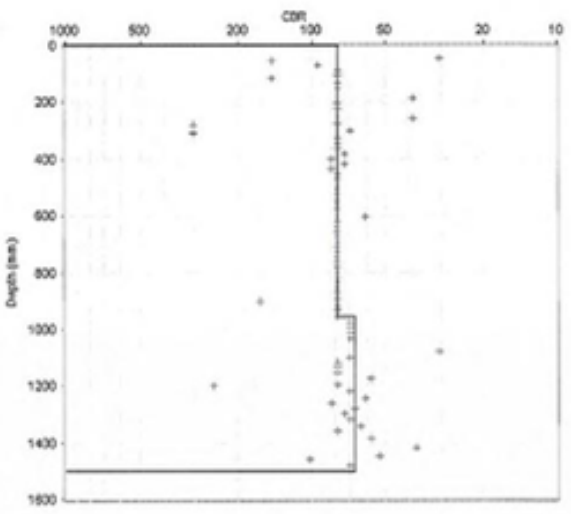

CBR Chart

No.	Penetration Rate (mm/blow)	CBR (%)	Thickness (mm)	Depth to layer bottom	Position	Strength Coefficient	SN	SNC	SNP
1	3.60	78	954	954	Subgrade	-	-	-	-
2	4.2	66	546	1500	Subgrade	-	-	-	-

Pavement Strength

	Layer Contribution		
Layer	SN	SNC	SNP
Surface	--	--	--
Base	--	--	--
Sub-Base	--	--	--
Subgrade	--	2.08	2.08
Pavement strength	--	2.08	2.08

CBR Relationship:

TRL equation: $\log_{10}(CBR) = 2.48 - 1.057 \times \log_{10}(strength)$

DCP Layer Strength Analysis Report

Project Name: 25+060 to 25+160 RHS DCP Test

Report produce By Sadik Husen

Chainage (Km):	25.160	Surface Type:	Unpaved
Direction:	RHS	Thickness(mm):	0
Location/Offset:	Lane 1/7.00m	Base Type:	
Cone Angle:	60 degrees	Thickness (mm):	
Zero Error(mm):	0	Surface Moisture:	Moderate
Test Date:	11/01/2025	Moisture adjustment factor:	Not adjusted

Layer Boundaries Chainage 25.100

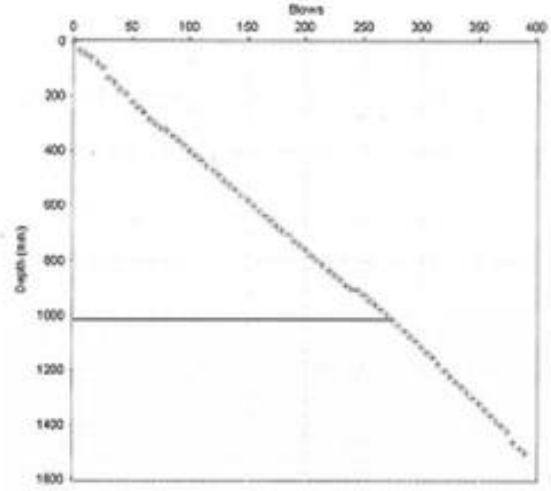

Layer Boundaries Chart

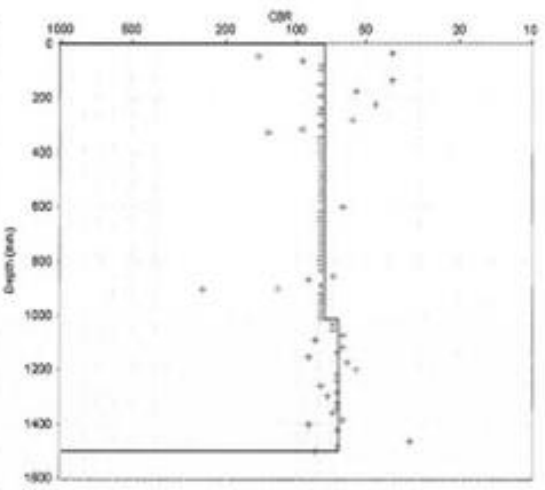

CBR Chart

No.	Penetration Rate (mm/blow)	CBR (%)	Thickness (mm)	Depth to layer bottom	Position	Strength Coefficient	SN	SNC	SNP
1	5.00	55	325	325	Subgrade	-	-	-	-
2	3.73	75	1175	1500	Subgrade	-	-	-	-

Pavement Strength

	Layer Contribution		
Layer	SN	SNC	SNP
Surface	--	--	--
Base	--	--	--
Sub-Base	--	--	--
Subgrade	--	2.08	2.08
Pavement strength	--	2.08	2.08

CBR Relationship:

TRL equation: $\log_{10}(CBR) = 2.48 - 1.057 \times \log_{10}(strength)$